AD-A087 126 NATIONAL TELECOMMUNICATIONS/INFORMATION ADMINISTRATIO--ETC F/G 17/3
POWER LINE CARRIER RADIATION AND THE LOW-FREQUENCY AERONAUTICAL--ETC(U)
MAY 80 W A KISSICK DOT-FA79WAI-023

UNCLASSIFIED FAA-RD-80-31 NL

1 OF 2
AD A
087126

Report No. FAA-RD-80-31

LEVEL II

(12)

ADA087126

POWER LINE CARRIER RADIATION AND THE LOW-FREQUENCY AERONAUTICAL RADIO COMPASS

WILLIAM A. KISSICK

MAY 1980

Document is available to the U.S. public through the National Technical Information Service, Springfield, Virginia 22161.

Prepared for

U.S. DEPARTMENT OF TRANSPORTATION
FEDERAL AVIATION ADMINISTRATION
Systems Research & Development Service
Washington, D.C. 20590

NOTICE

Technical Report Documentation Page

1. Report No.	2. Government Accession No.	3. Recipient's Catalog No.
(18) FAA-RD-80-31 (19)	AD-A087 226	

4. Title and Subtitle	5. Report Date
(6) POWER LINE CARRIER RADIATION AND THE LOW-FREQUENCY AERONAUTICAL RADIO COMPASS	May 1980
	6. Performing Organization Code: NTIA/ITS/1
7. Author(s): (10) William A. Kissick	8. Performing Organization Report No.: (11) May 80
9. Performing Organization Name and Address: Institute for Telecommunication Sciences, National Telecommunications and Information Admin., Department of Commerce, Boulder, Colorado 80303	10. Work Unit No. (TRAIS)
	11. Contract or Grant No.: (15) DOT-FA79WAI-023
12. Sponsoring Agency Name and Address: U.S. Department of Transportation, Federal Aviation Administration, Systems Research and Development Service, Washington, D.C. 20590 (12) 136	13. Type of Report and Period Covered: (9) Final rept.
	14. Sponsoring Agency Code: SRDS, ARD-450

15. Supplementary Notes

410137

16. Abstract

The power line carrier is a telecommunication technique widely used by the power utilities for communication and telemetry. This system uses the power ines as a propagation medium and operates largely in the LF band. Potential for interference to an aeronautical radio compass operationing in the 190-535 kHz aeronautical radionavigation band exists. The purpose of this work was to examine that potential for interference.

Laboratory measurements of radio compass receivers were made. These results indicate that 44 to 54 dBu of undesired signal or an undesired-to-desired signal ratio of 4 to 10 dB was required to cause measurable radio compass bearing errors, depending on the type of receiver.

An airplane equipped with a spectrum analyzer/data recording system was used to make power line carrier radiation measurements over two selected power lines in Tennessee. The results indicate that, for the limited measurements taken, radio compass bearing errors could be caused by power line carrier radiation for an injected carrier power of 4 W. The distance and height dependence of the power line carrier radiation is discussed.

17. Key Words	18. Distribution Statement
calibration; carrier current; electromagnetic compatibility; interference; LF; power lines; radiation; radio compass	Document is available to the U.S. public through the National Technical Information Service, Springfield, Virginia 22161.

19. Security Classif. (of this report)	20. Security Classif. (of this page)	21. No. of Pages	22. Price
Unclassified	Unclassified	133	

410937 vlt

METRIC CONVERSION FACTORS

Approximate Conversions to Metric Measures

Symbol	When You Know	Multiply by	To Find	Symbol
	LENGTH			
in	inches	*2.5	centimeters	cm
ft	feet	30	centimeters	cm
yd	yards	0.9	meters	m
mi	miles	1.6	kilometers	km
	AREA			
in^2	square inches	6.5	square centimeters	cm^2
ft^2	square feet	0.09	square meters	m^2
yd^2	square yards	0.8	square meters	m^2
mi^2	square miles	2.6	square kilometers	km^2
	acres	0.4	hectares	ha
	MASS (weight)			
oz	ounces	28	grams	g
lb	pounds	0.45	kilograms	kg
	short tons (2000 lb)	0.9	tonnes	t
	VOLUME			
tsp	teaspoons	5	milliliters	ml
Tbsp	tablespoons	15	milliliters	ml
fl oz	fluid ounces	30	milliliters	ml
c	cups	0.24	liters	l
pt	pints	0.47	liters	l
qt	quarts	0.95	liters	l
gal	gallons	3.8	liters	l
ft^3	cubic feet	0.03	cubic meters	m^3
yd^3	cubic yards	0.76	cubic meters	m^3
	TEMPERATURE (exact)			
°F	Fahrenheit temperature	5/9 (after subtracting 32)	Celsius temperature	°C

*1 in = 2.54 (exactly). For other exact conversions and more detailed tables, see NBS Misc. Publ. 286, Units of Weights and Measures, Price $2.25, SD Catalog No. C13.10:286.

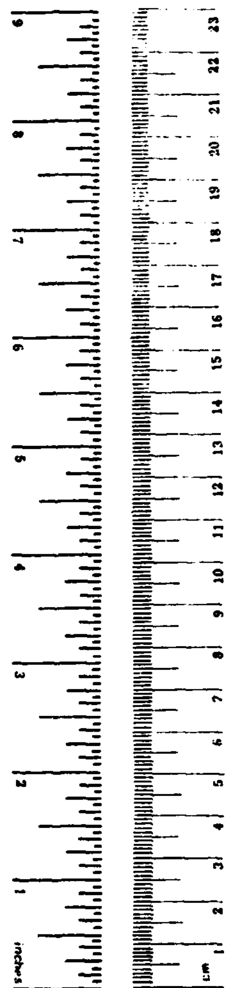

Approximate Conversions from Metric Measures

Symbol	When You Know	Multiply by	To Find	Symbol
	LENGTH			
mm	millimeters	0.04	inches	in
cm	centimeters	0.4	inches	in
m	meters	3.3	feet	ft
m	meters	1.1	yards	yd
km	kilometers	0.6	miles	mi
	AREA			
cm^2	square centimeters	0.16	square inches	in^2
m^2	square meters	1.2	square yards	yd^2
km^2	square kilometers	0.4	square miles	mi^2
ha	hectares (10,000 m^2)	2.5	acres	
	MASS (weight)			
g	grams	0.035	ounces	oz
kg	kilograms	2.2	pounds	lb
t	tonnes (1000 kg)	1.1	short tons	
	VOLUME			
ml	milliliters	0.03	fluid ounces	fl oz
l	liters	2.1	pints	pt
l	liters	1.06	quarts	qt
l	liters	0.26	gallons	gal
m^3	cubic meters	35	cubic feet	ft^3
m^3	cubic meters	1.3	cubic yards	yd^3
	TEMPERATURE (exact)			
°C	Celsius temperature	9/5 (then add 32)	Fahrenheit temperature	°F

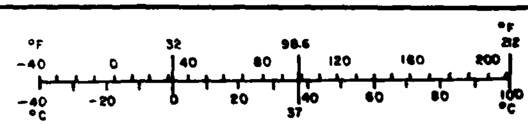

FEDERAL AVIATION ADMINISTRATION
SYSTEMS RESEARCH AND DEVELOPMENT SERVICE
SPECTRUM MANAGEMENT BRANCH

STATEMENT OF MISSION

The mission of the Spectrum Management Branch is to assist the Department of State, National Telecommunications and Information Administration, and the Federal Communications Commission in assuring the FAA's and the nation's aviation interests with sufficient protected electromagnetic telecommunications resources throughout the world and to provide for the safe conduct of aeronautical flight by fostering effective and efficient use of a natural resource--the electromagnetic radiofrequency spectrum.

This objective is achieved through the following services:

- Planning and defending the acquisition and retention of sufficient radio frequency spectrum to support the aeronautical interest of the nation, at home and abroad, and spectrum standardization for the world's aviation community.

- Providing research, analysis, engineering, and evaluation in the development of spectrum related policy, planning, and standards, criteria, measurement equipment, and measurement techniques.

- Conducting electromagnetic compatibility analyses to determine intra/intersystem viability and design parameters, to assure certification of adequate spectrum to support system operational use and projected growth patterns, to defend aeronautical services spectrum from encroachment by others, and to provide for the efficient use of the aeronautical spectrum.

- Developing automated frequency selection computer programs/routines to provide frequency planning, frequency assignment, and spectrum analysis capabilities in the spectrum supporting the National Airspace System.

- Providing spectrum management consultation, assistance, and guidance to all aviation interests, users, and providers of equipment and services, both national and international.

TABLE OF CONTENTS

TABLE OF CONTENTS - continued

LIST OF FIGURES

LIST OF FIGURES - continued

LIST OF FIGURES - continued

LIST OF FIGURES - continued

LIST OF TABLES

LIST OF TABLES - continued

LIST OF TABLES - continued

LIST OF TABLES - continued

LIST OF TABLES - continued

Page

POWER LINE CARRIER RADIATION

AND

THE LOW-FREQUENCY AERONAUTICAL RADIO COMPASS

William A. Kissick*

The power line carrier is a telecommunication technique widely used by the power utilities for communication and telemetry. This system uses the power lines as a propagation medium and operates largely in the LF band. Potential for interference to an aeronautical radio compass operating in the 190-535 kHz aeronautical radionavigation band exists. The purpose of this work was to examine that potential for interference.

Laboratory measurements of radio compass receivers were made. These results indicate that 44 to 54 dBu of undesired signal or an undesired-to-desired signal ratio of 4 to 10 dB was required to cause measurable radio compass bearing errors, depending on the type of receiver.

An airplane equipped with a spectrum analyzer/data recording system was used to make power line carrier radiation measurements over two selected power lines in Tennessee. The results indicate that, for the limited measurements taken, radio compass bearing errors could be caused by power line carrier radiation for an injected carrier power of 4 W. The distance and height dependence of the power line carrier radiation is discussed.

Key Words: calibration; carrier current; electromagnetic compatibility; interference; LF; power lines; radiation; radio compass

* The author is with the Institute for Telecommunication Sciences, National Telecommunications and Information Administration, U.S. Department of Commerce, Boulder, Colorado 80303.

1. INTRODUCTION

The power line carrier (PLC) is a telecommunication technique used by the electric power utilities for voice communication, protective relaying, and general supervision of the power system. This technique is favored by the utilities due to its high inherent reliability and economy. This is due to the simple fact that the power distribution system itself is the propagation medium, with the PLC transmitters and receivers coupled to the lines with matching networks. The useful frequencies for PLC systems are the low-frequency (LF) and medium-frequency (MF) bands up to about 500 kHz. However, the LF band (30 to 300 kHz) is the most used and useful frequency range.

The automatic direction-finder (ADF) radio compass is an aeronautical navigation aid that operates in the LF and MF frequency ranges. The ADF radio compass makes use of two antennas: a pair of orthogonal loops and a separate, omnidirectional "sense" antenna. With some signal manipulation the desired output--the direction of signal arrival--is obtained. The most used signal source is a nondirectional beacon (NDB). The beacons are operated either by the airport or the Federal Aviation Administration (FAA), and those not operated by the government are licensed by the Federal Communications Commission (FCC). The ADF radio compasses operate in the 190-535 kHz aeronautical radionavigation band, can be used with AM radio broadcasting signals, and NDB's as high in frequency as 1715 kHz.

With the PLC systems operating in the same frequency bands as the ADF systems, one can readily imagine some unacceptable situations. Several plane crashes in Europe appear to have been caused by ADF navigation errors induced by interfering PLC signals. Investigations of several plane crashes in this country have considered PLC interference to be a possible factor; whether or not the PLC interference was a factor is unknown. Then, too, several complaints about ADF performance in specific areas have been received by the FAA. Naturally, PLC interference is considered a possible reason.

Some of the observed ADF errors may indeed be due to the power lines, but not necessarily to the PLC radiation. The power lines and/or towers may be reradiating a beacon signal, a situation of several apparent sources. In other words, poor siting of an NDB could produce significant bearing errors in the ADF radio compass.

In order to help resolve some of the questions the preceding discussion raises, this study was initiated by the FAA. It is not well known how the ADF radio compass reacts to an interfering signal. Then, too, it is not well known to what degree the PLC signals radiate from transmission lines. So, in this work, we first studied the above two items: the ADF receiver susceptibility to interference, and the degree to which PLC signals radiate. Then we made an assessment, based on the information collected, of the degree to which PLC systems can interfere with the proper operation of the ADF radio compass.

It should be emphasized at this point that this work is not a comprehensive study. We made measurements of ADF receiver susceptibility, but only on two particular receivers and not all types of signals were considered. Some measurements of PLC radiation have been made by others and a few theoretical models have been developed. We made more measurements of PLC radiation, and we feel that these are a significant contribution to the knowledge of PLC radiation. The theories that describe the propagation of radio frequency (rf) signals along power lines can, in general, be considered unrealistic due to the many simplifying assumptions. They are, however, informative in a qualitative manner.

As stated above, this work was initiated and supported by the FAA, more specifically, by the Spectrum Management Branch at the FAA Systems Research and Development Service in Washington, D.C. Measurements of the ADF receiver susceptibility were made by FAA personnel at the FAA Aeronautical Center in Oklahoma City. Airborne PLC radiation measurements were made by FAA personnel from the National Aviation Facilities Experimental Center (NAFEC) in Atlantic City, N.J. The aircraft and data collection instrumentation were also supplied by NAFEC. The power lines, ground support, and instrumentation necessary to generate specific PLC signals with various coupling configurations were provided by the Tennessee Valley Authority (TVA) in Chattanooga, Tennessee. The responsibilities of the Institute for Telecommunication Sciences were to provide the measurement plans, reduce the data, and perform the necessary analyses--all of which are described in this report.

2. BACKGROUND

This section presents more detail on both the ADF radio compass receivers and the PLC systems. The principles of operation of both systems are described and references are provided for those readers needing more detail.

2.1 The LF Radio Compass

The LF radio compass is a radio navigation technique that falls under the general heading of "direction-finding," hence the name, automatic direction-finding (ADF) radio compass has come into common usage. Direction-finding represents the earliest and most basic use of radio for navigational purposes. The radio compasses that we are interested in for this work are of the airborne type that are useful in the frequency range of about 200 to 1700 kHz. The radio compass can determine the direction to any transmitter in that frequency range. As we described in the Introduction, the source signal is usually a nondirectional beacon, but could just as well be an AM broadcast station.

The essential output of an ADF radio compass is the direction of signal arrival relative to the aircraft heading. In principle, then, all that is needed is a rotatable, directional antenna. However, a single rotating, directional antenna with sufficient directivity and small size is impossible to build. The solution is to make use of the nulls in the pattern of a simple loop antenna. The loop antenna has a sufficiently large effective area and small size for the airborne application. The following paragraphs will develop the principles of using the loop antenna in the ADF system.

Consider a simple rotatable loop, and assume that it is rotated until the incoming signal is in one of the two sharp nulls. The direction of arrival is then in the plane that is perpendicular to the plane of the loop. There is, however, an ambiguity since there are two nulls. The ambiguity can be removed by using an omnidirectional antenna to sense the phase of the incoming signal; this antenna is usually a "tee" antenna, i.e. a top-loaded vertical element. Now, the loop is rotated so that one of its two lobes is directed at the incoming signal and the phase of the signal received by the loop is compared to the phase of the signal received by the sense antenna. The signal received on one of the lobes of the loop pattern will be in phase with the sense antenna, and the signal received on the other lobe will be 180° out of

phase. One simple way of determining which lobe of the loop pattern is receiving the signal is to add the outputs of the loop and sense antennas. The loop, sense, and combined patterns are shown in Figure 1.

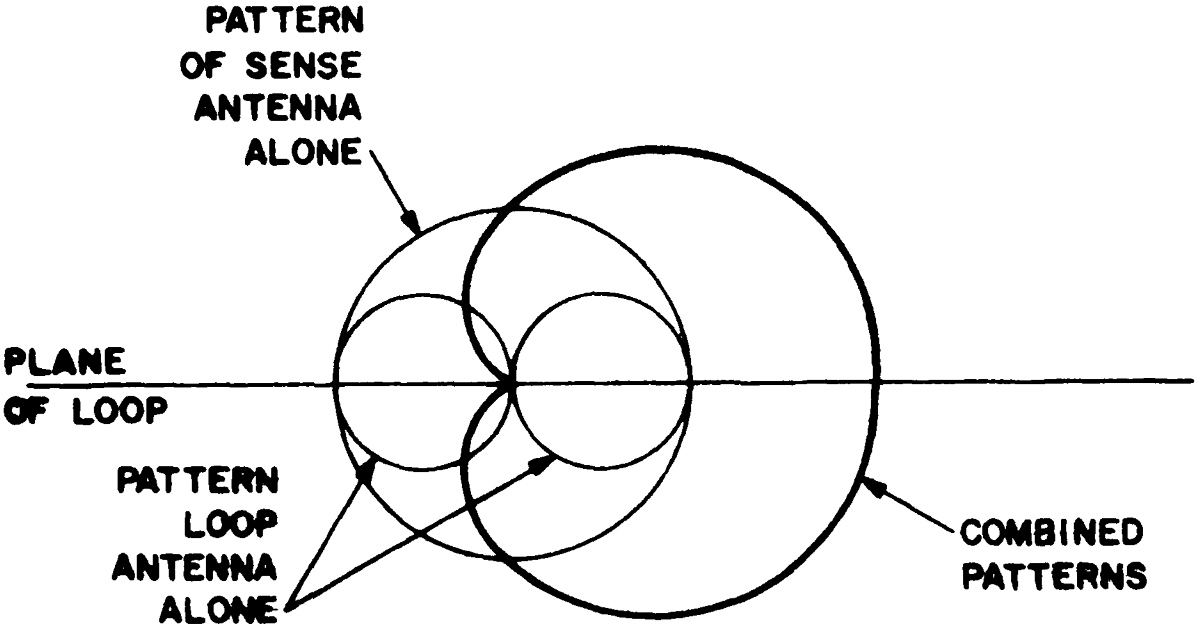

Figure 1. Loop, sense, and combined antenna patterns for the ADF radio compass.

It is not necessary to rotate the loop antenna physically in order to null the incoming signal. The alternative is to use a pair of fixed loops placed at right angles to each other and connect them to the stator windings of a goniometer. The goniometer has two sets of stator windings, and in the magnetic field of these windings is a rotatable loop that is connected to the receiver. The rotor can then be made a part of a feedback circuit that automatically determines the direction of signal arrival. More information can be found in Kayton and Fried (1969).

2.2 Power Line Carrier Systems

The transmission of electric energy from the production plants to the load centers and the interconnection of both plants and load centers requires a complex communication and control network. The primary purpose of the

communication network is to provide the optimum configuration to suit the demand. These networks require extensive telecommunication facilities for speech, telemetering, telecontrol, and protection signals. The electric utilities use a variety of techniques, which include circuits rented from a common carrier and microwave radio links, as well as PLC. The technique chosen for any circuit is a function of the information bandwidth, economics, and various technical factors.

One of the needs for a communication circuit is for the transmission of "protection" signals. The protection signals control the automatic operation of circuit-breakers. In this application, it is often necessary to exchange signals at a high speed and with high reliability between switching stations already linked by the power lines. The use of PLC in this instance is ideal, since the power lines are quite reliable mechanically.

The PLC signals may be propagated along the lines in various ways (modes) such as between one conductor and the earth. Since most power lines carry a three-phase system and the three phases are often arranged asymmetrically, the choice of conductor or conductors is a function of the efficiencies of coupling, attenuation, and radiation. In many cases the power line towers support two three-phase lines as well as one or two ground continuity conductors for lightning and fault protection. The mutual couplings can be quite complex. A number of papers have been published that describe the theory of propagation along power lines. Some of these papers are: Perz (1964), Wedepohl (1965), Wedepohl and Wasley (1966), and Ushirozawa (1964). It should be noted that these papers deal with the characteristics of the PLC from the application engineering point of view, and do not describe the RF fields surrounding the lines.

Consider the specific case of a single three-phase line with the conductors disposed horizontally, i.e. equally spaced and running side-by-side at the same height above the ground. This case has been studied by the Institute for Electrical and Electronic Engineers (IEEE) Power Line Carrier Subcommittee (Dobson, 1979). There may be two shield (ground) wires above the power conductors, located at the top of the towers and grounded to them. There are three important modes of propagation along this line:

<u>Mode 1</u>: This is the least attenuated of the modes. It has current flowing out the two outer phases and returning on the center phase.

Mode 2: This mode has current flowing out one of the outer phases and returning on the other outer phase. The attenuation for this mode is greater and more frequency dependent than for mode 1.

Mode 3: This mode has equal current on all phases with a ground return. It has a high attenuation.

A typical PLC channel, with center phase-to-ground coupling is shown in Figure 2. In this drawing are the basic components of any PLC system: the transmitter and the receiver, tuners, coupling capacitors, and line traps. The tuner in conjunction with the coupling capacitor provides for impedance matching between the transmitter or receiver and the power line. The coupling capacitor blocks the high voltage, has a typical capacitance of 2000-4000 pF, and is a physically large unit. A protection circuit is usually contained within the tuner to protect the transmitter or receiver against electrical surges induced by lightning or other transient disturbances. The line trap is needed to minimize PLC signal power loss into the substation bus or in unwanted directions along the power lines. The choke coil in the line trap has an inductance that is usually in the range of 100 μH to 2 mH. A capacitor is usually placed in parallel with the choke coil to produce a parallel tuned circuit.

There are a number of ways to effect the coupling of the PLC signal to the power line; these include the following:

- center phase-to-ground
- outer phase-to-ground
- phase-to-phase
- "mode 1"
- intercircuit
- intrabundle

Figure 2 is an example of the first of these, center phase-to-ground. Figure 3, then, is an example of phase-to-phase coupling. There is a scheme using two transformers, three tuners, three coupling capacitors, and three line traps to effect a current injection that very effectively excites mode 1 propagation. Intercircuit coupling uses a single phase from each of two three-phase lines on the same tower. Intrabundle coupling can be used on those lines where each phase conductor is composed of several closely spaced

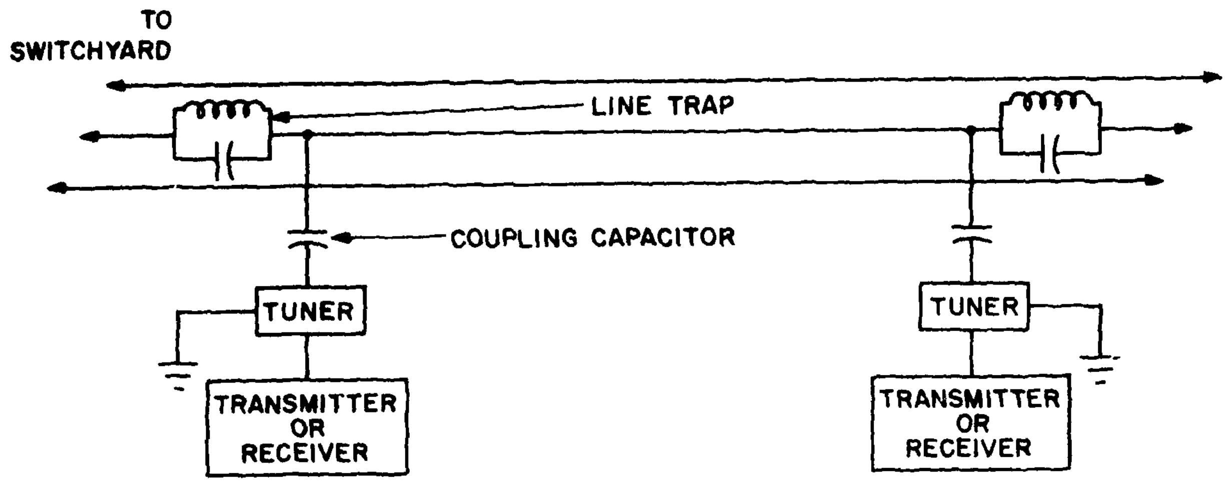

Figure 2. Diagram of a power line carrier circuit on a three-phase power line with center phase-to-ground coupling.

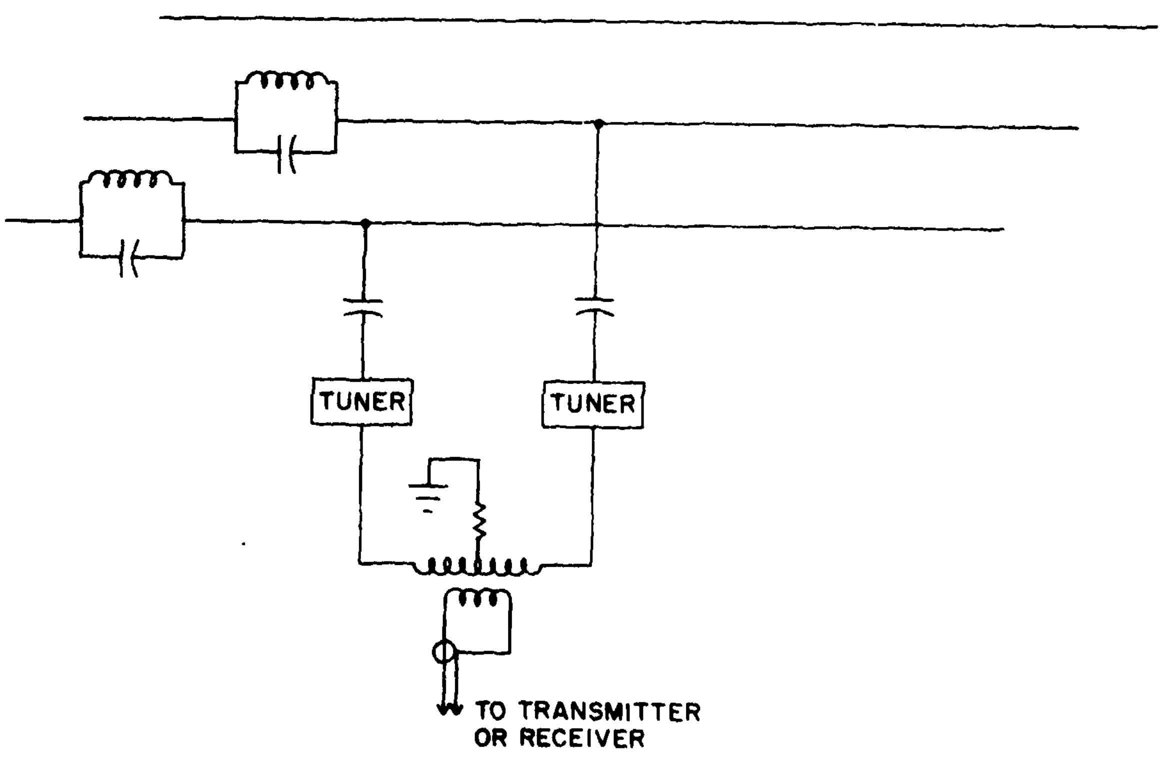

Figure 3. Diagram of adjacent phase-to-phase power line carrier coupling.

wires (the bundle). Intrabundle PLC propagation exhibits very low attenuation due to the close spacing of the conductors.

The mode of propagation at large distances (several tens of kilometers or more) is nearly always the least attenuated mode, that is, in the case considered here, mode 1. This is true regardless of the coupling method, however, the different coupling methods will have different coupling efficiencies. Most simple coupling methods, such as phase-to-ground will excite several modes of propagation, with the more attenuated modes becoming less significant as the distance from the transmitter increases. In practice, the phase-to-ground and the phase-to-phase coupling methods are by far the most commonly used.

3. RADIO COMPASS RECEIVER SUSCEPTIBILITY MEASUREMENTS

The essential purpose of these laboratory measurements is to determine the susceptibility of the typical ADF radio compass receiver to an interfering signal. In other words, we wish to determine the nature and degree of the bearing indication error. The measurements were performed on only two ADF receivers, so the results should not be considered comprehensive. However, of the two receivers chosen, one would most likely be used by commercial aviation and the other by general aviation. The former unit operates with a goniometer as described in section 2.1 and is designated "receiver A" in this report. The latter unit makes use of an electronic circuit to replace the goniometer. It is designated "receiver B" in this report.

Measurements were made to examine the effects of the undesired signal arriving from the same or a different direction from the desired signal. The information sought was the bearing error as a function of the undesired signal level and frequency separation of the two signals. These data were obtained by holding some other parameters constant for each measurement. These parameters are: the level and frequency of the desired signal, the modulation types for the two signals, and the direction of arrival for the desired and undesired signals. The bearing error is defined as the difference in the indicated bearing with and without the undesired signal present.

Two test configurations were used: one for the case where desired and undesired signals arrive from different directions, and another for the case where they arrive from the same direction. Figures 4a and 4b are the block

diagrams for the two configurations. The values of the parameters used for each measurement are given in Table 1a for the configuration of Figure 4a and in Table 1b for the configuration of Figure 4b. As shown in these Tables, a wide range in the desired signal level was used. The 40 $^{\mu V}/m$ at 200 kHz and 30 $^{\mu V}/m$ at 400 kHz are the minimum required signal levels as specified for receiver A by the manufacturer. The 100,000 $^{\mu V}/m$ desired signal level is the specified maximum operating level for receiver A. Two types of desired signal modulation were used: CW, continuous wave or no modulation; and MCW, modulated continuous wave which is an 80% AM modulation with a 1020 Hz tone. The MCW modulation simulates the presence of the identification code on the typical NDB. Two kinds of undesired signal modulation were used: CW or none and FSK, frequency shift keying with a rate of 75 baud and a frequency shift of 200 Hz.

The "antenna simulator" shown in Figures 4a and 4b is a device designed to provide signals to the loop and sense antenna ports of a receiver in a manner that simulates actual reception by the loop and sense antennas. Since proper account is taken of antenna and transmission line efficiencies, a 1 μV input signal simulates a field strength at the antennas of 1 $^{\mu V}/m$.

The standard performance tests were performed on both receiver A and receiver B before the measurements were begun to ensure that the receivers were operating as specified.

Figure 5 is an example of the data collected for each measurement; this particular one is for receiver B, measurement no. 2. Appendix A contains tables of the data for each measurement and graphs for those measurements where the desired and undesired signals arrive from different directions. The results are discussed in detail in Section 6.

Table 1a. The Values of the Parameters for each Measurement Associated with the Configuration of Figure 4a.

MEASUREMENT NUMBER	DESIRED SIGNAL FREQUENCY (kHz)	DESIRED SIGNAL LEVEL (μV/m)	DESIRED SIGNAL MODULATION TYPE	UNDESIRED SIGNAL MODULATION TYPE	UNDESIRED SIGNAL LEVEL (μV/m)	UNDESIRED SIGNAL FREQUENCY (kHz)
1	200	40	CW	CW	VARIED DURING MEASUREMENT	VARIED DURING MEASUREMENT
2	200	500	CW	CW		
3	200	500	MCW*	CW		
4	200	1,000	CW	CW		
5	200	1,000	CW	FSK		
6	400	30	CW	CW		
7	400	500	CW	CW		
8	400	500	CW	FSK		
9	400	1,000	CW	CW		
10	400	100,000	CW	CW		

* Modulated Continuous Wave, see text.

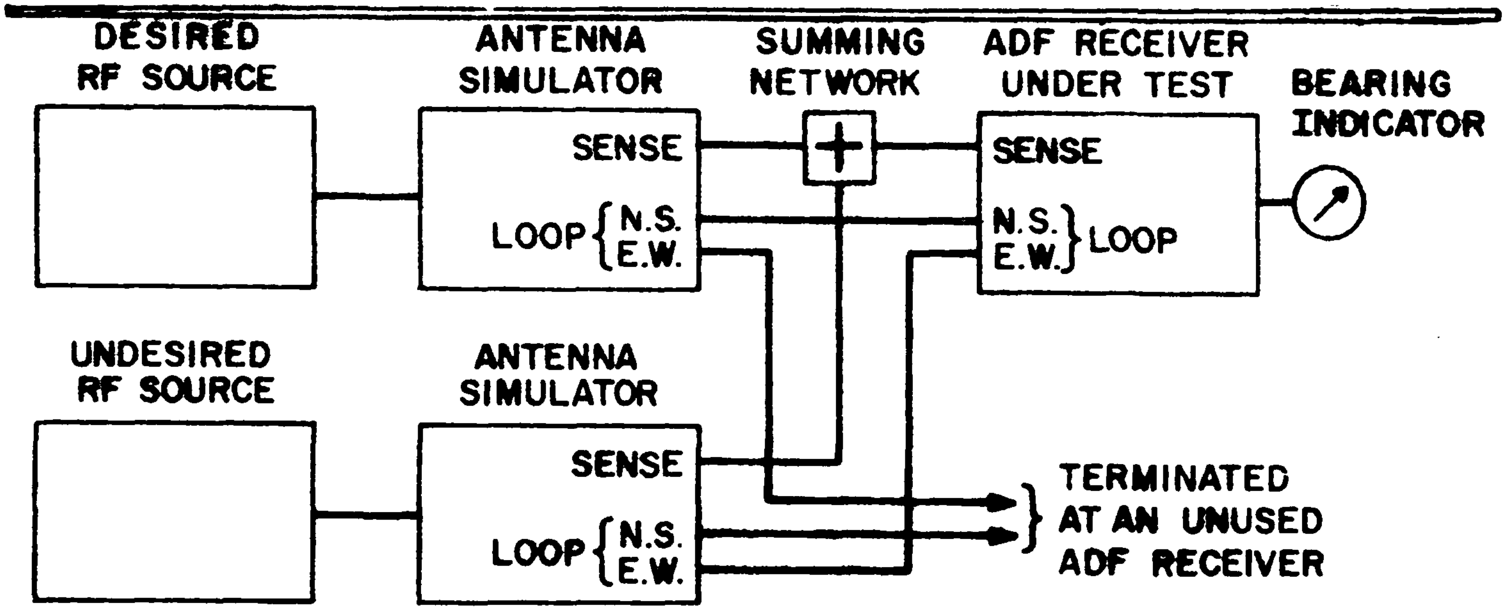

Figure 4a. Equipment configurations used to measure the ADF bearing error for the cases where the desired and undesired signals arrive from different directions.

Table 1b. The Values of the Parameters for each Measurement Associated with the Configuration of Figure 4b.

	DESIRED SIGNAL			UNDESIRED SIGNAL		
MEASUREMENT NUMBER	FREQUENCY (kHz)	LEVEL (μV/m)	MODULATION TYPE	MODULATION TYPE	LEVEL (μV/m)	FREQUENCY (kHz)
11	200	40	CW	CW	VARIED DURING MEASUREMENT	VARIED DURING MEASUREMENT
12	200	1,000	CW	CW		
13	200	500	CW	FSK		
14	400	30	CW	CW		
15	400	500	CW	CW		

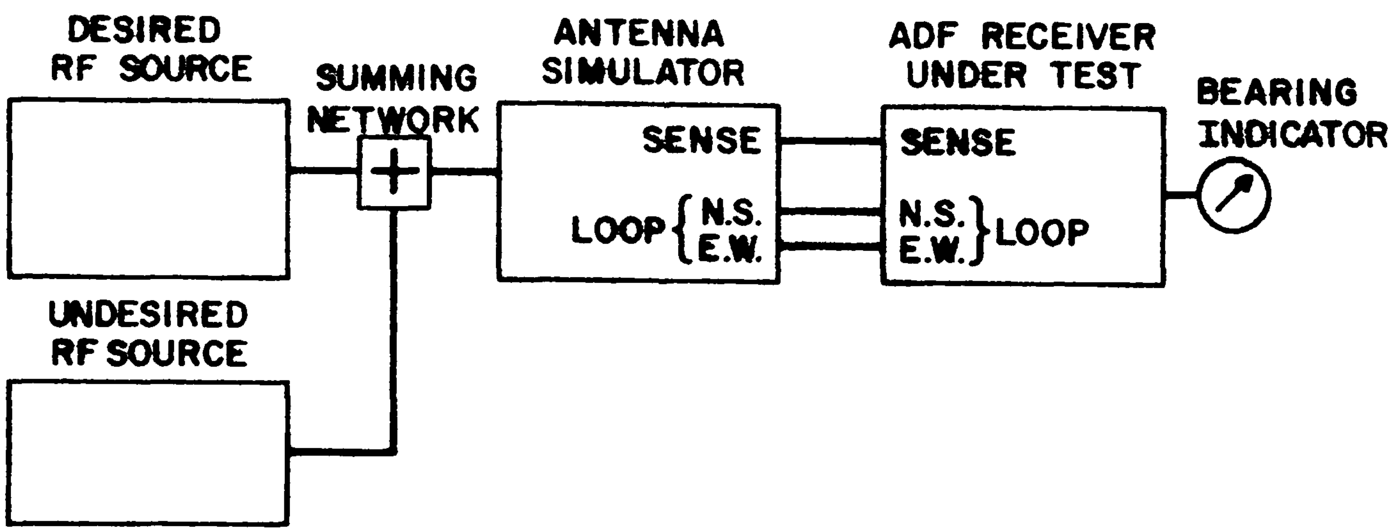

Figure 4b. Equipment configurations used to measure the ADF bearing error for the cases where the desired and undesired signals arrive from the same direction.

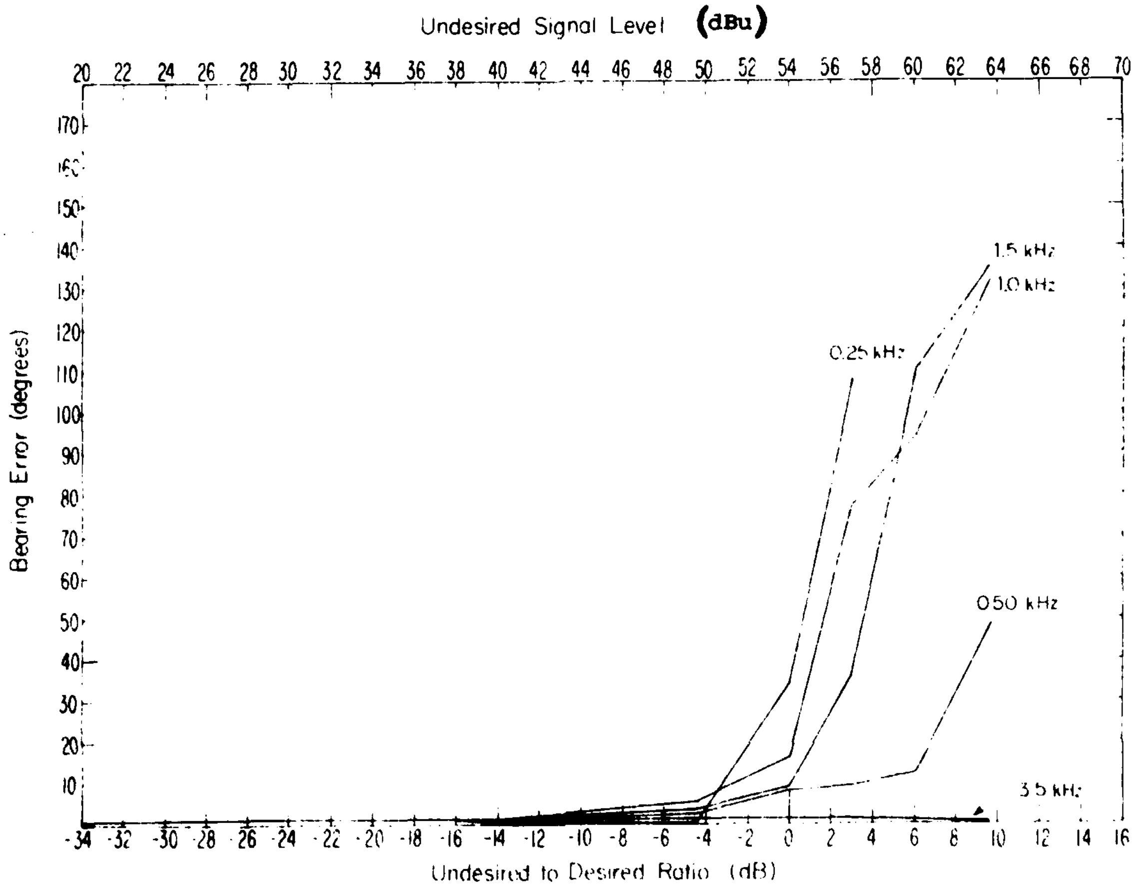

Figure 5. Measured bearing error for ADF receiver B as a function of the undesired signal level and the frequency separation (Δf) between the desired and undesired signals. The desired signal level is 500 $\mu V/m$ at 200 kHz with no modulation. The undesired signal is unmodulated, and arrives from a simulated bearing of 90°.

4. POWER LINE CARRIER RADIATION

The aspect of PLC systems that we are interested in for this work is not how poorly or how well PLC signals propagate along power lines, but how much of the PLC signal is present in the airspace above the power lines. The PLC signal, when propagating along the power line, can be viewed as a guided wave and as such has some field distribution surrounding the power line. This kind of a guided wave is predictable if the geometry of the power line and its environment (the earth's surface and the support towers) is simple; e.g.,

conductors at all times parallel to a planar earth. This kind of an analysis does not portray the real world very well, however. The point we wish to make is this: there is some field structure due to the guided wave nature of the propagation and there is some radiation due to the departures from ideal geometry. This radiation is very difficult to predict and may be the dominant source of signal in the airspace above the power line. Note that there can be some confusion as to the meaning of "PLC radiation." This term is often used to mean all of the fields that surround the power line regardless of geometry and distance. Strictly speaking, PLC radiation ought to describe only those fields that will propagate independently after being launched by the power line. These radiated fields, then, are not a part of the guided wave mode of propagation.

4.1 Propagation and Radiation Theories

In this subsection, we will examine the theories that have been set forth on PLC radiation (actually, PLC propagation). None of the theories account for the many anomalies in geometry, such as line sag and bends, but they are instructive as to the propagation mechanisms involved.

One of the most recent and detailed works on the subject is by Pullen (1975). The most interesting aspect of Pullen's derivation is an identification of the induction field and the radiation field. He states that "These two components are not separated precisely but regions in space are chosen such that one component dominates the other." In his development he defines the two regions as follows:

> "Region 1, close to the line at a large distance from the origin ($z \gg r$). This will correspond to the induction field. Region 2, at a large distance from the line. This will correspond to the radiation field."

For the first statement, z is the distance along the semi-infinite line and r is the transverse distance from the point on the earth's surface below the line to the observation point. So, we agree that Pullen's induction field solution is the total field.

Pullen's basic assumptions are not unlike what others (Jensen, 1972;

Gronlie, 1956) have done. First, it is assumed that the power line conductors are straight, semi-infinite, and parallel to a planar earth. Second, it is assumed that the carrier currents flowing in other phases are small compared to those flowing in the injected phases. Third and last, it is assumed that the earth is perfectly conducting. Based on these assumptions, Pullen's work is interesting to us because he has calculated the field strengths for a horizontally disposed three-phase line. Below, in Table 2, are his propagation mode definitions. Pullen's mode 3 is the same as the IEEE mode 1 (see section 2.2). Then, in Figures 6 and 7, we have reproduced Pullen's results for the three modes.

Table 2 PLC Mode Definitions Used by Pullen

MODE NUMBER	RELATIVE CURRENTS		
	PHASE A	PHASE B	PHASE C
1	1	1	1
2	1	0	-1
3	1	$-(2+\delta)$	1

Looking at Pullen's results, we can make one observation readily: the rate at which the fields decrease with distance, say, beyond 100 m. Pullen's mode 1 has the slowest decrease with a $^1/r^2$ dependence, his mode 2 is next with a $^1/r^3$ dependence, and his mode 3 shows the most rapid decrease with a $^1/r^4$ dependence. We would expect this result since Pullens' mode 3 is the mode that propagates along the power lines with the least attenuation. Recalling the discussion of section 2.2, we know that no matter what carrier coupling method is used, beyond a sufficient distance the dominant mode of propagation is mode 3 (the IEEE mode 1). One other point should be noted here. In Table 2, mode 3 has the factor δ associated with the center conductor current. Pullen states that if δ is non-zero an induction field component with a $^1/r^2$ dependence will result.

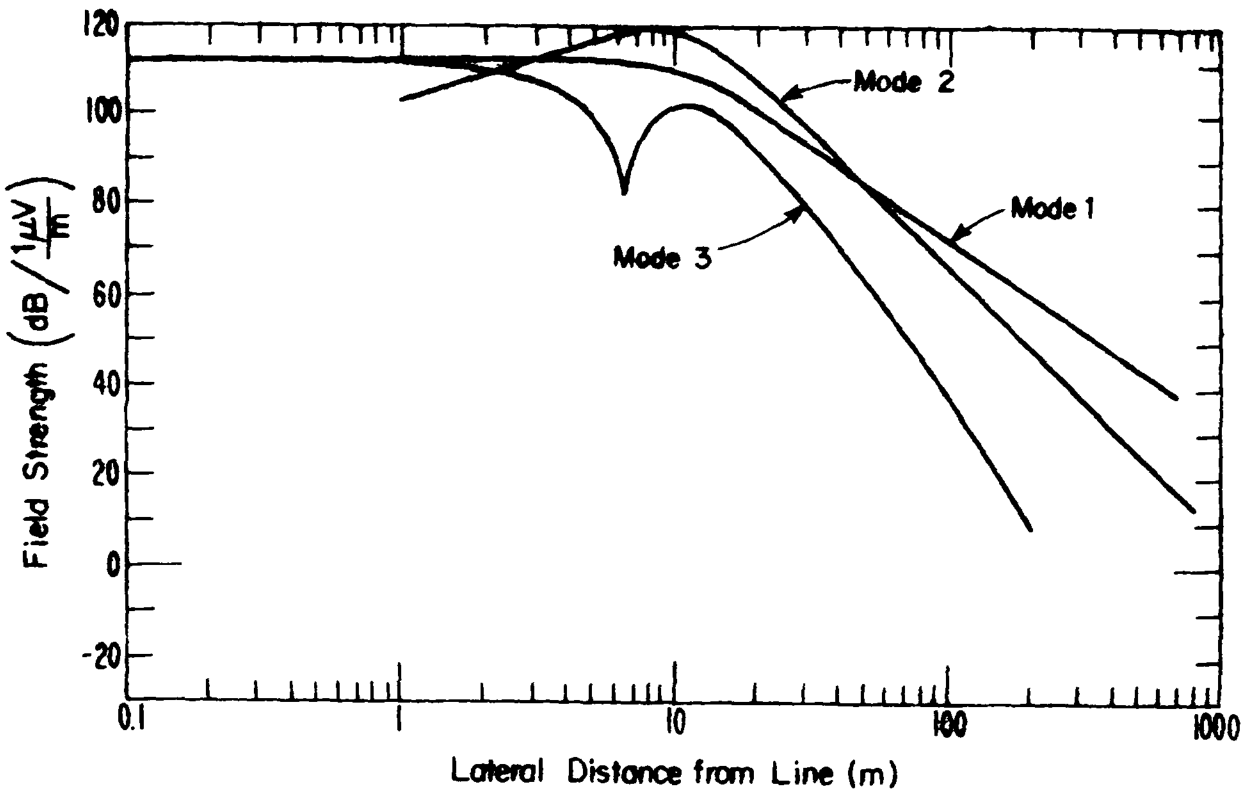

Figure 6. The induction field strength at ground level for a horizontally disposed three-phase line at a height of 20 m. After Pullen (1975).

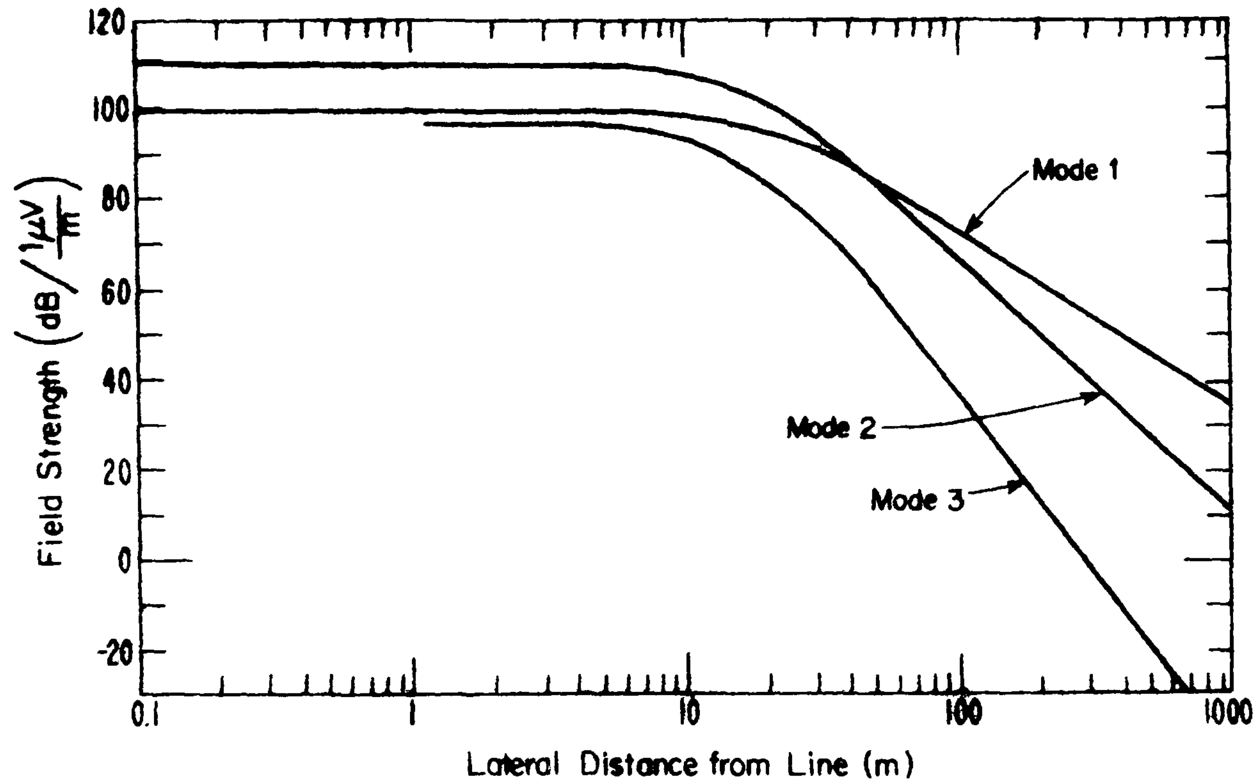

Figure 7. The induction field strength at a height of 20 m for a horizontally disposed three-phase line at a height of 20 m. After Pullen (1975).

4.2 Previous Measurements

Some PLC radiation measurements that have been made by others will be briefly described here. The earliest measurements we found were those by Gronlie (1956). Somewhat later, Jones (1965) made measurements of PLC field strength over a 19 mi (30.6 km) length of line in Ontario, Canada. In his paper he presents measured field strengths along both longitudinal and transverse paths for 283 kHz. He also measured the "end-fire" effect behind the transmitter and the effects of a fault placed several miles from the transmitter end of the line. Jones concludes his paper with a deduction of a zone of influence about a power line carrying PLC signals. His zone is defined as that region where the PLC signals could be strong enough to interfere with aeronautical navigation. He also suggests that the power utilities and aeronautical radio services coordinate their frequency use so that the zone of influence for a PLC link and the service area of a radio beacon do not overlap for any particular channel or frequency.

Some interesting, but limited, measurements are presented by Jensen (1972). The interesting aspect of his paper is that he makes some comparisons of predictions from theory and measured data. His comparisons essentially confirm the predicted lateral dependence for various line geometries and coupling methods.

The most extensive and recent measurements were made by the Telecommunications Laboratory of Electricité de France (1978). We obtained a translation of a portion of that report from the FAA. In Appendix V of the report is a large amount of PLC radiation data for a wide variety of conditions. The conditions include the line configuration, carrier frequency, ground conductivity, carrier coupling method, etc. Radiation from transformers and the effects of parallel or crossing lines and of towers are also examined.

4.3 Measurements Over TVA Power Lines

With the assistance of the Tennessee Valley Authority (TVA) and FAA's National Aviation Facilities Experimental Center (NAFEC), we took measurements of the PLC field strength over two of TVA's power lines. In this section we will describe the measurement technique, the choice of power lines, coupling methods, the PLC test signals that were injected into the lines, and the resulting measured field strengths.

While we were making airborne measurements of the field strength of the PLC test signals, the TVA conducted a few measurements of their own. Those measurements were of the field strength at the ground level. The TVA measurements are described in Appendix C of this report. The aircraft used was an FAA flight inspection aircraft (see Figure 8) equipped with a variety of avionics and a general-purpose spectrum analyzer/data recording system. One great advantage of this particular system is that it is interfaced with the aircraft inertial navigation system (INS). This means that data such as the location (latitude and longitude), heading, and ground speed could be recorded at essentially the same time as the signal level data were being recorded.

The aircraft is equipped with dual ADF radio compass systems with an independent set of antennas. This provided the opportunity to use one of the ADF sense antennas to make the desired measurements. This equipment and a few additional items form the measurement system that we used. This system is shown in block diagram form in Figure 9. Then, in Figure 10, a photograph of the belly of the airplane, the two ADF sense antennas can be seen. This type of antenna is sometimes called a "tee" antenna. It is essentially a top-loaded vertical stub; that is, the horizontal wire is the electrical top-loading.

For our purposes, it would be most informative to measure the actual field strength of the PLC signal. To do so, however, we must calibrate the aircraft and receiving system as a unit. This is because the only thing we can really measure is the signal level present at the antenna terminals (a voltage or power). So, the calibration we seek is a relationship between the field strength (in volts/meter) external to the aircraft and the received signal level as observed with the spectrum analyzer (in watts). This, in itself is no trivial exercise. A brief description is given below and more detail on this procedure may be found in Appendix B of this report.

In order to perform the aircraft calibration, a known electric field is needed through which the aircraft can be flown. This, in effect, is the crux of the calibration procedure. The known field was obtained by identifying several suitable NDB's, then measuring the ground level field strengths with a calibrated field strength meter, and lastly, predicting the field strength at some fixed altitude in the airspace above the beacons. An ideal beacon for

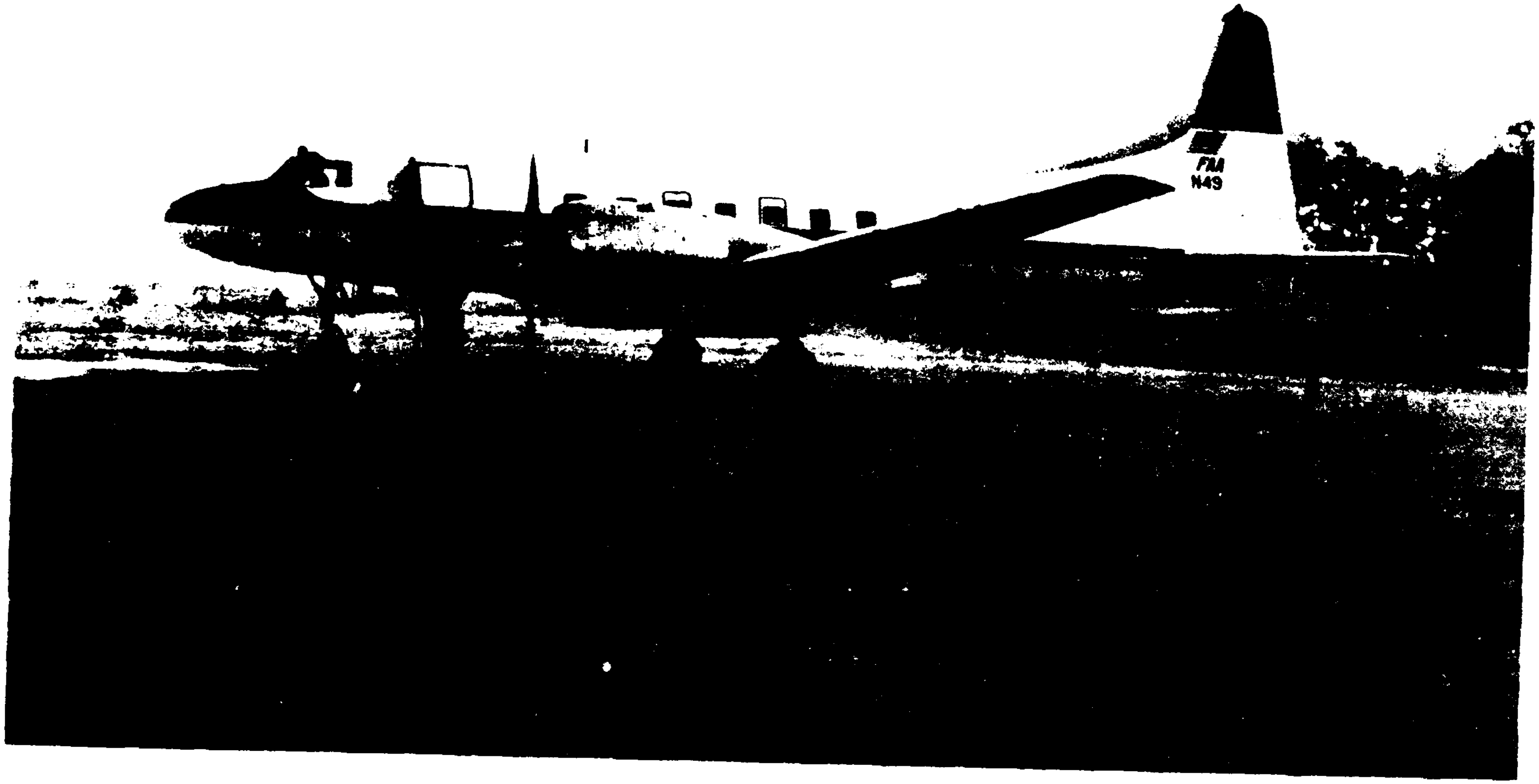

Figure 8. The FAA flight inspection aircraft used to make the PLC field strength measurements.

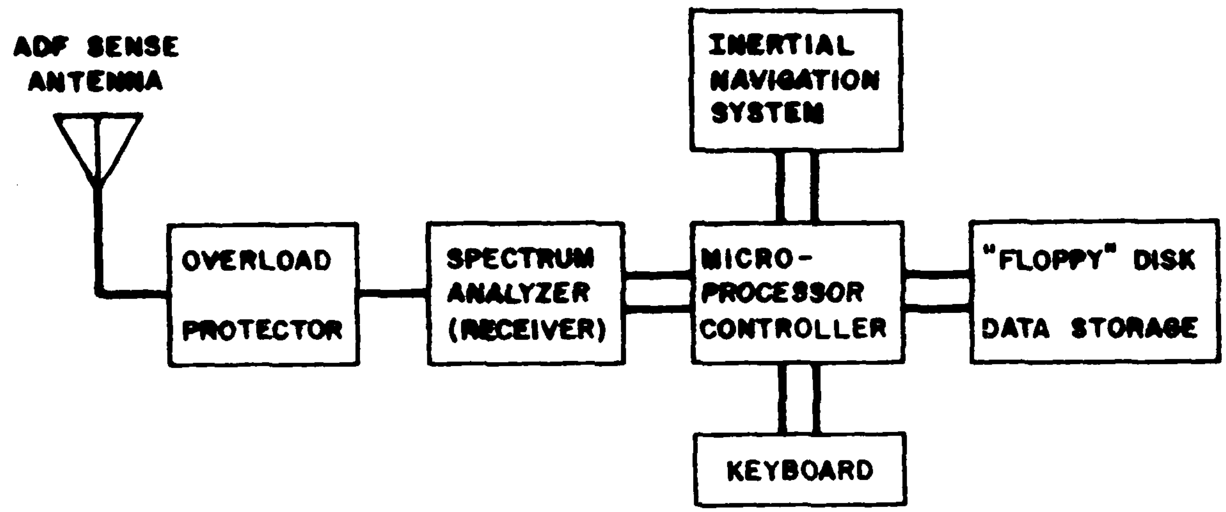

Figure 9. Block diagram of the spectrum analyzer/data recording system used to make the PLC field strength measurements.

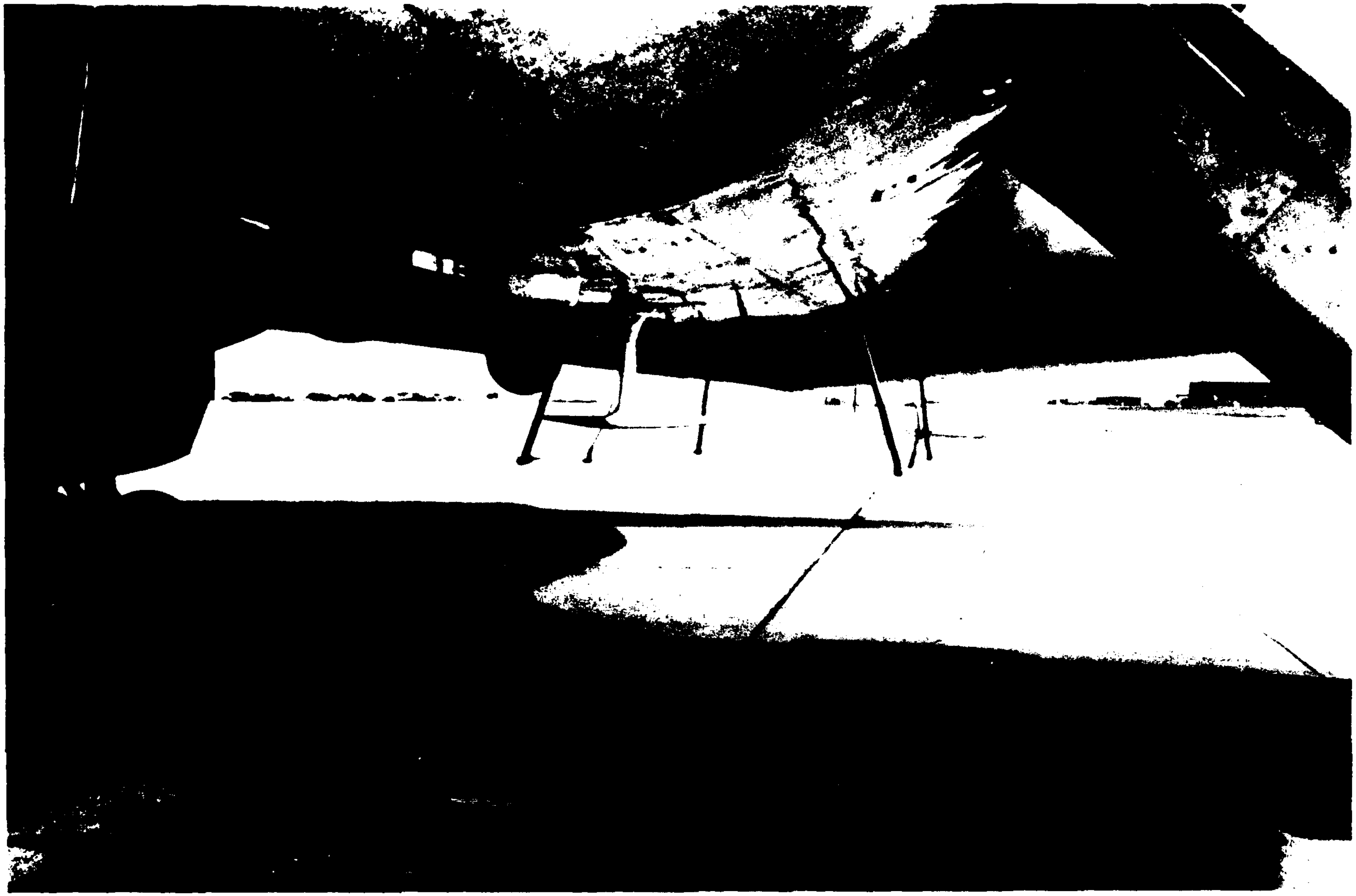

Figure 10. The belly of the FAA aircraft showing the two ADF sense antennas. The sense antenna on the left side of the photograph is partly obscured by a VHF omni-range (VOR) antenna.

this procedure is one that has a circularly symmetric (vertical) antenna, no nearby obstructions, and is located on flat, homogeneous earth. Of course, ideal beacons are impossible to find, but one with excellent conditions and two with reasonable conditions were found in the Texas panhandle and Oklahoma, respectively.

The two power lines that were chosen for the PLC radiation measurements have different characteristics and features. Both lines are horizontally disposed three-phase transmission lines with shield wires above the phase conductors. The relevant characteristics of these lines are listed in Table 3, below.

Table 3 Characteristics of the TVA Power Lines Used for the PLC Measurements

LINE	GREAT FALLS - SPRING CITY	JOHNSONVILLE - CUMBERLAND
Voltage	161 kV	500 kV
Terrain	Relatively Rugged	Relatively Level
Tower Type	Wood Pole	Steel Structure
Span Length	Variable	Relatively Constant
Line Length	About 72 km	About 48 km
Location	80 km N of Chattanooga	100 km W of Nashville
PLC Coupling	Center Phase-to-Ground	Phase-to-Phase

For each line, several test configurations are specified and for each configuration a set of flight paths over which measurements are taken are also specified. The test configurations are shown schematically in Figure 11. Then in Figure 12, we show a generalized set of flight paths, some combination of which are used for each configuration. Each particular flight path or set of flight paths are flown at a constant altitude. Table 4 gives the set of flight paths and measurements for each line and test configuration, and a key to which figure contains the data. Note that the measured signals have been normalized to 1 W of injected PLC power.

The results are presented in two ways. The grid data are handled statistically and the transverse or longitudinal path data are plotted on a graph showing the field strength versus the percent of the path. This means that all of the data taken along a particular path are plotted sequentially. It was planned that the INS location data would be used to determine the distance along the line for the longitudinal paths or the lateral distance

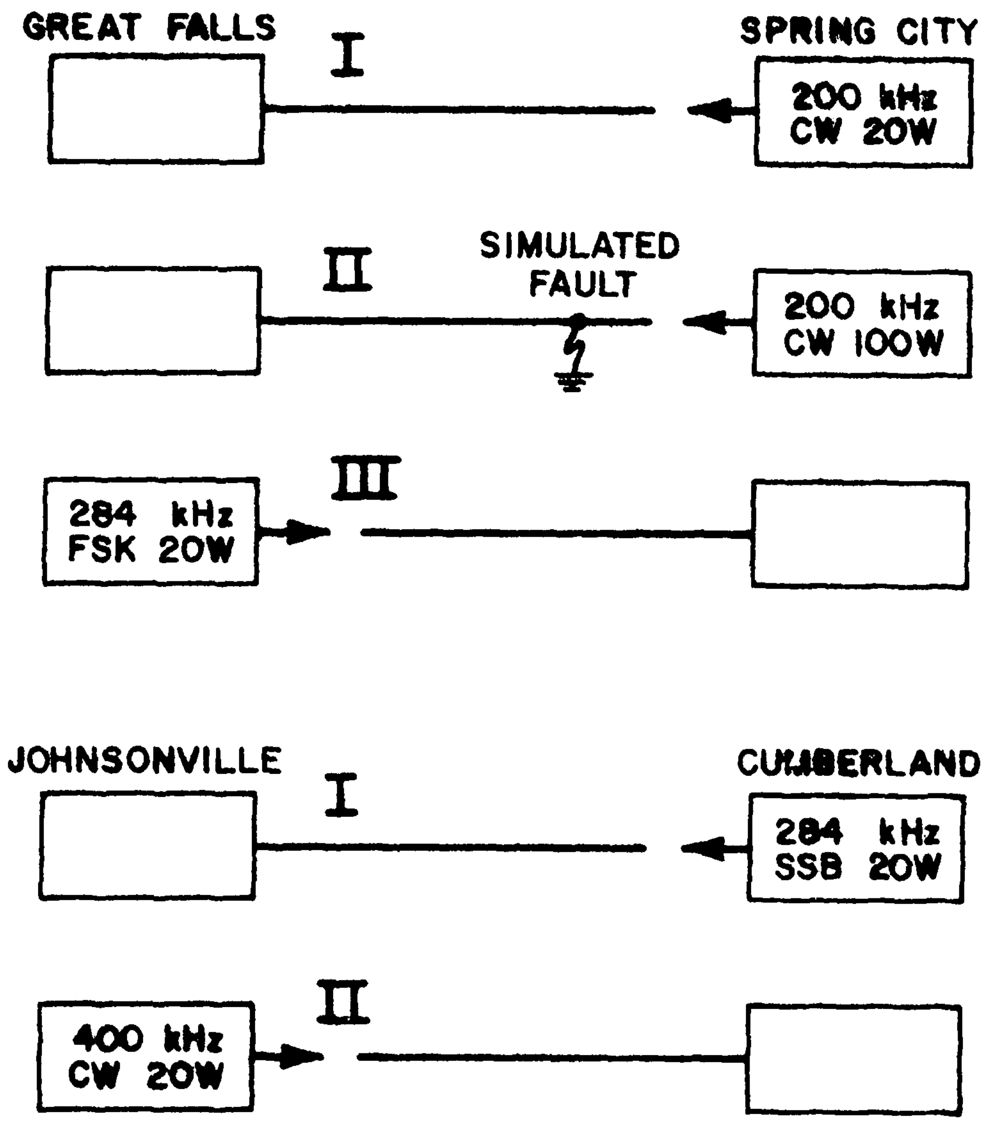

Figure 11. The test configurations for the two TVA power lines.

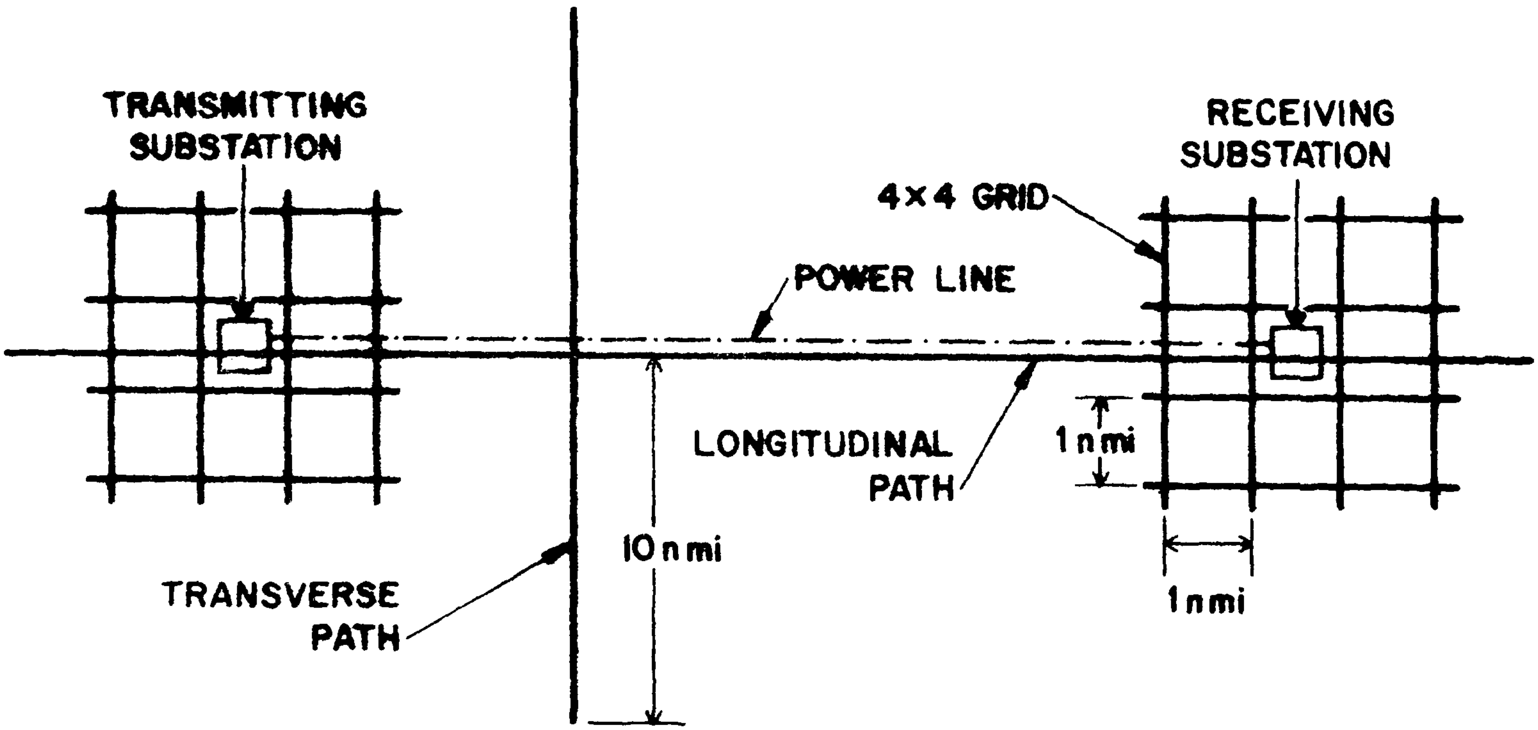

Figure 12. A generalized set of flight paths over which PLC field strength measurements are made. See Table 4 to determine the particular set of flight paths used for each configuration.

Table 4. Flight Paths over which PLC Field Strength Measurements were Made for each Power Line and Test Configuration (see Figure 12).

LINE	CONFIGURATION (SEE FIG. 11)	TYPE OF FLIGHT PATH	ALTITUDE (ft/MSL)	RECEIVER BANDWIDTH (Hz)	FIGURE OR TABLE
GREAT FALLS SPRING CITY	I	LONGITUDINAL	3600	30	FIGURE 13
		TRANSVERSE	3600	30	FIGURE 14
		GRID AT GREAT FALLS	3600	30	TABLE 5
		GRID AT SPRING CITY	3600	30	TABLE 5
	II	LONGITUDINAL	3600	30	FIGURE 15
		LONGITUDINAL (DISPLACED)	3600	30	FIGURE 16
		GRID OVER FAULT	3200	30	TABLE 5
	III	GRID AT GREAT FALLS	3600	1000	TABLE 5
JOHNSONVILLE CUMBERLAND	I	LONGITUDINAL	2100	3000	FIGURE 17
		GRID AT CUMBERLAND	2100	3000	TABLE 5
	II	LONGITUDINAL	3500	?	FIGURE 18
		TRANSVERSE	2750	?	FIGURE 19
		TRANSVERSE	2750	?	FIGURE 20
		GRID AT JOHNSONVILLE	2100	30	TABLE 5
		GRID AT CUMBERLAND	2100	?	TABLE 5

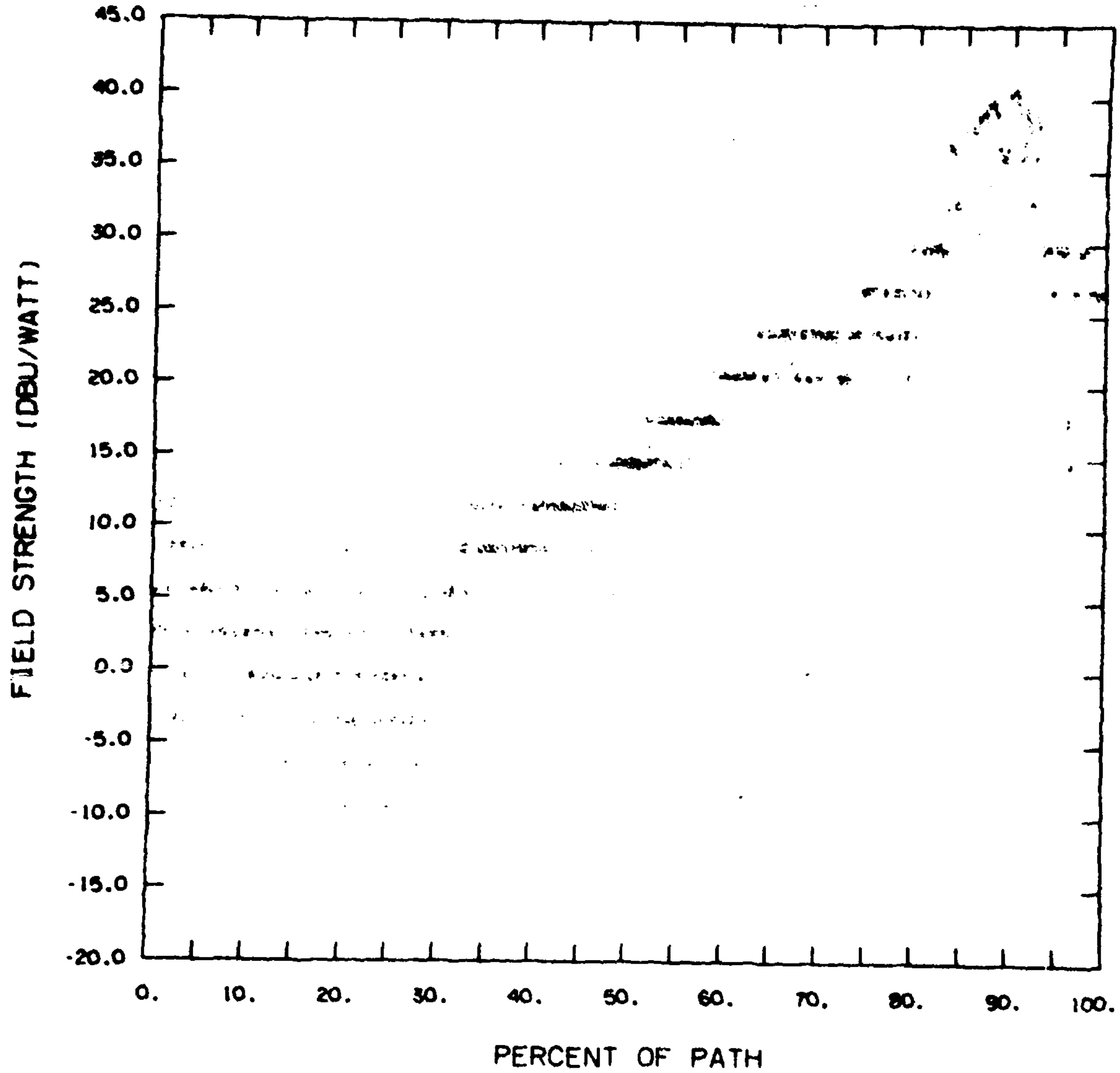

Figure 13. The field strength on a longitudinal path at about 400 m (~1312 ft) above the highest point along the Great Falls - Spring City line for configuration I.

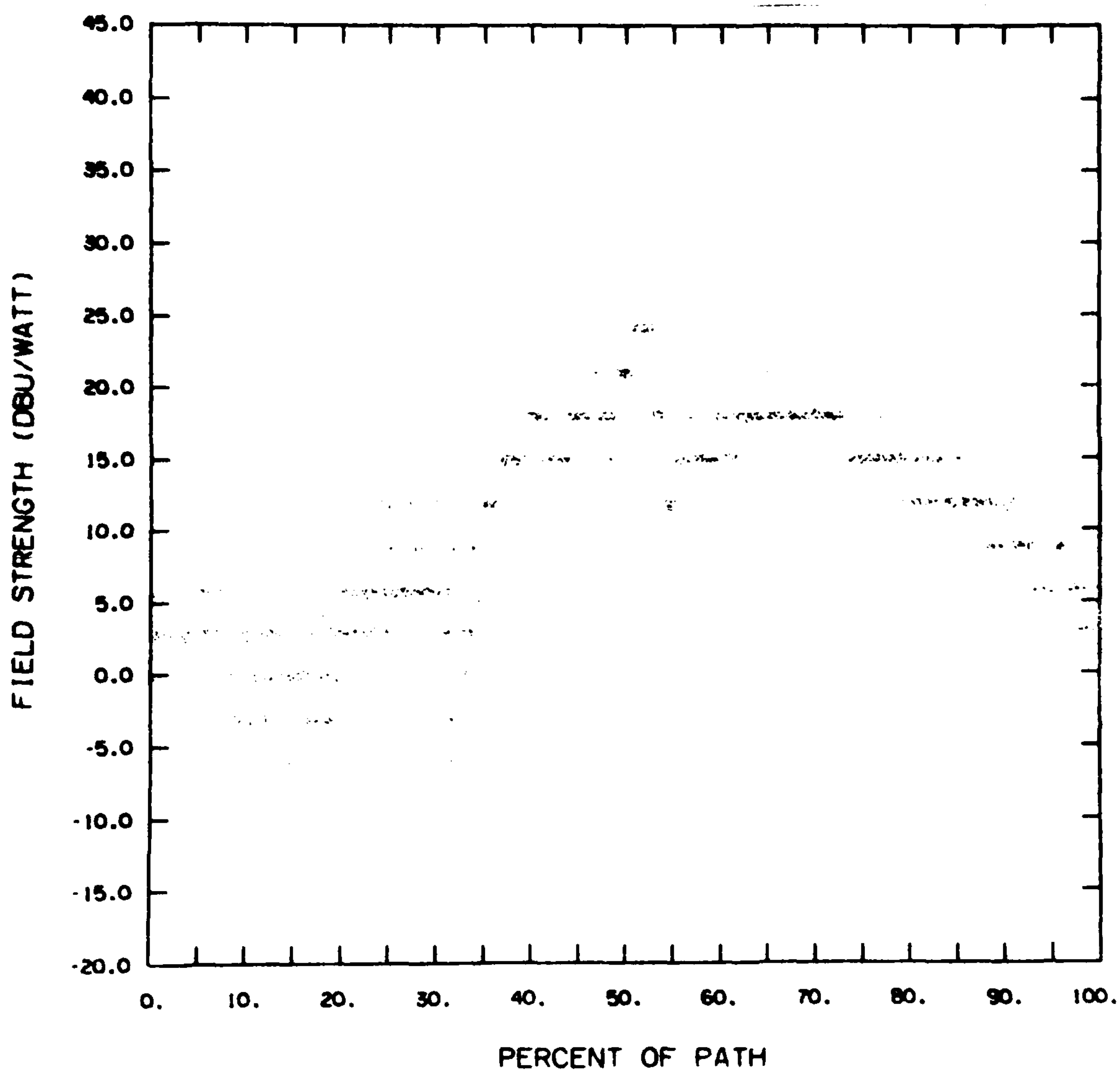

Figure 14. The field strength on a transverse path at about 21 km from Spring City at about 810 m (~2658 ft) above the Great Falls-Spring City line for configuration I.

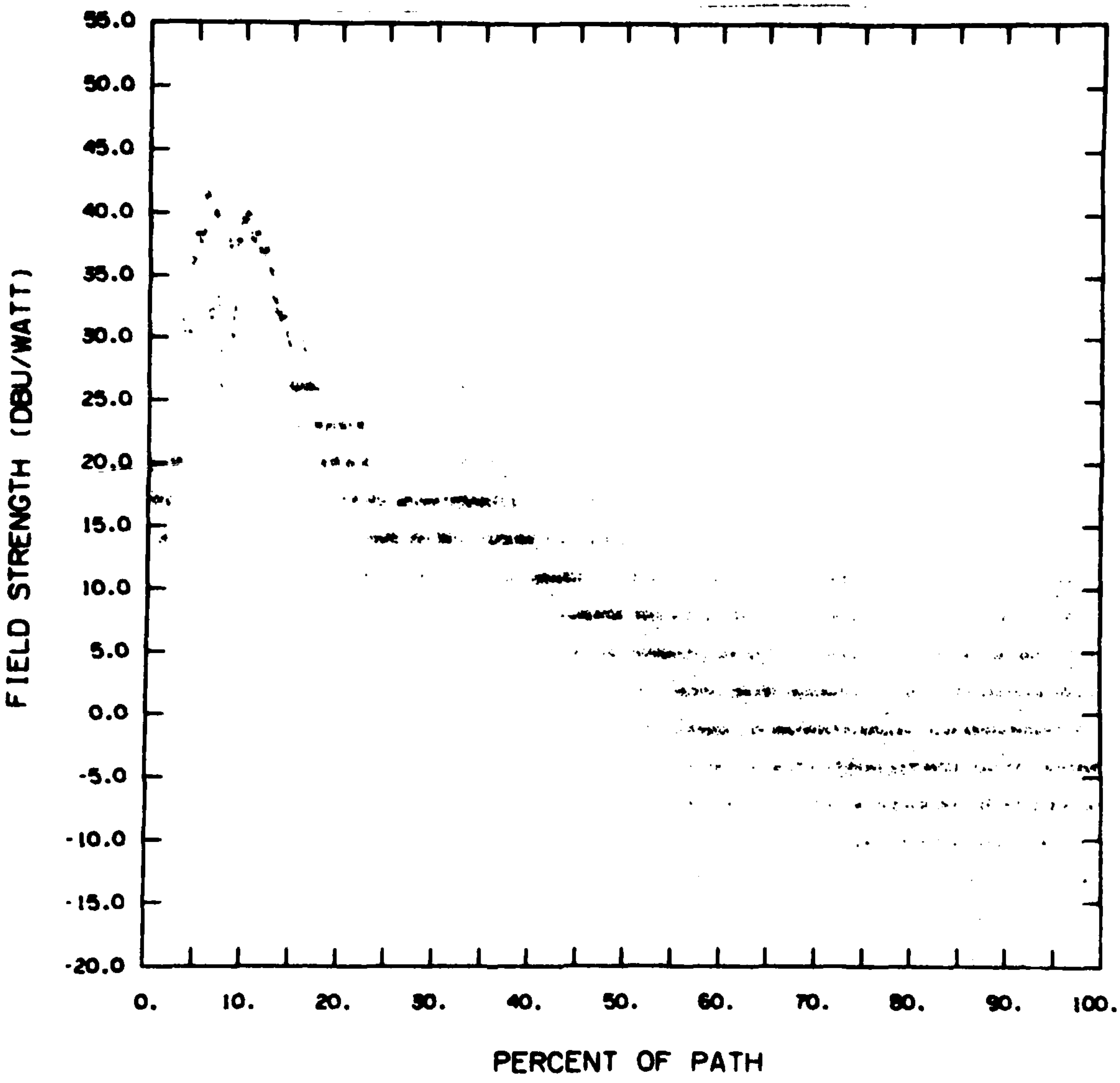

Figure 15. The field strength on a longitudinal path at about 400 m (~1312 ft) above the highest point along the Great Falls - Spring City line for configuration II.

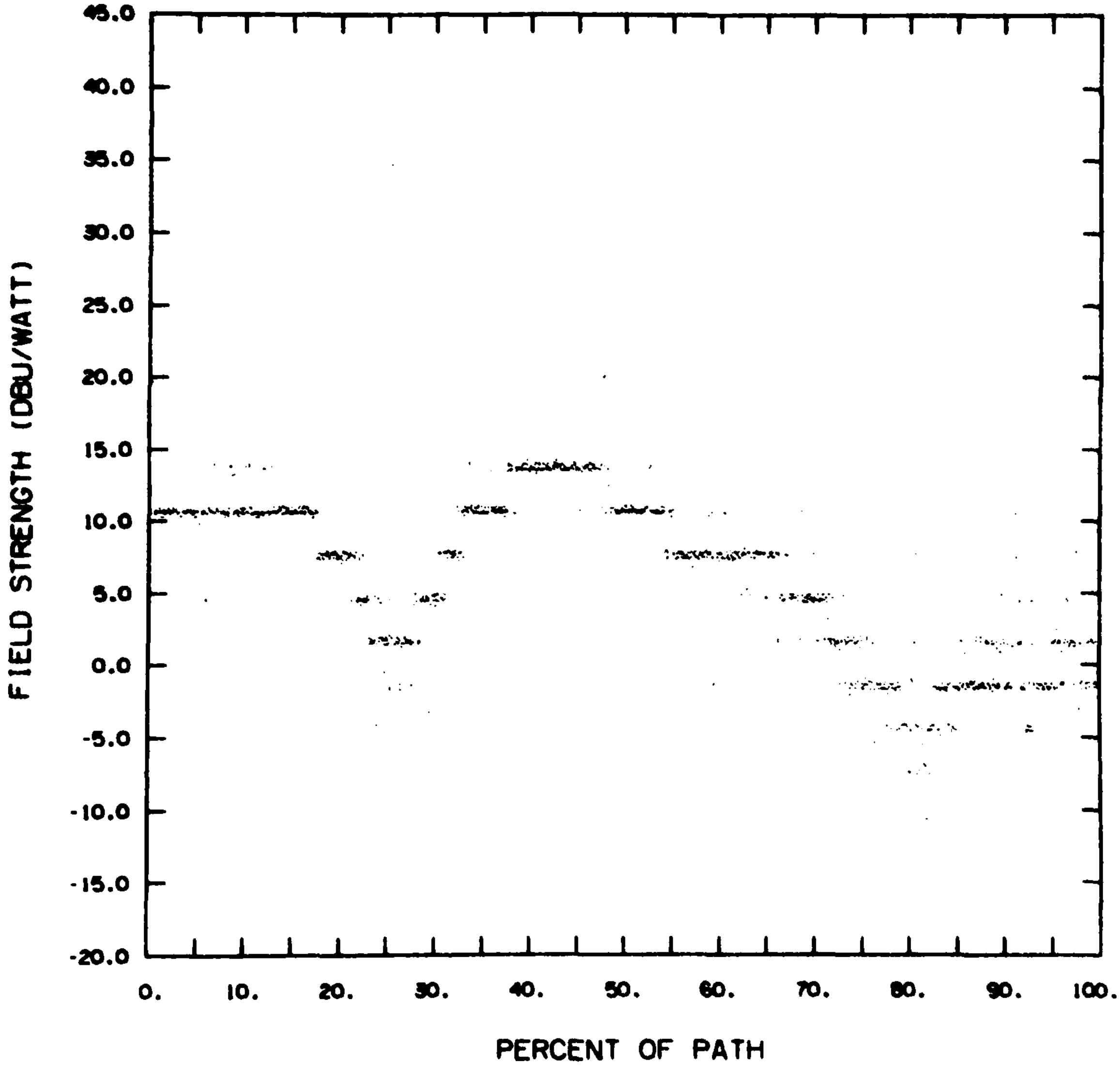

Figure 16. The field strength on a displaced longitudinal path at about 400 m (~1312 ft) above the highest point along the Great Falls - Spring City line for configuration II. The displacement is 1.85 km (1.0 n mi) north of the line.

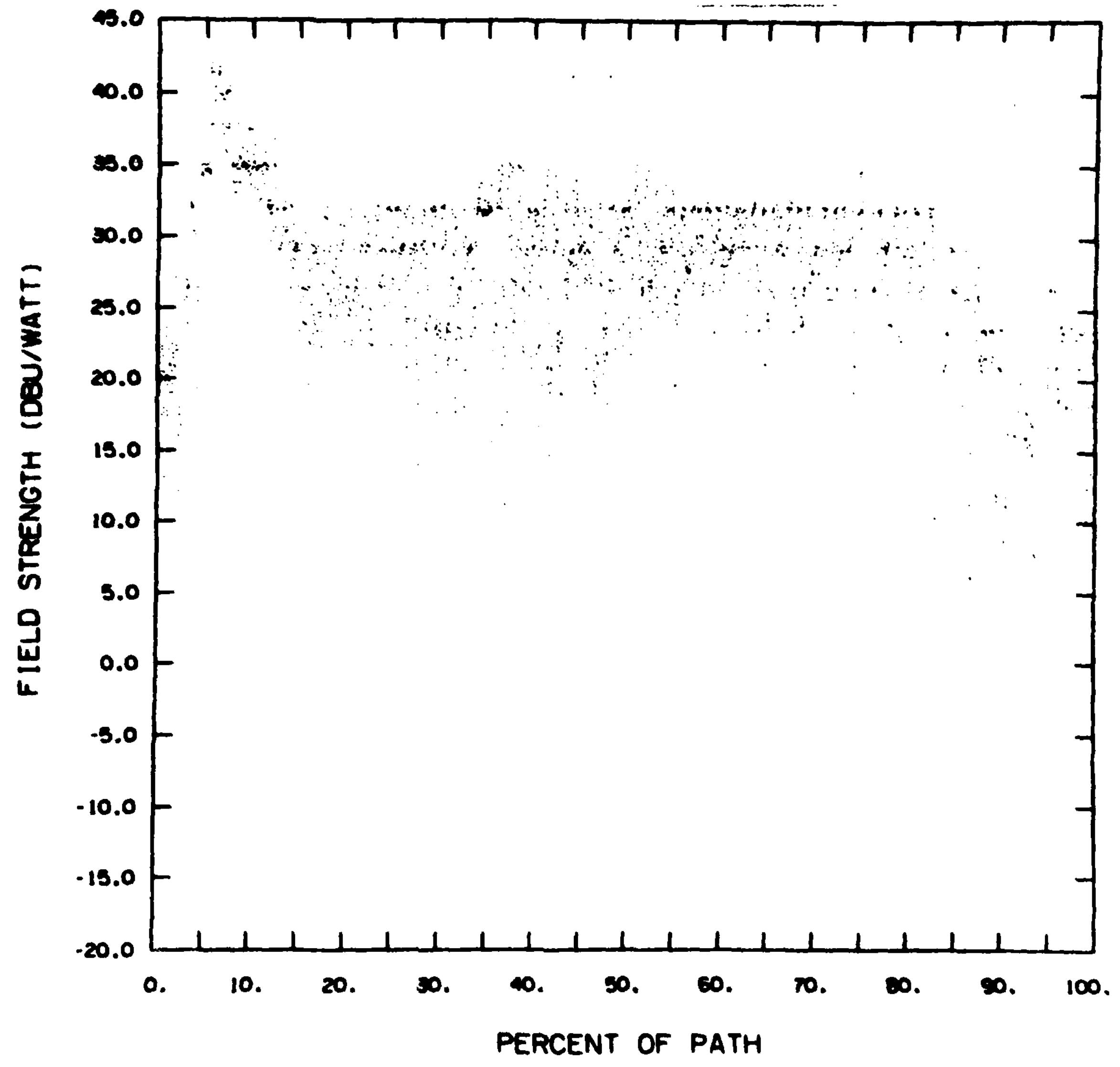

Figure 17. The field strength on a longitudinal path at about 390 m (~1280 ft) above the highest point along the Johnsonville - Cumberland line for configuration I.

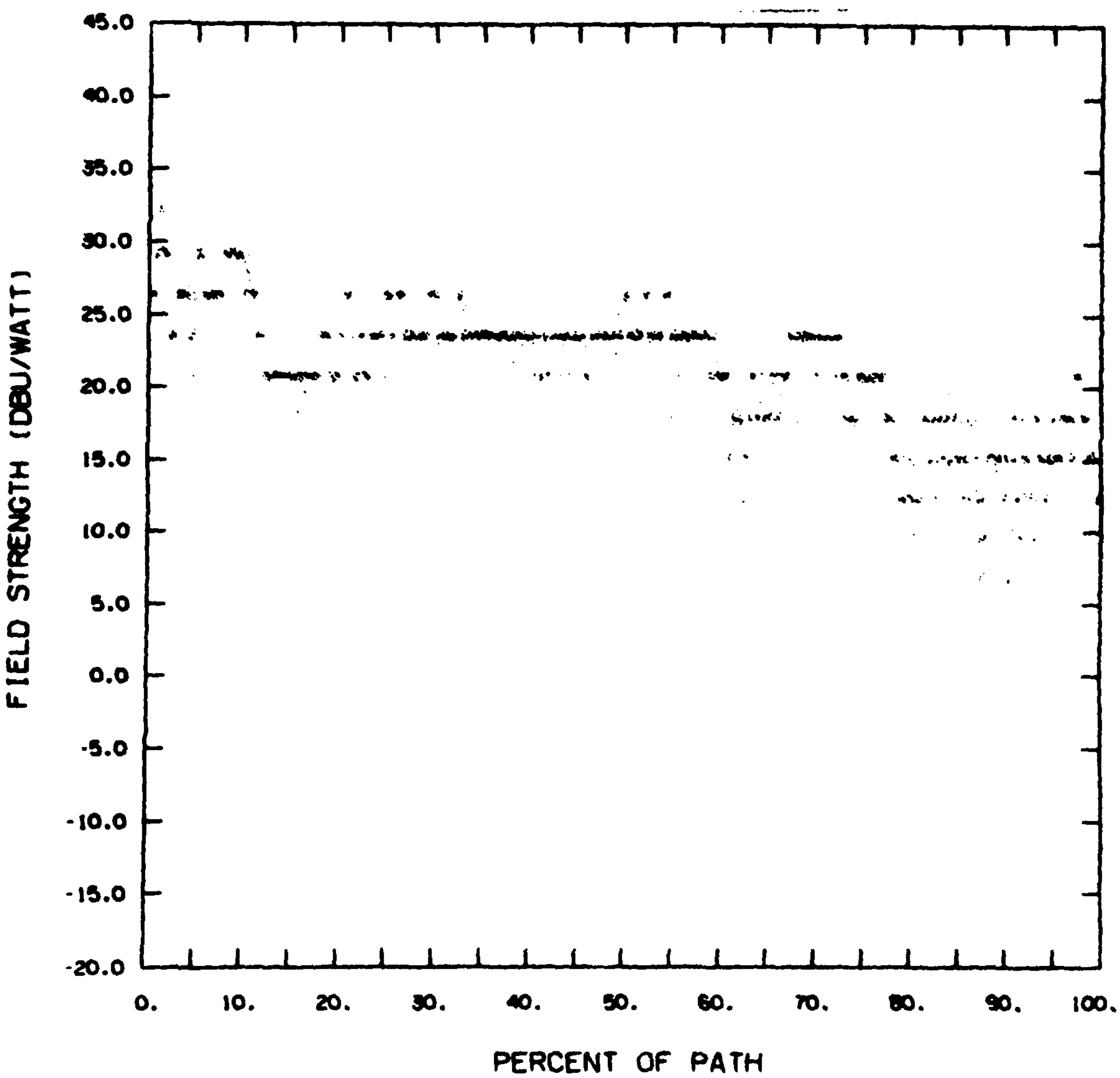

Figure 18. The field strength on a longitudinal path at about 820 m (2690 ft) above the highest point along the Johnsonville - Cumberland line for configuration II.

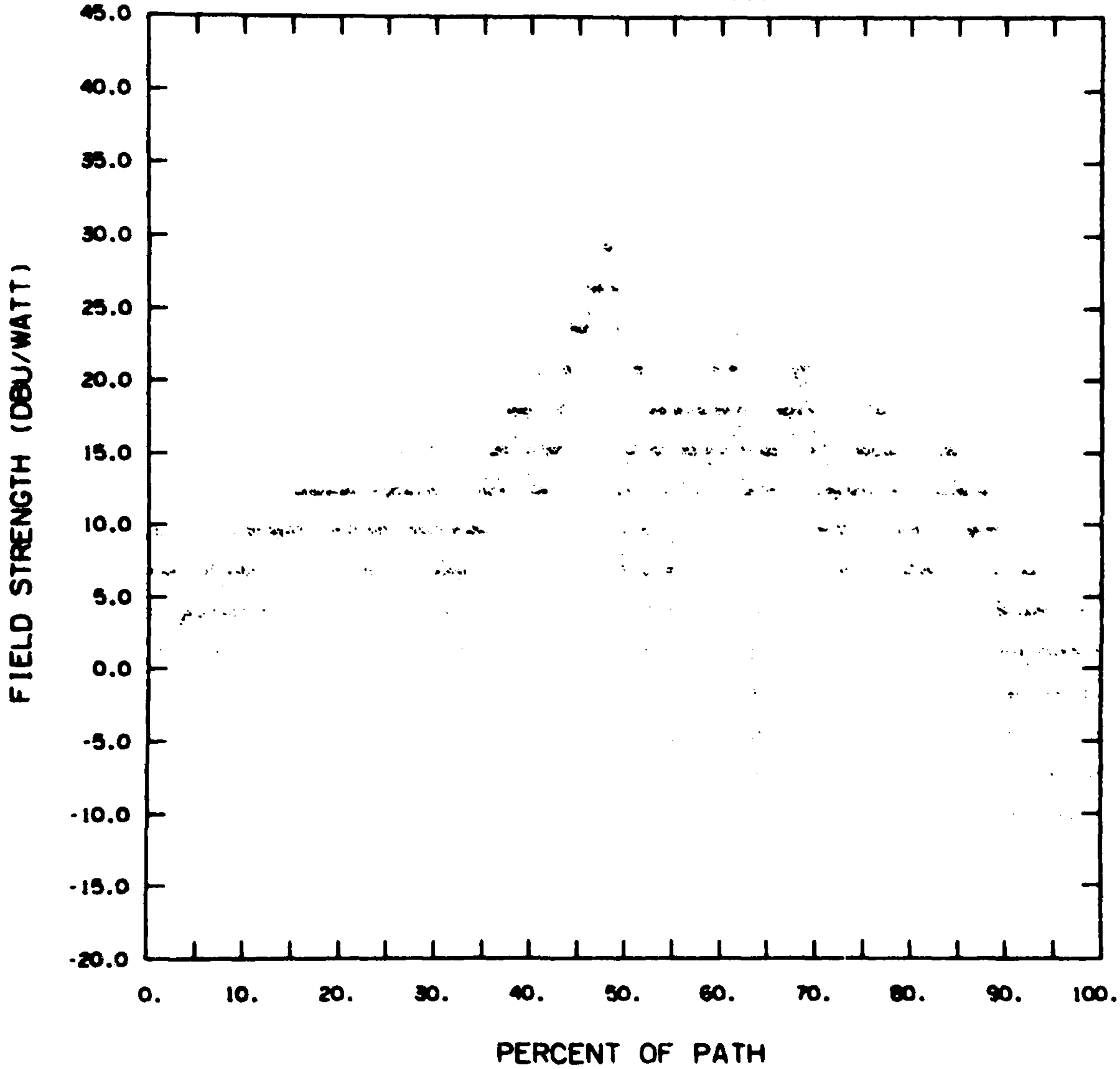

Figure 19. The field strength on a transverse path at about 15 km from Johnsonville at about 590 m (~1936 ft) above the Johnsonville-Cumberland line for configuration II.

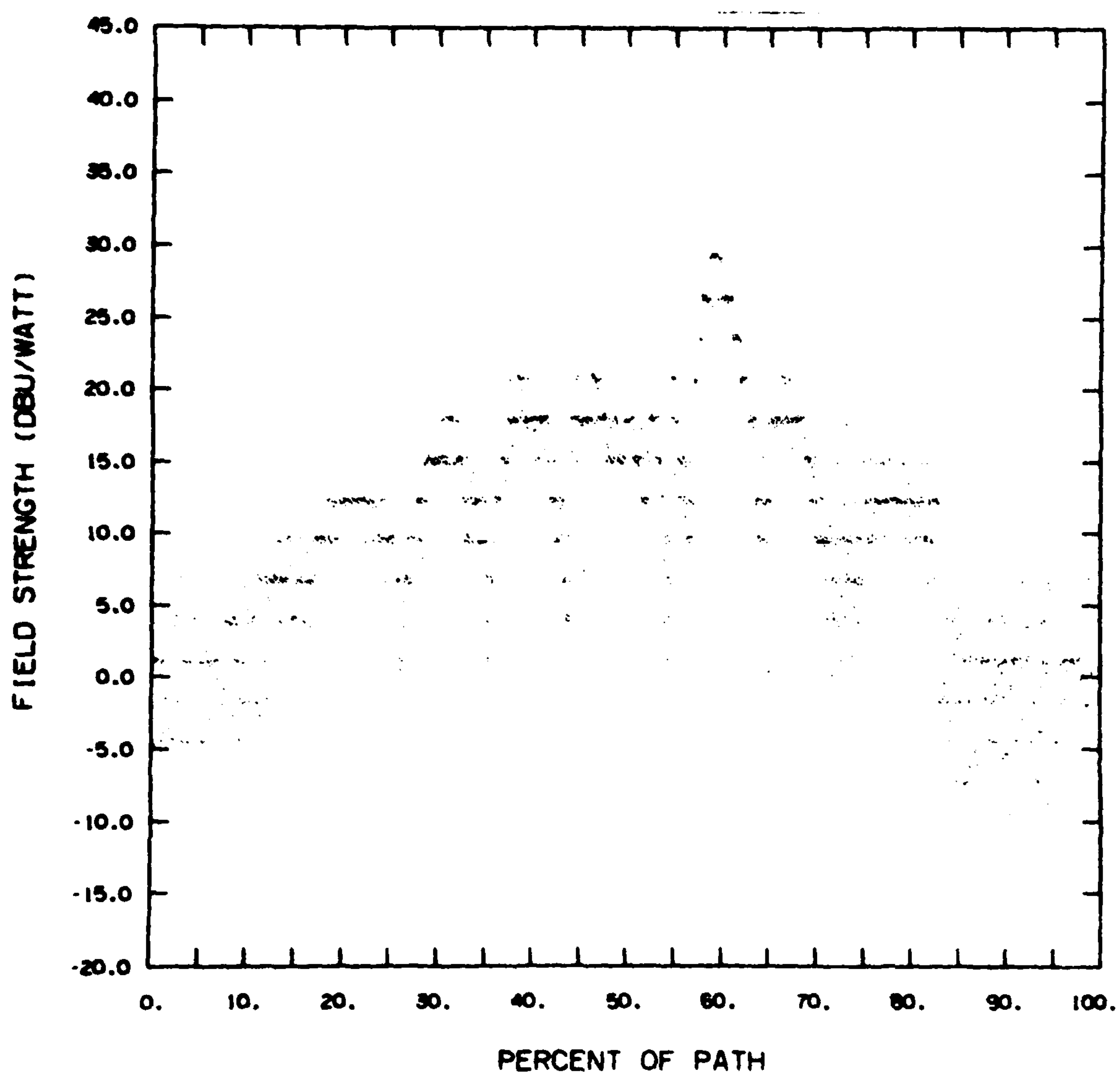

Figure 20. The field strength on the same transverse path as Figure 19, except flown in the opposite direction.

Table 5 Statistics of the Measured PLC Radiation Field Strengths, Normalized to 1 W of Injected Power for the Grid Flight Paths

LINE	CONFIGURATION	GRID LOCATION	STATISTICS OF FIELD STRENGTH MEAN dBu/W	STANDARD DEVIATION dB	10 PERCENTILE dBu/W	MEDIAN dBu/W	90 PERCENTILE dBu/W	NUMBER OF SAMPLES
GREAT FALLS-SPRING CITY	I	SPRING CITY	23.75	4.201	19.03	24.46	25.40	441
		GREAT FALLS	15.64	7.537	6.85	15.84	25.21	2,122
	II	OVER FAULT	18.81	4.301	13.81	19.80	23.08	2,091
	III	GREAT FALLS	18.67	4.213	13.04	19.12	22.96	132
JOHNSONVILLE-CUMBERLAND	I	CUMBERLAND	23.45	6.741	14.75	23.45	32.23	1,575
	II	JOHNSONVILLE	18.48	6.442	9.96	17.88	26.67	1,737
		CUMBERLAND	10.73	9.200	-1.70	10.66	23.36	1,072

from the line for the transverse paths. However, due to software or interface problems the INS location information was not recorded properly during the PLC radiation measurements. The flight paths are, however, fairly well-defined. The longitudinal path data begin about 3 n mi (~5.6 km) before one substation and continue to about the same distance beyond the other substation.

At the same time the airborne measurements were being made, the TVA made some ground-level field strength measurements of the PLC test signals on the power lines. These measurements are described and presented in Appendix C.

4.4 Beacon Signal Reradiation

In order to test the hypothesis that a power line may reradiate a beacon signal or, at least, disrupt the wave structure, we made some measurements on an NDB located very close (~1 km) to a 500 kV power line. This particular NDB is located at the Sparta-White County airport in north central Tennessee and operates on 233 kHz. Signal level data were taken on a 10 n mi (~18.5 km) radius orbit of the NDB. A holographic technique (Wieder, 1979) was then applied to the data to locate the scatterers. The technique draws on holographic principles. In holography (and related technologies such as synthetic aperture imaging) a bias signal is superimposed upon the signal scattered from the object under study in order to record phase and amplitude information in the scattered signal on a photographic screen. An image of the scatterer can then later be derived by illuminating the screen with a replicated bias wave. Since the direct wave in a communications system can be taken as equivalent to the bias wave, and spatial variations in the measured signal as the interference between the direct (bias) wave and signals from scatterers, it should be possible to "image" the scatterers through a holographic type analysis of the measurements.

The results of the application of the technique to the Sparta-White beacon indicate that the power line is an insignificant scatterer. The terrain is the dominant scatterer and the effects of several hills and ridges were clearly seen, and there were no strong scatterers in the immediate vicinity of the beacon. Although this does not conclusively prove that a power line cannot act as a scatterer, it provides some significant support for the concept that the terrain, in general, has the most significant effect on the NDB wave structure.

5. OBSERVATIONS AND CONCLUSIONS

In this section we make some observations based on the various measurements that were made. Using some of these observations we then go on to describe the conditions under which the PLC systems may interfere with the ADF radio compass systems. In addition to the observations and conclusions concerning the compatibility of the PLC and ADF systems, we wish to comment on the good and bad points of the measurement procedures that were used to collect the data presented in this report.

One important consideration must be emphasized: this work cannot be used as a comprehensive study. The observations and conclusions presented below are based on the data we collected and these data do not cover all the possible environmental and geometric conditions, and equipment types that are in use. For example, we used only two of the many available ADF receivers and only single-circuit, three-phase, horizontally disposed power lines.

5.1 Radio Compass Receiver Susceptibility

- The bearing error is independent of frequency in the 200 to 400 kHz range for both receivers.

- The bearing error observed on the B receiver was more dependent upon the absolute undesired (U) signal level than on the undesired-to-desired (U/D) ratio. Significant bearing errors were observed at 44 to 54 dBu and above for the U signal level. The desired (D) signal level ranged from 30 to 60 dBu.

- The bearing error observed on the A receiver was more dependent on the U/D ratio than absolute signal levels. Significant bearing errors were observed at about 4 to 10 dB for the U/D ratio. The D signal level ranged from 30 to 60 dBu.

- Both the A and B receivers were less susceptible to the interference from the U signal at very high levels of the D signals.

- Little or no bearing error was observed for a U and D signal frequency separation of 3.5 kHz for the B receiver and 2.0 kHz for the A receiver.

5.2 Power Line Carrier Radiation

In this section we make some observations regarding the PLC radiation measurements. PLC systems, in practice, operate with injected powers that range from a fraction of a watt to tens of watts. We used powers of 20 and 100 W so that we would have a strong, reliable signal to measure. These high powers are not meant to represent typical usage. For the purpose of comparison to other measurements or predictions, the measurements we made were normalized to 1 W of injected PLC powe a convenient reference level. Keep in mind that what is measured is always (signal + noise) so that where the measured data appears to be predominately composed of noise that this is not the true noise level, due to the normalization.

- There is about 5 to 10 dB more radiation from the lower frequency signal (coupled phase-to-ground on the 161-kV line) than from the higher frequency signal (coupled phase-to-phase on the 500-kV line).

- The transmitting substation shows a strong peak in field strength directly above the substation which drops 10 dB or more in the first few kilometers of horizontal distance in any direction.

- The transverse runs indicate that the field strength decreases with lateral distance at the rate of 18 to 22 dB/decade. This represents a $^1/r$ dependence for the field strength.

- Comparison of the results in Figures 15 and 16 indicate that the signal directly above the power line may be less than at some distance to the side. The transverse runs did not show this behavior. The reason may be that the field is not vertically polarized directly above the line.

- Although the simulated fault was located such that it would have a high potential for radiation, it caused little (about 2 or 3 dB) increase in the radiated fields in the vicinity. This is only a single, isolated test of radiation from a fault and the conclusion should not be considered general; but we feel this is a strong indication that any fault would have little effect, except perhaps a fault in or very near the transmitting substation.

- The highest levels of field strength that we measured were about 40 dBu. These are in good agreement with the field strengths that Jones (1965) and the Electricité de France (1978) measured.

5.3 Interference to the Radio Compass

The conclusions made in this section are based on the assumptions that the injected PLC power is 1 W, and that the aircraft is located about 400 m (~1312 ft) above the transmitting substation (where the PLC radiation is the greatest).

- The PLC field strengths for 1 W of injected power are not sufficient to affect the B receiver except where the NDB signal (the desired signal) is very weak (30 $\mu V/m$) at the upper end of the NDB band (400 kHz).

- Assuming that the minimum NDB signal (the desired signal) is 36.9 dBu (70 $\mu V/m$), the PLC field strengths for 1 W of injected power are not sufficient to affect the A receiver.

- If the injected PLC power was increased by 6 dB (to 4 W), the point where perceptible interference to the radio compass is reached. This is true for the locations where the PLC radiation is greatest.

- The lateral distance dependence of the PLC field strengths, based on our measurements, was observed to be no more than -18 dB/decade. The height dependence of the PLC field strength may be the same as the lateral distance dependence if no surface wave propagation mode is present. However, for that portion of the PLC signal that propagates as a surface wave there will be very little decrease in field strength with height for those heights below one or two wavelengths, then it will decrease rapidly.

- The holographic scatter technique showed that, in one case, the power line causes insignificant reradiation of the NDB signal. This should not be considered as a broad conclusion. Further study is recommended if reradiation is to be understood sufficiently.

5.4 General Summary: The Compatibility of Power Line Carrier and the Radio Compass

The data we collected could be used to predict a zone of incompatibility embodied in geographic and frequency separations. To do so, one must make some broad and conservative assumptions based on our data.

For the PLC field strengths: the lateral distance dependence is $^1/r$. The longitudinal distance dependence can be obtained from the measured field strengths on the longitudinal paths. The vertical distance dependence, although difficult to obtain from our data, could be assumed to be $^1/r$. The relationship between the field strength and injected power can be taken directly from our data.

For the radio compass: A frequency separation of less than 3.5 kHz (or even 4 kHz) would cause the radio compass to be susceptible to interference. The undesired-to-desired signal ratio and the absolute undesired signal level must be less than 4 dB and 44 dBu, respectively.

Radio compass errors due to PLC radiation could be guarded against by defining an appropriate zone of incompatibility. We do not feel that this definition would place unreasonable restraints on PLC power or spectrum use.

5.5 Experimental Techniques

- The receiver susceptibility measurements provided more than what we needed to know for this work. It was sufficient (and efficient) to have made laboratory measurements. It would have been difficult to assess or to quantitavely measure the ADF bearing error using actual PLC signals. The area where some improvement to the measurements can be made is in the antenna simulation or the way in which it is used. It would be more informative to be able to arbitrarily set the direction of arrival for both the desired and undesired signals.

- The method of calibrating the measurement aircraft, although somewhat cumbersome, worked well. The Perryton site gave excellent results for the ground-level measurements which, in turn, lends a degree of confidence to the field strength extrapolation procedure. The Alva and Elk City sites were not as good. It is very important that the terrain be level and homogeneous.

- The problems encountered with the measurement system, both software and hardware, are the cause of the loss of about half of the data and the lack of good INS data for the PLC radiation measurements. The tendency for the PLC data to be striated for smaller receiver bandwidths was caused by the measurement system. Any field system should be very reliable and the software should incorporate a variety of diagnostics to ensure continued system reliability while in the field.

6. ACKNOWLEDGMENTS

The author wishes to acknowledge the Spectrum Management Branch of the Federal Aviation Administration for their support of this work. In particular, the author thanks Mr. Charles Cram for his assistance with the development of the concept and his continued help coordinating the various parts of the project.

The author wishes to express strong appreciation for the assistance provided by the following people:

Dan Jernigan, Ted Swingle and the staff of the Communications Engineering Branch at the Tennessee Valley Authority. In particular, Herb Dobson for his coordination efforts; Lawrence Bryant and Bob Bratton for their help in providing the test PLC signals; Leslie Longmire and Sharon Ogle for making the ground-level PLC radiation measurements.

Edward Sawtelle, James Dong, and Wayne Bell of the National Aviation Facilities Experimental Center for the data recording system. Al Bazer, Bob Powell, and Jess Terry, the pilots, for their precise flying of the specified flight paths.

Dick Vaughn of the FAA Aeronautical Center for engineering the radio compass susceptibility measurements, and Don Wilson and Daryl Hill for performing the measurements.

Leslie Berry of the Institute for Telecommunication Sciences for his assistance with the aircraft calibration procedures and LF radio predictions. Dr. Bernard Wieder for the use of his holographic techniques. Eric Rehm for his painstaking efforts reducing the recorded data.

Last, the large number of people such as the airport managers, the radio engineers responsible for maintaining the beacons we used, and Paul Hopkins and his staff at the Alabama Power Company for some special PLC signal scheduling.

7. REFERENCES

Dobson, H. I. (1979), Private communication, Chairman of the IEEE Power Line Carrier Subcommittee, Tennessee Valley Authority, Chattanooga.

Electricite de France (1978), An experimental study of the electromagnetic field caused by carrier-current-links, Telecommunications Laboratory, Appendix V, Translation No 677 by the Library of the Electricity Supply Board, Lower Fitzwilliam St., Dublin, 2, Ireland.

Gronlie, L. (1956), High-frequency transmission along power lines, ETT, 69, June, pp 201-208.

Jensen, K. Kolbaek (1972), Felder von Tragerfrequenzverbindungen uber Hochspannungsleitungen, ETZ-A, Bd. 93, H4, pp 197-201.

Jones, D. E. (1965), Power line carrier radiation from high voltage lines, Ontario Hydro Research Quarterly, 17, no. 3, pp 10-16.

Kayton, M. and W. R. Fried (1969), Editors, Avionics Navigation Systems, John Wiley and Sons, New York.

Perz, M. C. (1964), A method of analysis of PLC problems on three-phase lines, IEEE Transactions on Power Apparatus and Systems, 83, July, pp 586-692.

Pullen, F. D. (1975), The calculated electromagnetic fields surrounding carrier-bearing power line conductors, IEEE Transactions on Power Apparatus and Systems, PAS-94, no. 2, March/April, pp 530-538.

Ushirozawa, M. (1964), HF propagation on non-transposed power lines, IEEE Transactions on Power Apparatus and Systems, 84, November, pp 1137-1142.

Wedepohl, L. M. (1965), Electrical characteristics of polyphase transmission systems with special reference to boundary value calculations at power line carrier frequencies, Proc. IEE, 112, No. 11, November.

Wedepohl, L. M. and R. G. Wasley (1966), Wave propagation in multiconductor overhead lines, Proc. IEE, 113, No. 4, April.

APPENDIX A

RADIO COMPASS RECEIVER SUSCEPTIBILITY DATA

Contained in this Appendix are the data collected on the ADF receiver susceptibility to the presence of an undesired signal. The measurement procedure is described in Section 3 in the body of the report. The Table below gives the correspondence between the measurement number, the parameters, and the data Tables and Figures in this Appendix. The measurements numbered 1-10 are for the case where the desired and the undesired signals arrive from different directions and those numbered 11-15 are for the case where the desired and undesired signals arrive from the same direction. No figures were prepared for measurements 11-15 because the bearing error was so small.

Table A-0. The Values of the Parameters for each Measurement and the Table and Figure Number of the Data Presented in this Appendix

DESIRED SIGNAL				UNDESIRED SIGNAL			TABLE NUMBER		FIGURE NUMBER	
MEASUREMENT NUMBER	FREQUENCY (kHz)	LEVEL (μV/m)	MODULATION TYPE	MODULATION TYPE	LEVEL (μV/m)	FREQUENCY (kHz)	RECEIVER A	B	RECEIVER A	B
1	200	40	CW	CW	VARIED DURING MEASUREMENT	VARIED DURING MEASUREMENT	A-1	A-16	A-1	A-11
2	200	500	CW	CW			A-2	A-17	A-2	A-12
3	200	500	MCW	CW			A-3	A-18	A-3	A-13
4	200	1,000	CW	CW			A-4	A-19	A-4	A-14
5	200	1,000	CW	FSK			A-5	A-20	A-5	A-15
6	400	30	CW	CW			A-6	A-21	A-6	A-16
7	400	500	CW	CW			A-7	A-22	A-7	A-17
8	400	500	CW	FSK			A-8	A-23	A-8	A-18
9	400	1,000	CW	CW			A-9	A-24	A-9	A-19
10	400	100,000	CW	CW			A-10	A-25	A-10	A-20
11	200	40	CW	CW			A-11	A-26		
12	200	1,000	CW	CW			A-12	A-27		
13	200	500	CW	FSK			A-13	A-28		
14	400	30	CW	CW			A-14	A-29		
15	400	500	CW	CW			A-15	A-30		

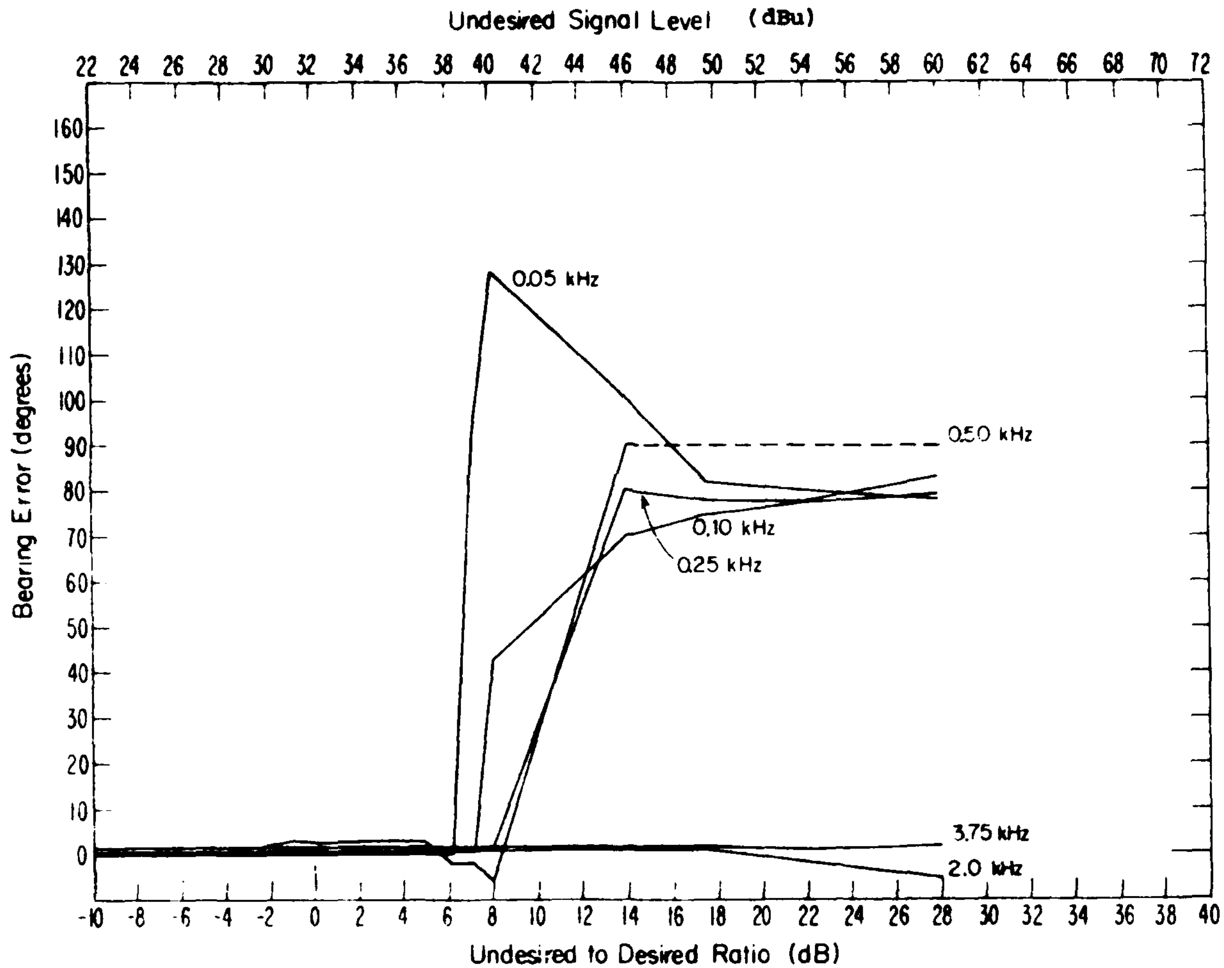

Figure A-1. Measured bearing error for ADF receiver A as a function of the undesired signal level and the frequency separation (Δf) between the desired and undesired signals. The desired signal level is 40 μV/m at 200 kHz with no modulation. The undesired signal is unmodulated.

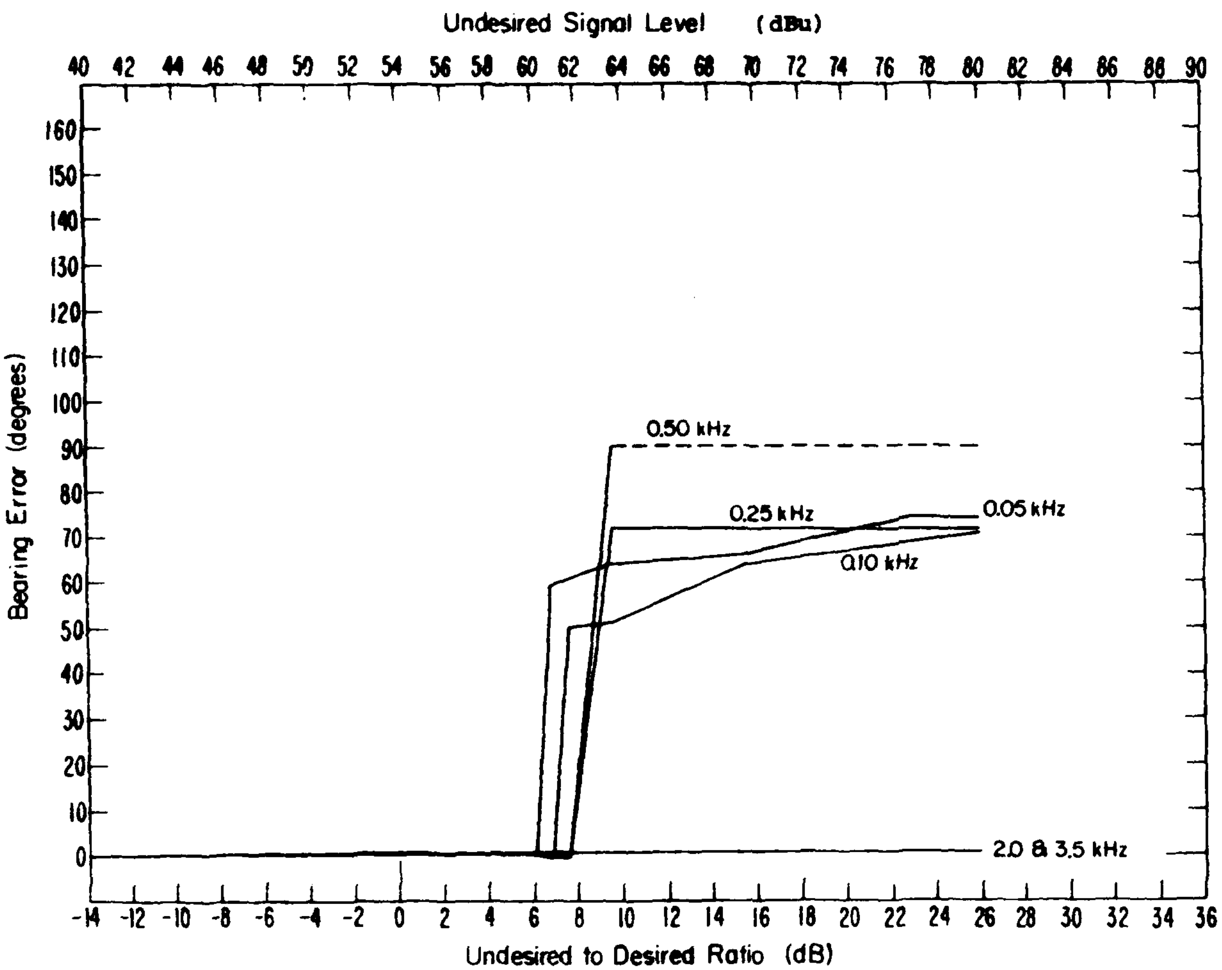

Figure A-2. Measured bearing error for ADF receiver A as a function of the undesired signal level and the frequency separation (Δf) between the desired and undesired signals. The desired signal level is 500 $\mu V/m$ at 200 kHz with no modulation. The undesired signal is unmodulated.

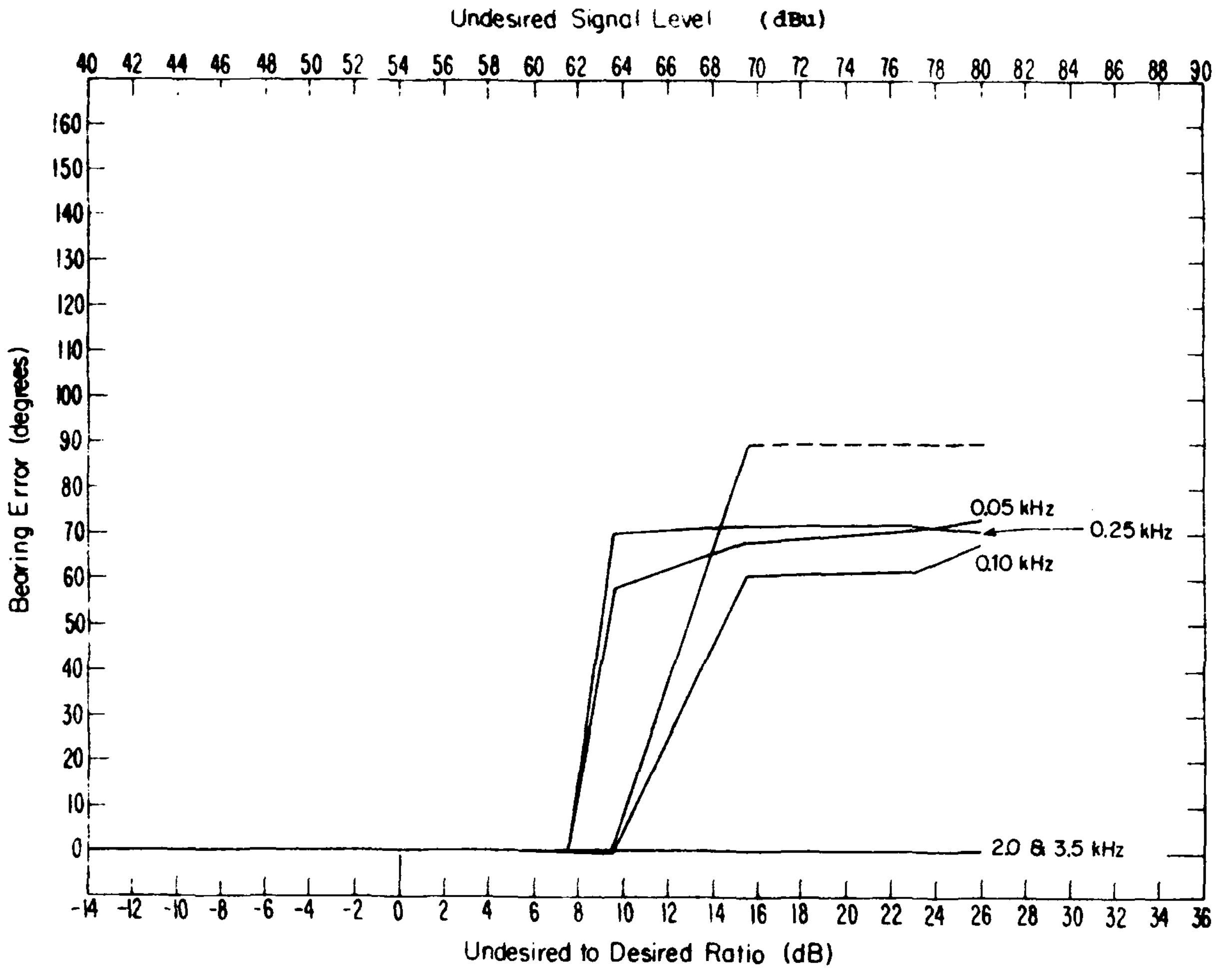

Figure A-3. Measured bearing error for ADF receiver A as a function of the undesired signal level and the frequency separation (Δf) between the desired and undesired signals. The desired signal level is 500 $\mu V/m$ at 200 kHz with tone modulation. The undesired signal is unmodulated.

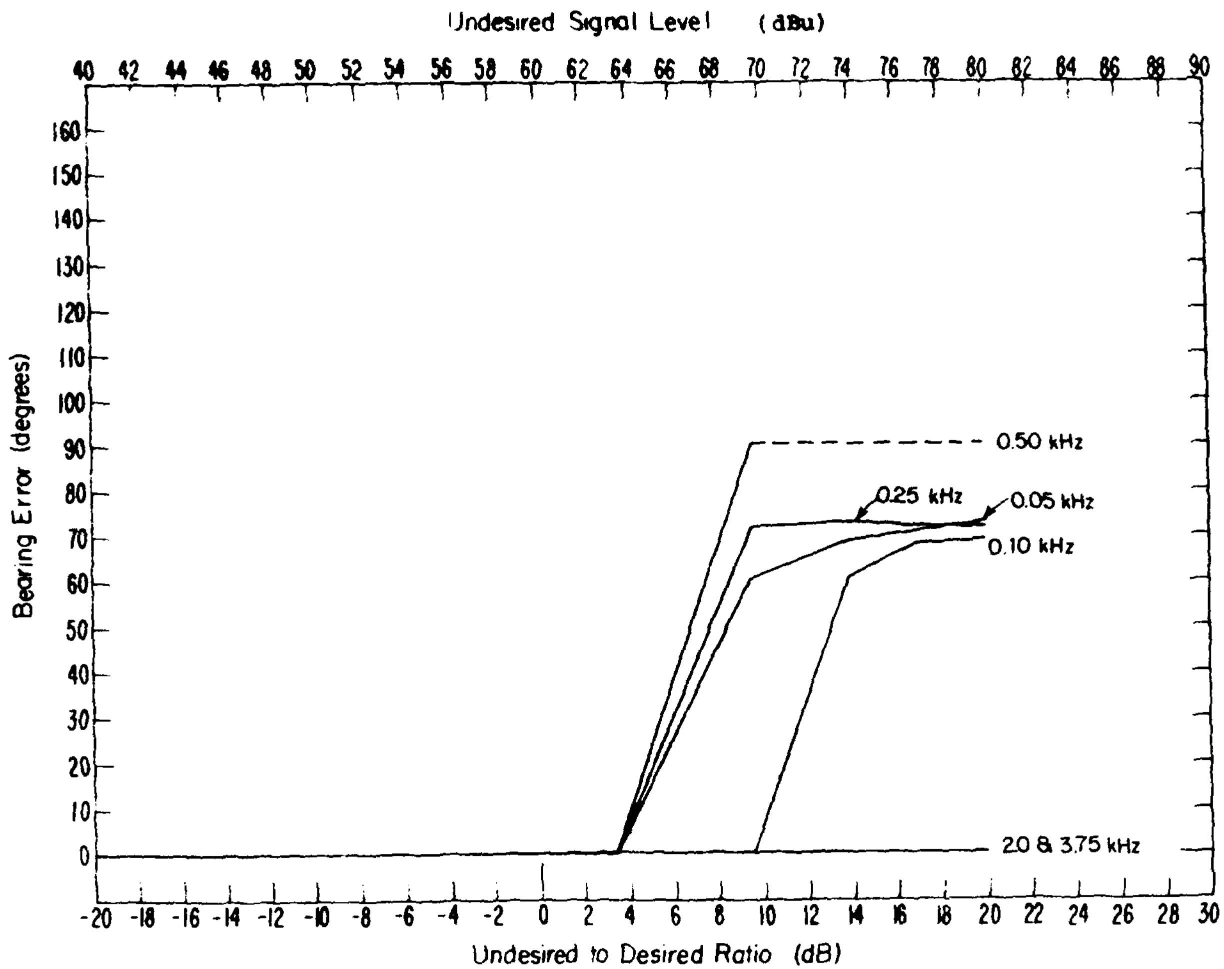

Figure A-4. Measured bearing error for ADF receiver A as a function of the undesired signal level and the frequency separation (Δf) between the desired and undesired signals. The desired signal level is 1,000 $\mu V/m$ at 200 kHz with no modulation. The undesired signal is unmodulated.

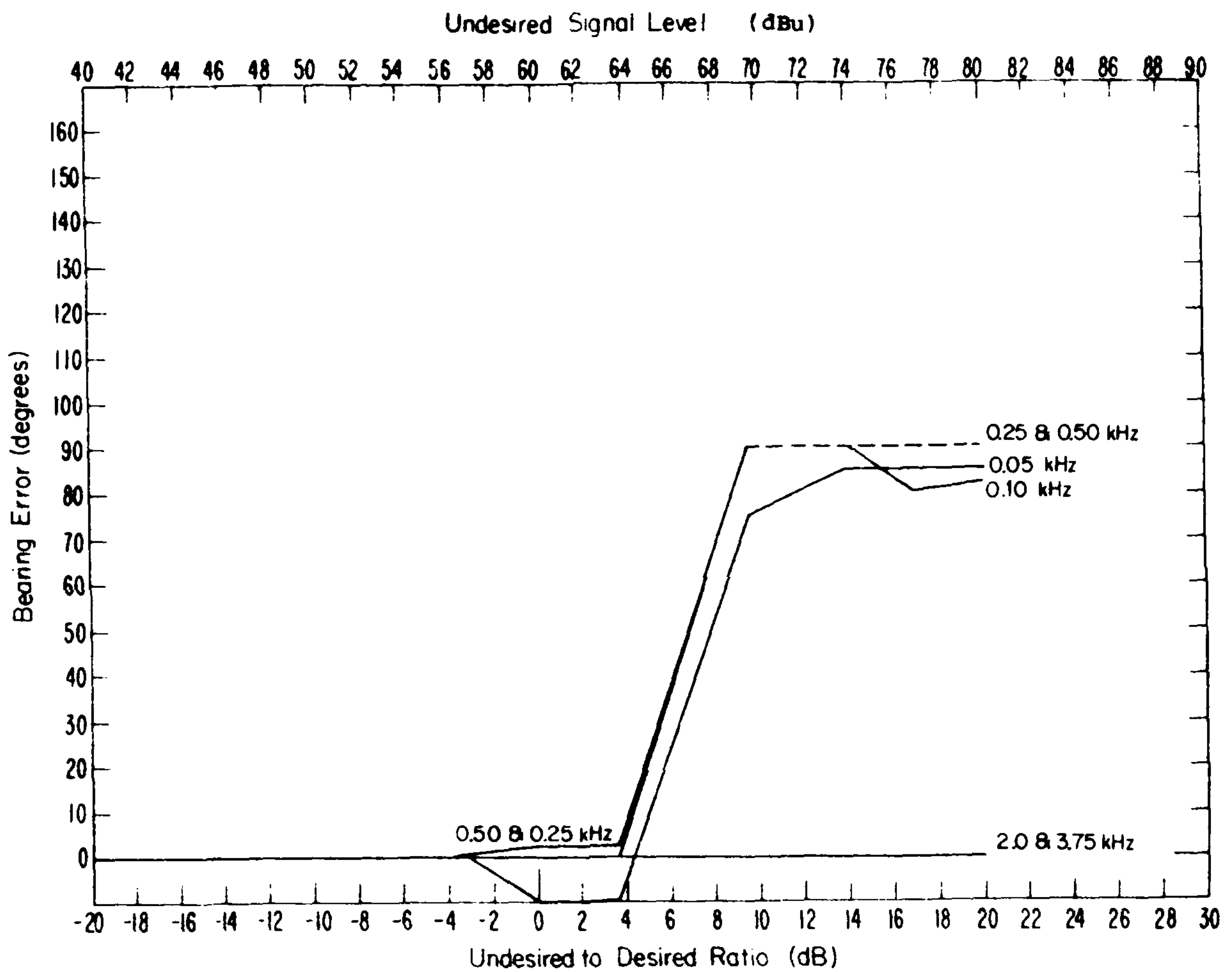

Figure A-5. Measured bearing error for ADF receiver A as a function of the undesired signal level and the frequency separation (Δf) between the desired and undesired signals. The desired signal level is 1,000 μV/m at 200 kHz with no modulation. The undesired signal is frequency shift keyed.

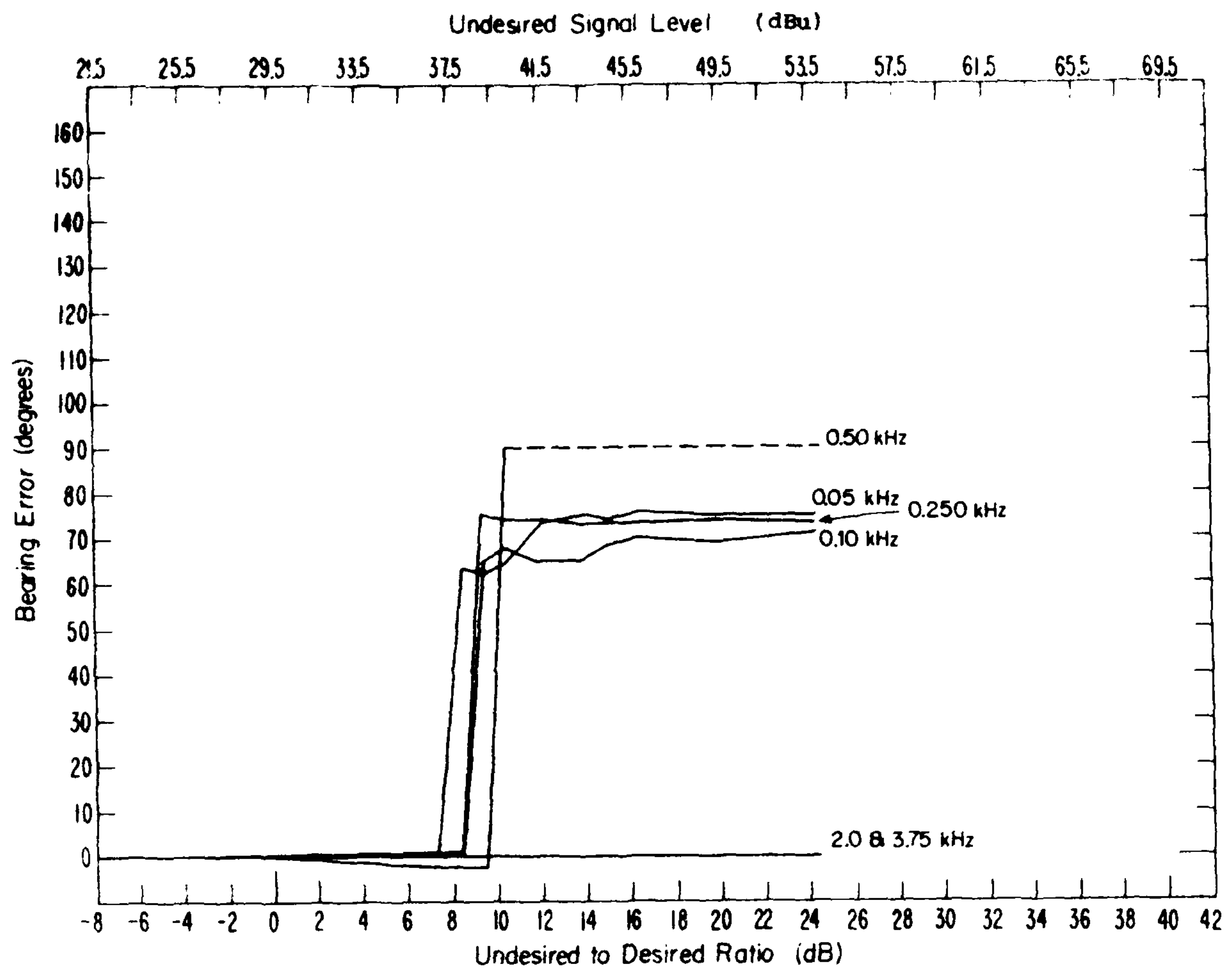

Figure A-6. Measured bearing error for ADF receiver A as a function of the undesired signal level and the frequency separation (Δf) between the desired and undesired signals. The desired signal level is 30 $\mu V/m$ at 400 kHz with no modulation. The undesired signal is unmodulated.

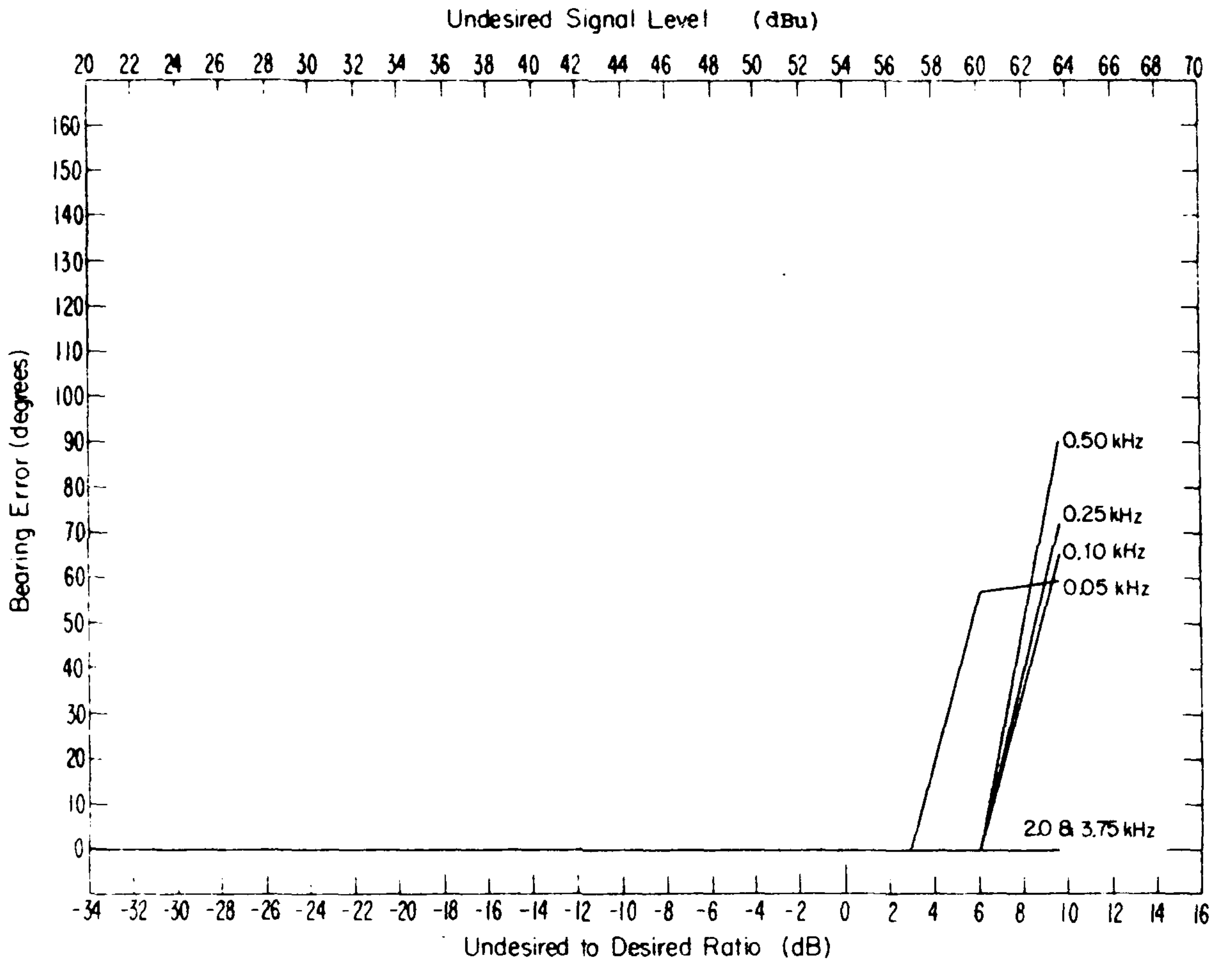

Figure A-7. Measured bearing error for ADF receiver A as a function of the undesired signal level and the frequency separation (Δf) between the desired and undesired signals. The desired signal level is 500 μV/m at 400 kHz with no modulation. The undesired signal is unmodulated.

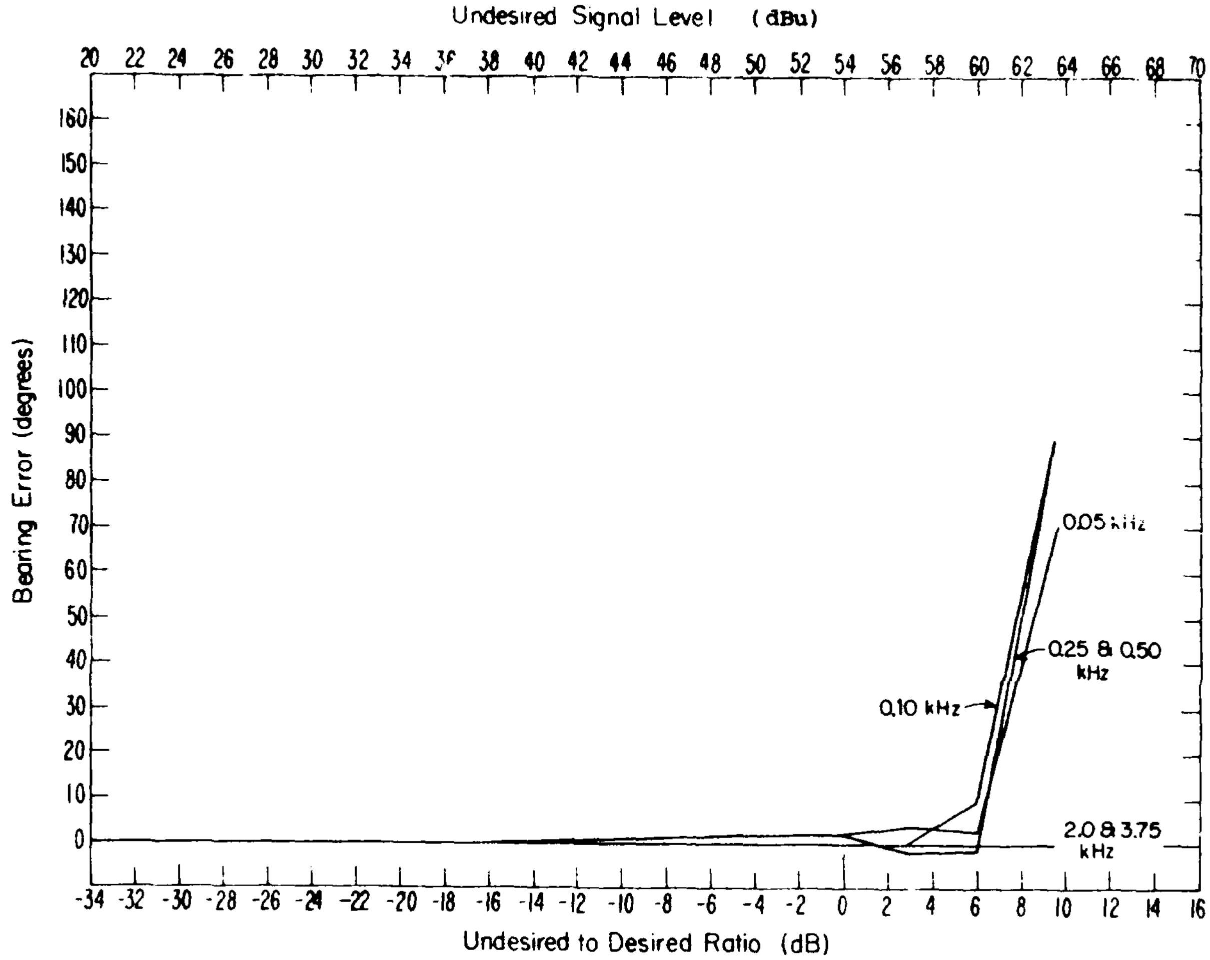

Figure A-8. Measured bearing error for ADF receiver A as a function of the undesired signal level and the frequency separation (Δf) between the desired and undesired signals. The desired signal level is 500 μV/m at 400 kHz with no modulation. The undesired signal is frequency shift keyed.

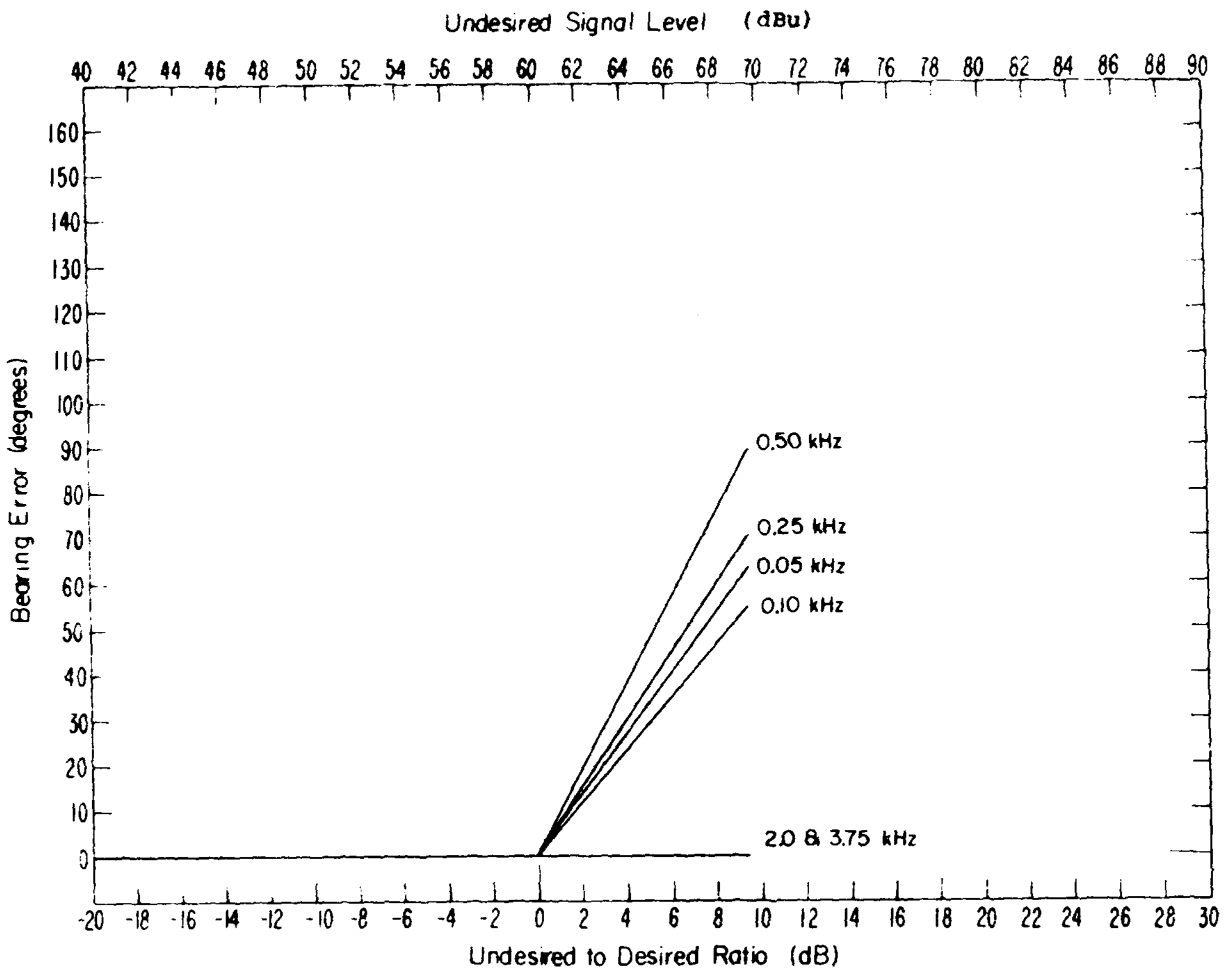

Figure A-9. Measured bearing error for ADF receiver A as a function of the undesired signal level and the frequency separation (Δf) between the desired and undesired signals. The desired signal level is 1,000 $\mu V/m$ at 400 kHz with no modulation. The undesired signal is unmodulated.

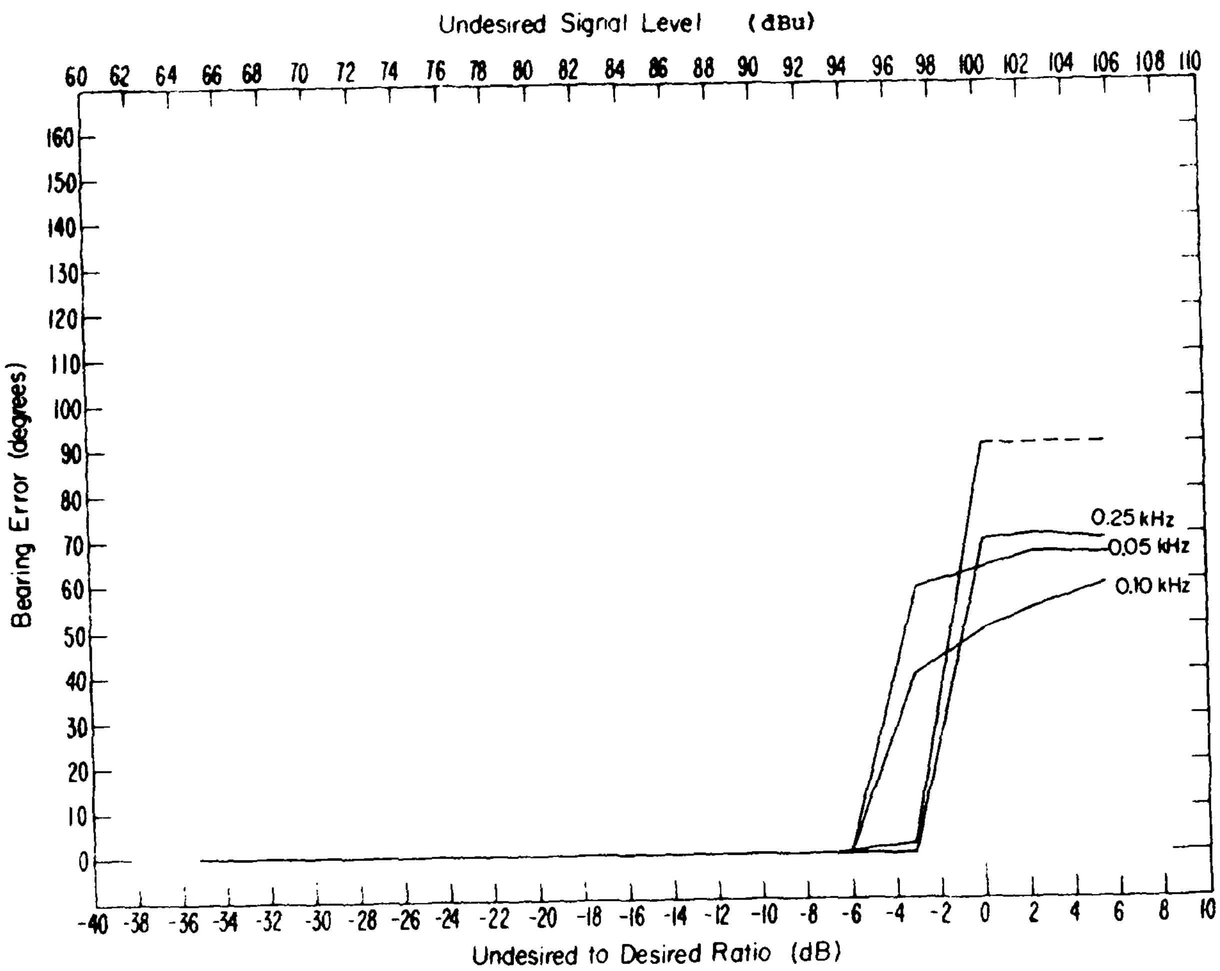

Figure A-10. Measured bearing error for ADF receiver A as a function of the undesired signal level and the frequency separation (Δf) between the desired and undesired signals. The desired signal level is 100,000 μV/m at 400 kHz with no modulation. The undesired signal is unmodulated.

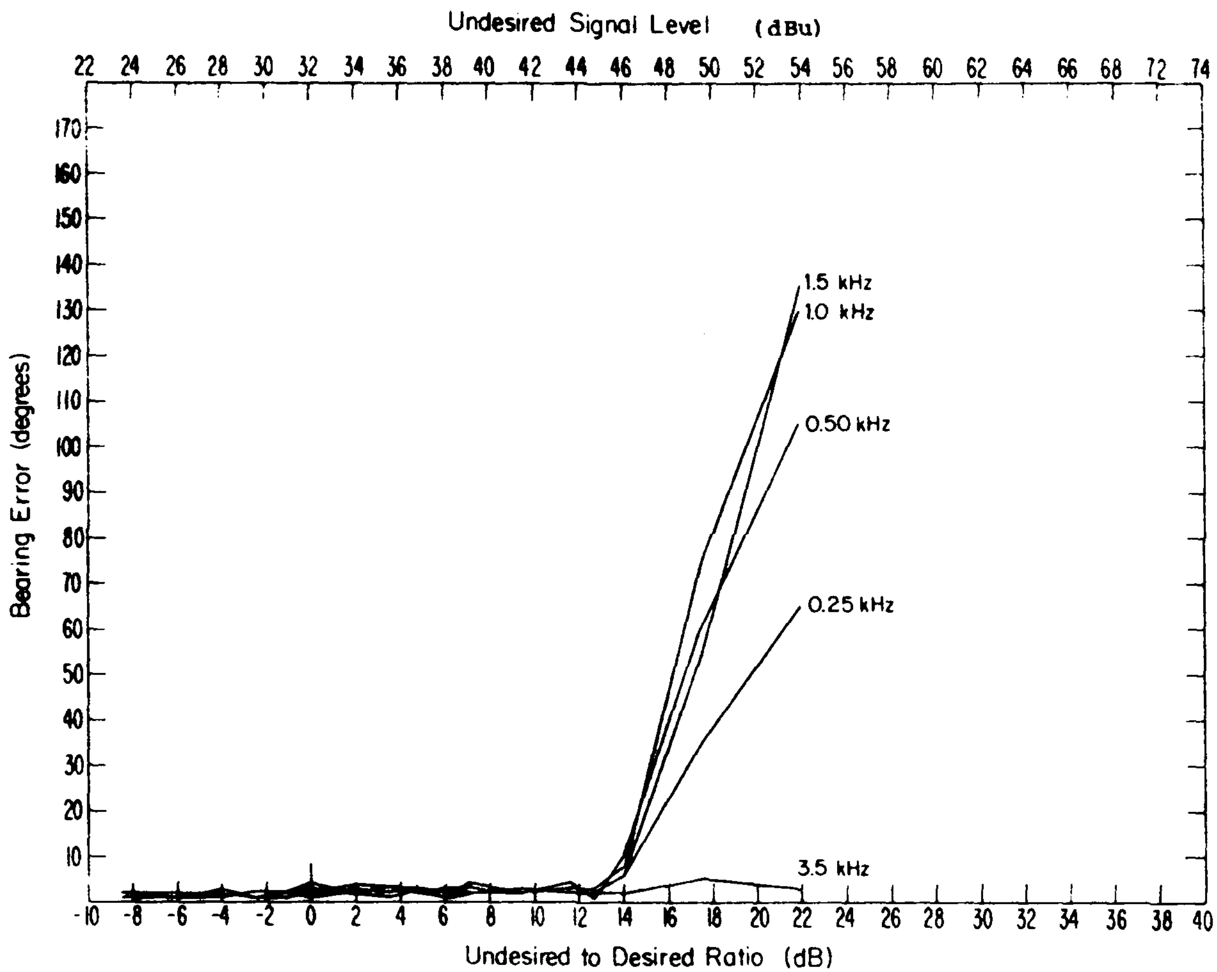

Figure A-11. Measured bearing error for ADF receiver B as a function of the undesired signal level and the frequency separation (Δf) between the desired and undesired signals. The desired signal level is 40 μV/m at 200 kHz with no modulation. The undesired signal is unmodulated.

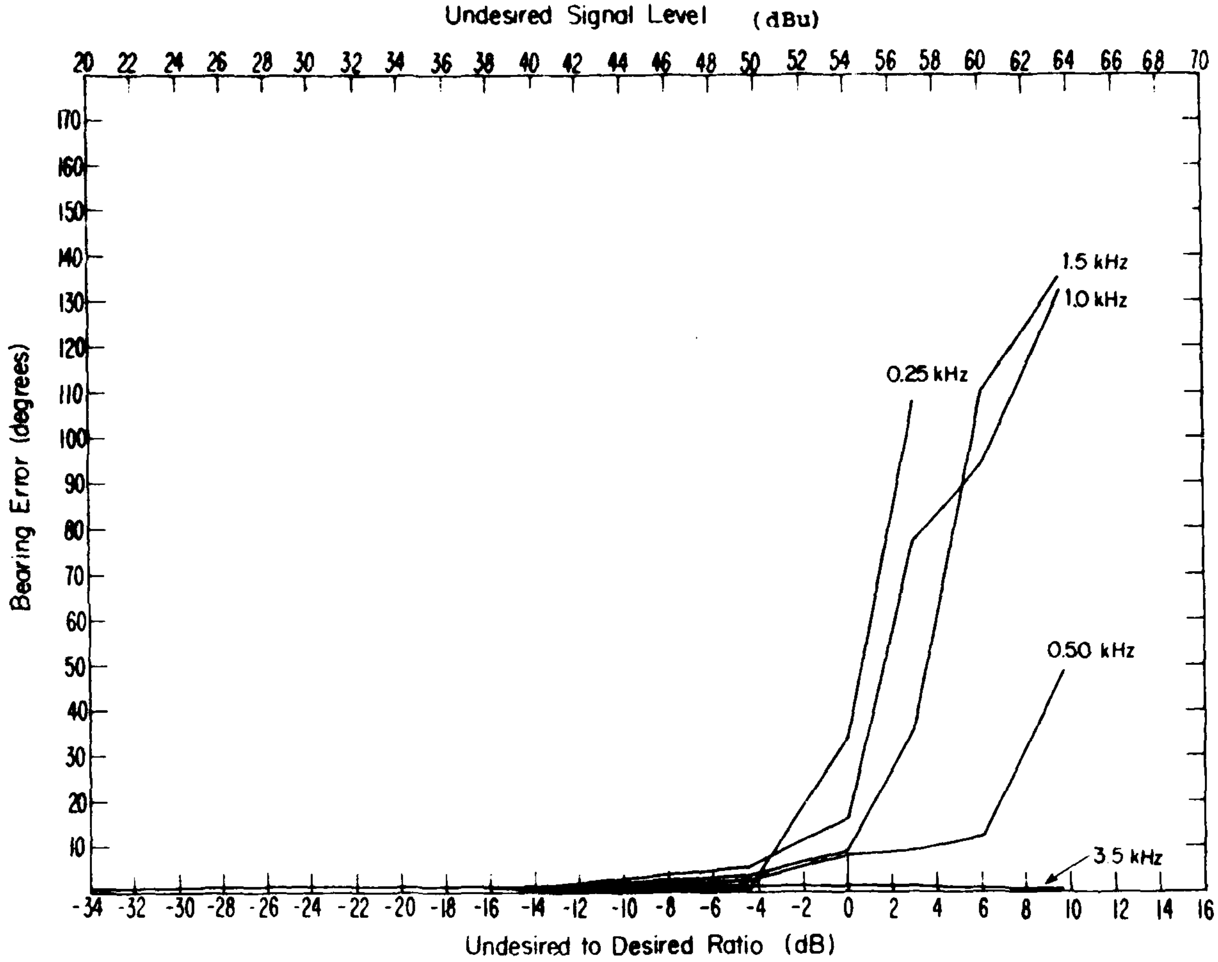

Figure A-12. Measured bearing error for ADF receiver B as a function of the undesired signal level and the frequency separation (Δf) between the desired and undesired signals. The desired signal level is 500 $\mu V/m$ at 200 kHz with no modulation. The undesired signal is unmodulated.

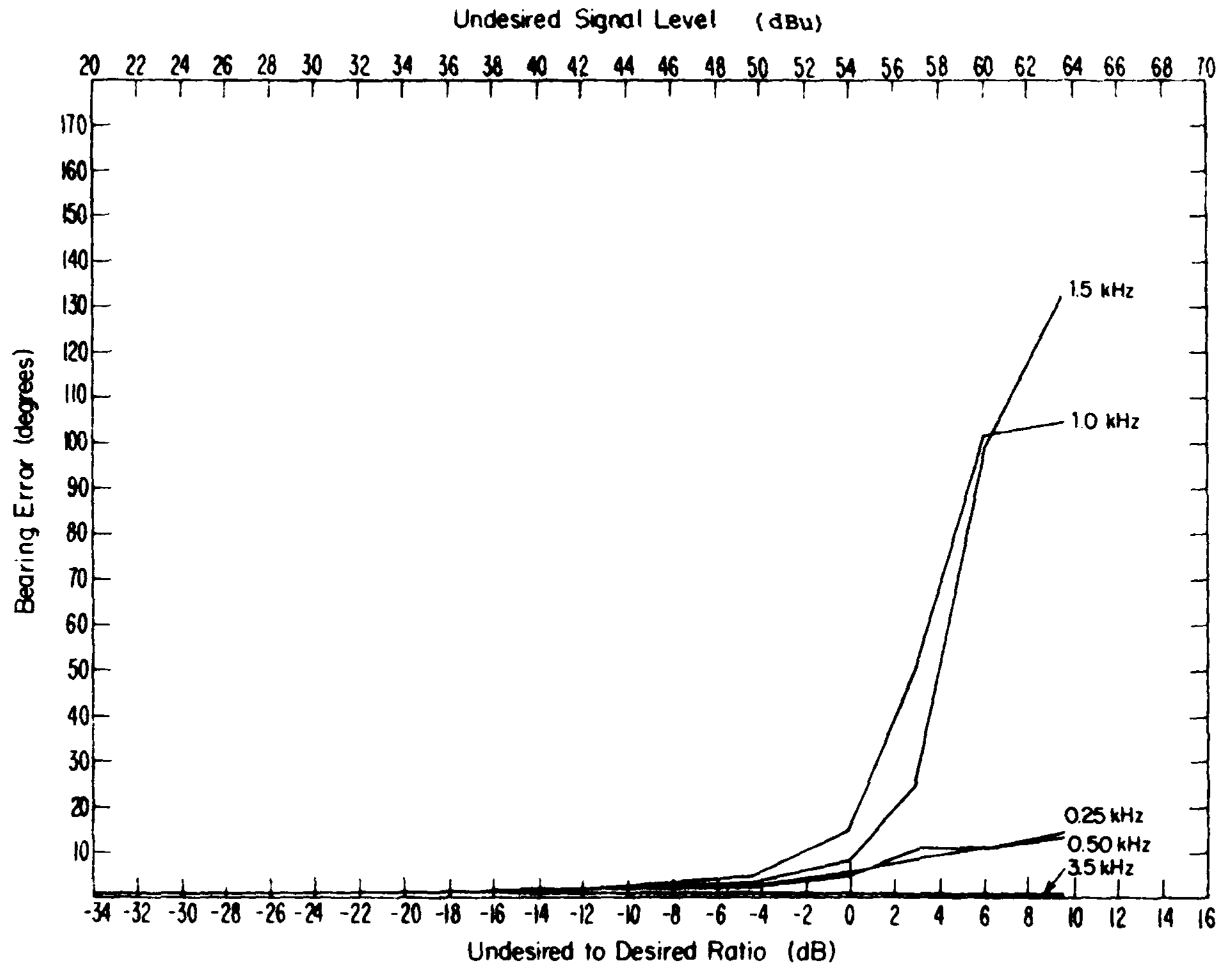

Figure A-13. Measured bearing error for ADF receiver B as a function of the undesired signal level and the frequency separation (Δf) between the desired and undesired signals. The desired signal level is 500 μV/m at 200 kHz with tone modulation. The undesired signal is unmodulated.

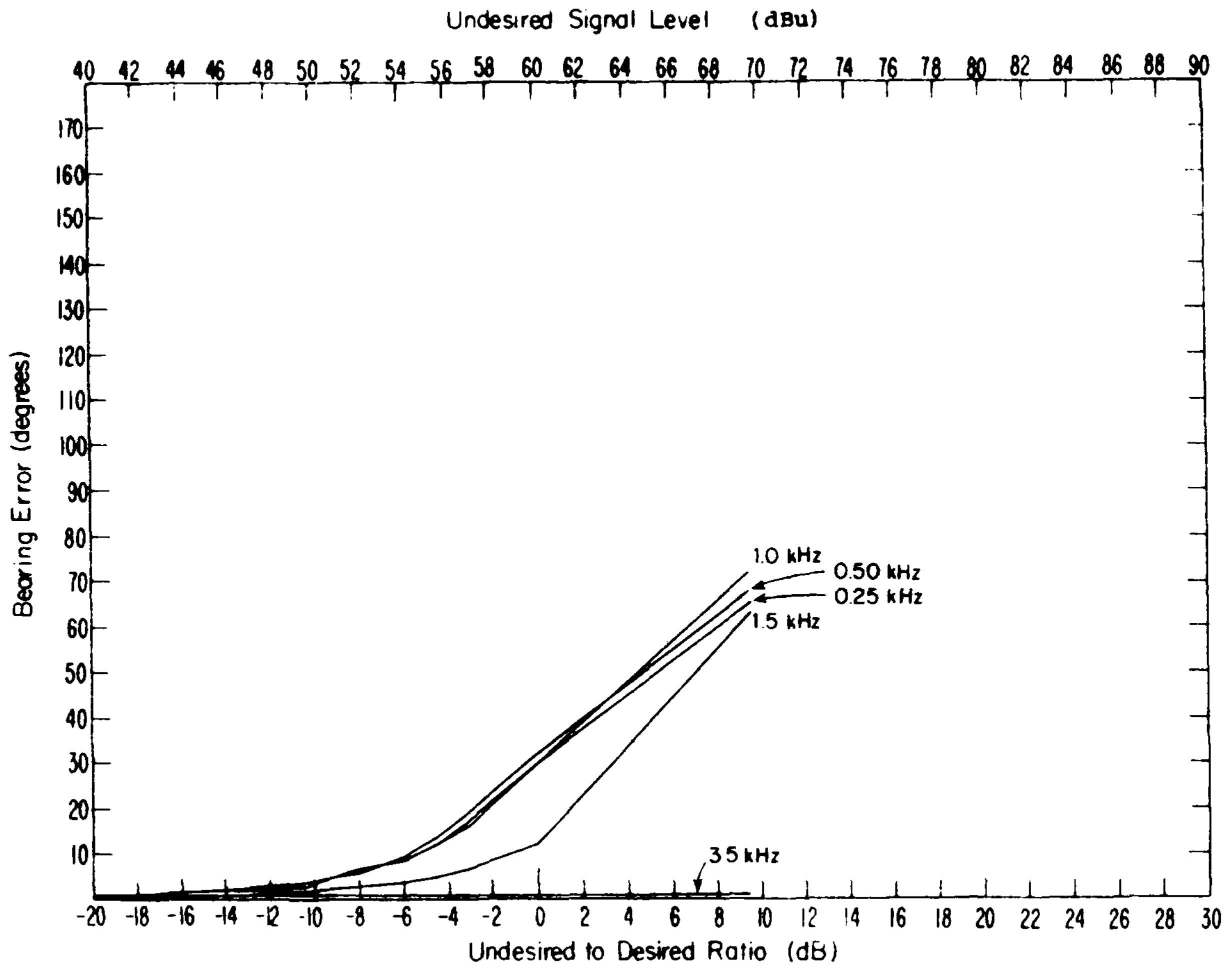

Figure A-14. Measured bearing error for ADF receiver B as a function of the desired signal level and the frequency separation (Δf) between the desired and undesired signals. The desired signal level is 1,000 μV/m at 200 kHz with no modulation. The undesired signal is unmodulated.

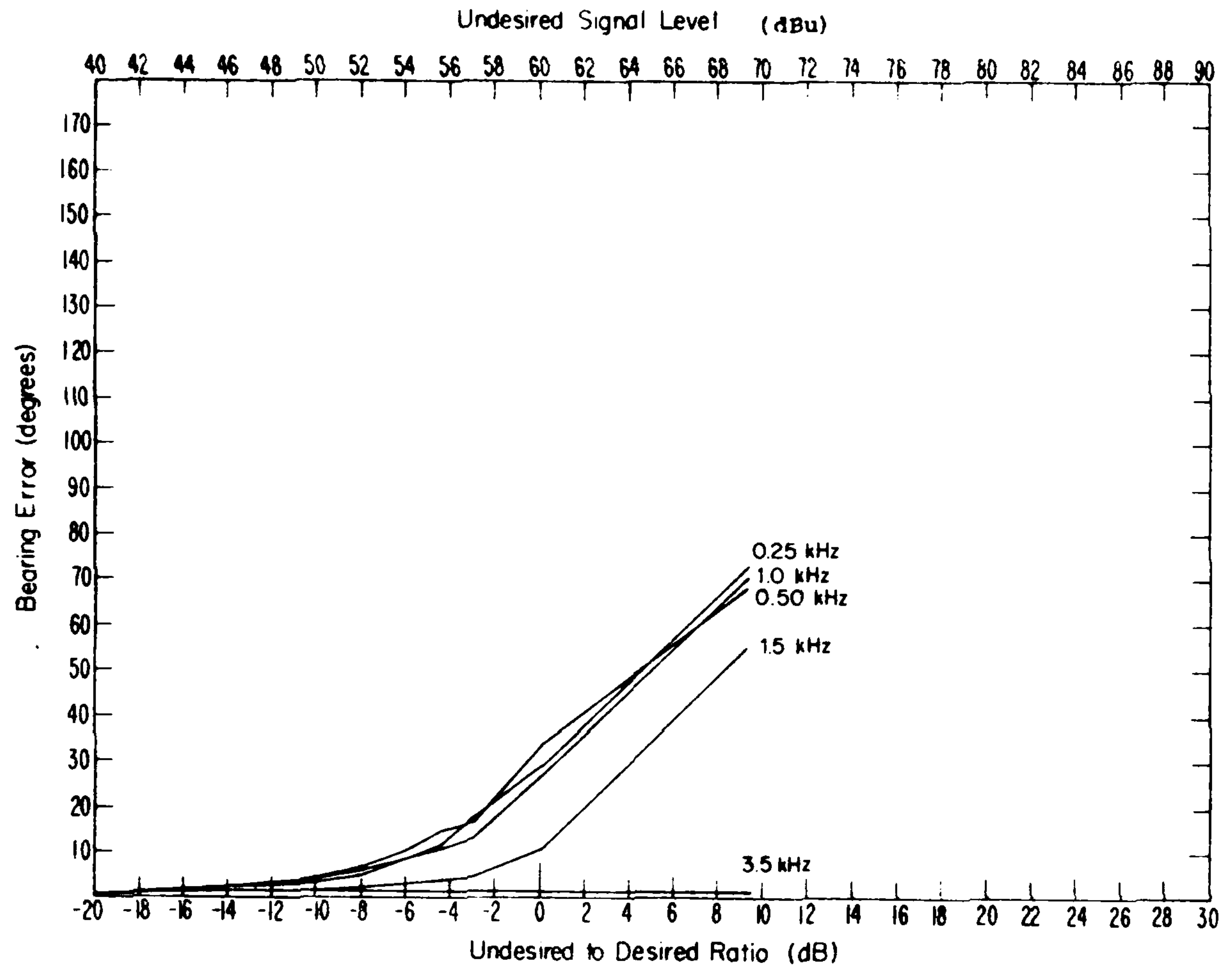

Figure A-15. Measured bearing error for ADF receiver B as a function of the undesired signal level and the frequency separation (Δf) between the desired and undesired signals. The desired signal level is 1,000 $\mu V/m$ at 200 kHz with no modulation. The undesired signal is frequency shift keyed.

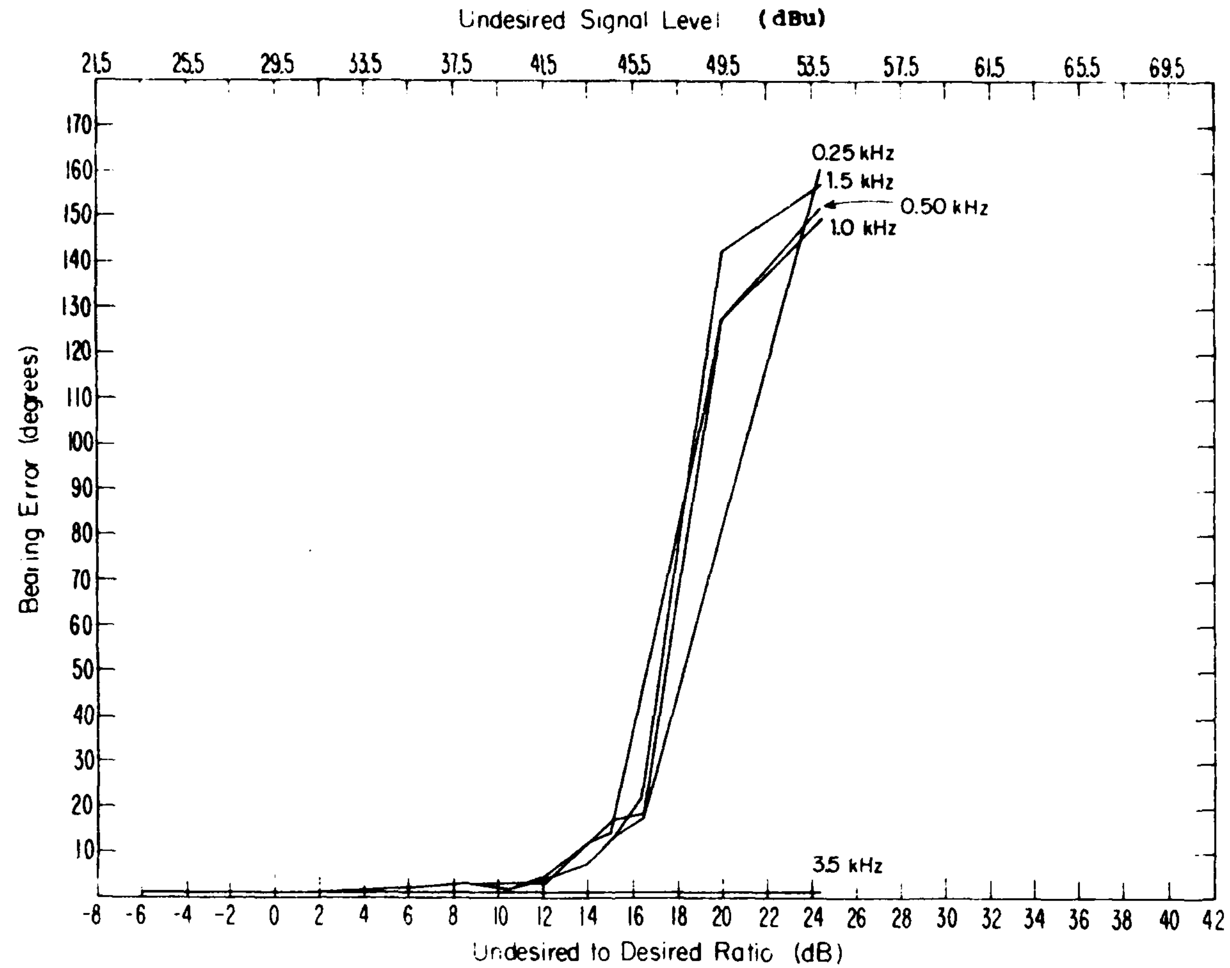

Figure A-16. Measured bearing error for ADF receiver B as a function of the undesired signal level and the frequency separation (Δf) between the desired and undesired signals. The desired signal level is 30 $\mu V/m$ at 400 kHz with no modulation. The undesired signal is unmodulated.

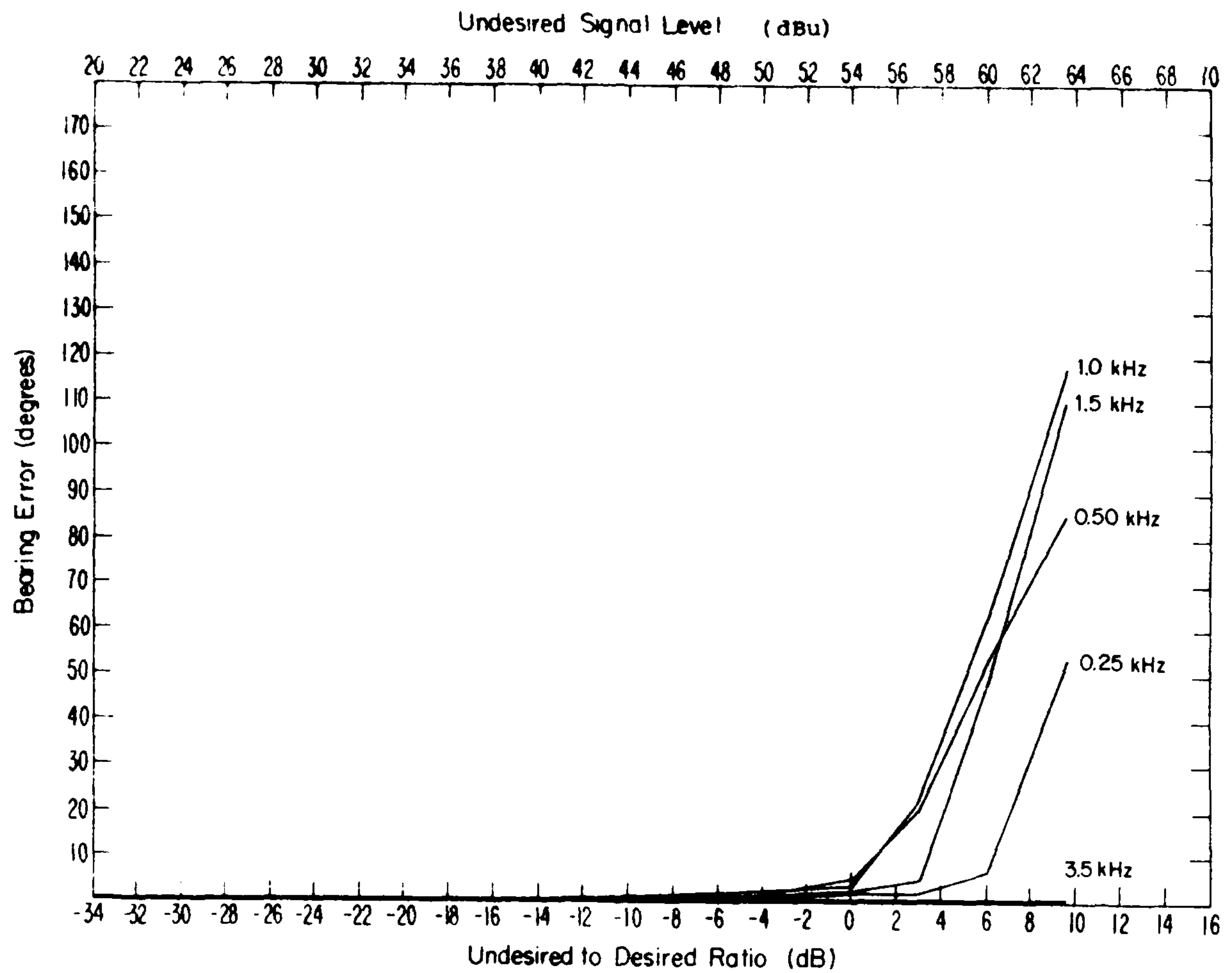

Figure A-17. Measured bearing error for ADF receiver B as a function of the undesired signal level and the frequency separation (Δf) between the desired and undesired signals. The desired signal level is 500 μV/m at 400 kHz with no modulation. The undesired signal is unmodulated.

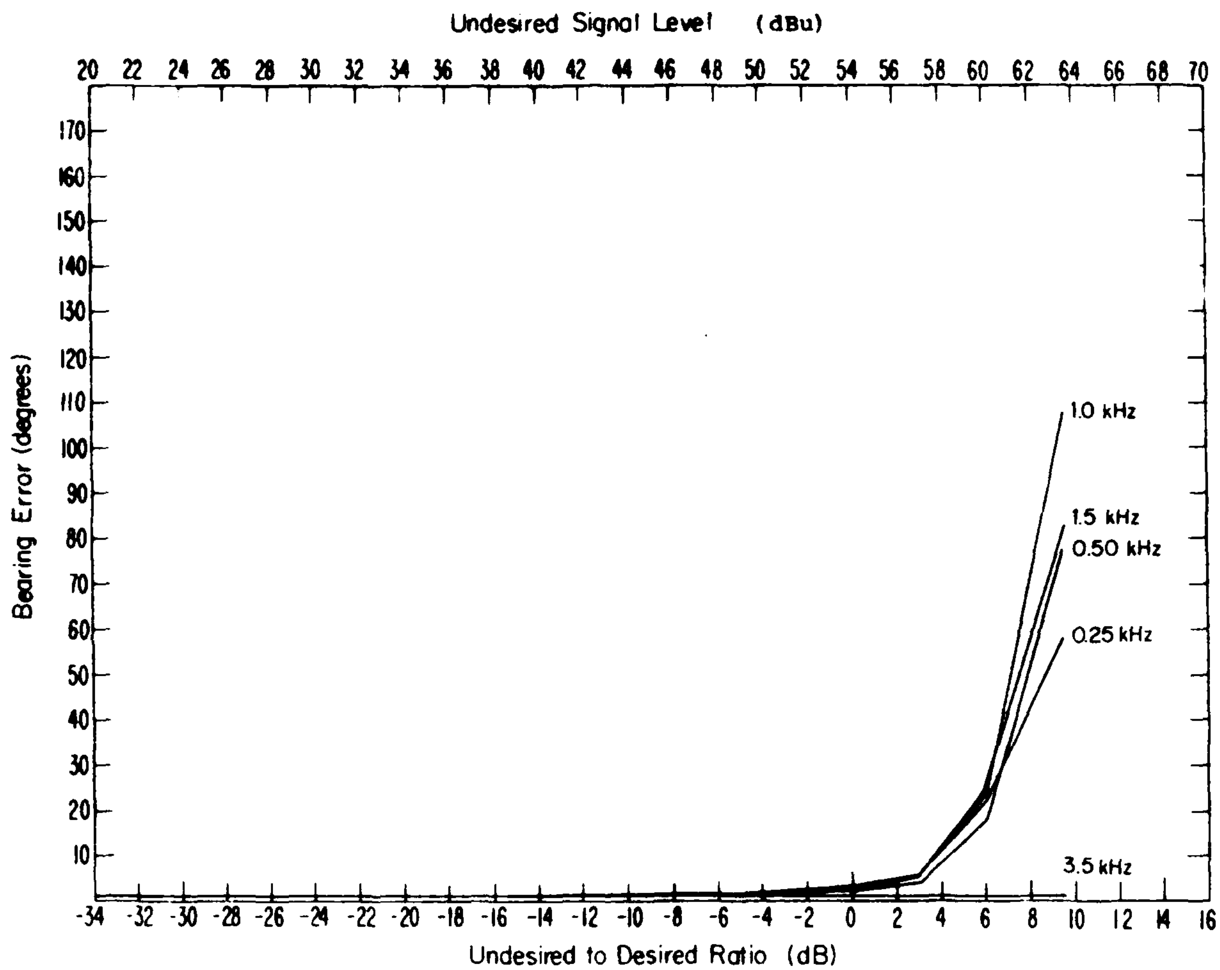

Figure A-18. Measured bearing error for ADF receiver B as a function of the undesired signal level and the frequency separation (Δf) between the desired and undesired signals. The desired signal level is 500 $\mu V/m$ at 400 kHz with no modulation. The undesired signal is frequency shift keyed.

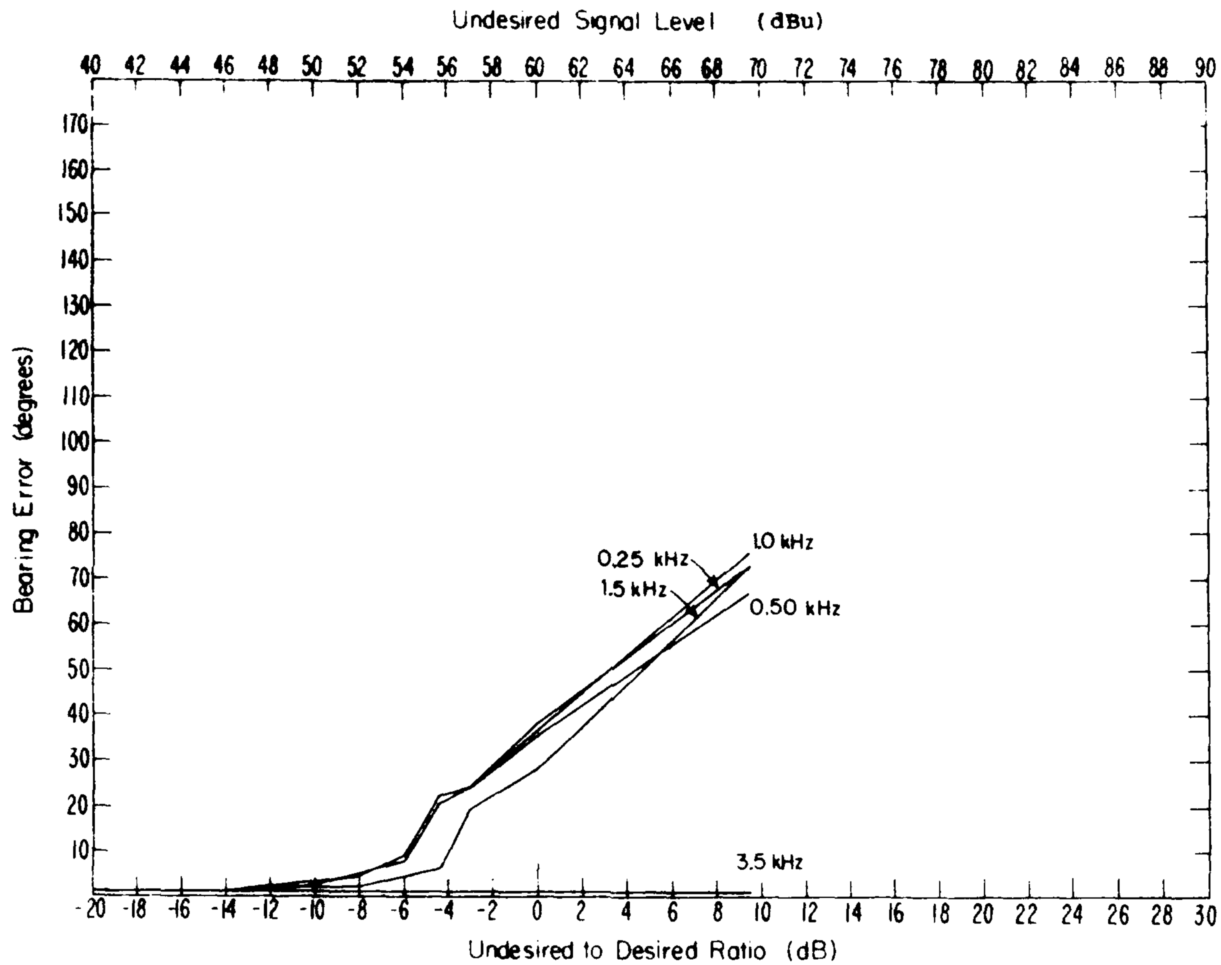

Figure A-19. Measured bearing error for ADF receiver B as a function of the undesired signal level and the frequency separation (Δf) between the desired and undesired signals. The desired signal level is 1,000 μV/m at 400 kHz with no modulation. The undesired signal is unmodulated.

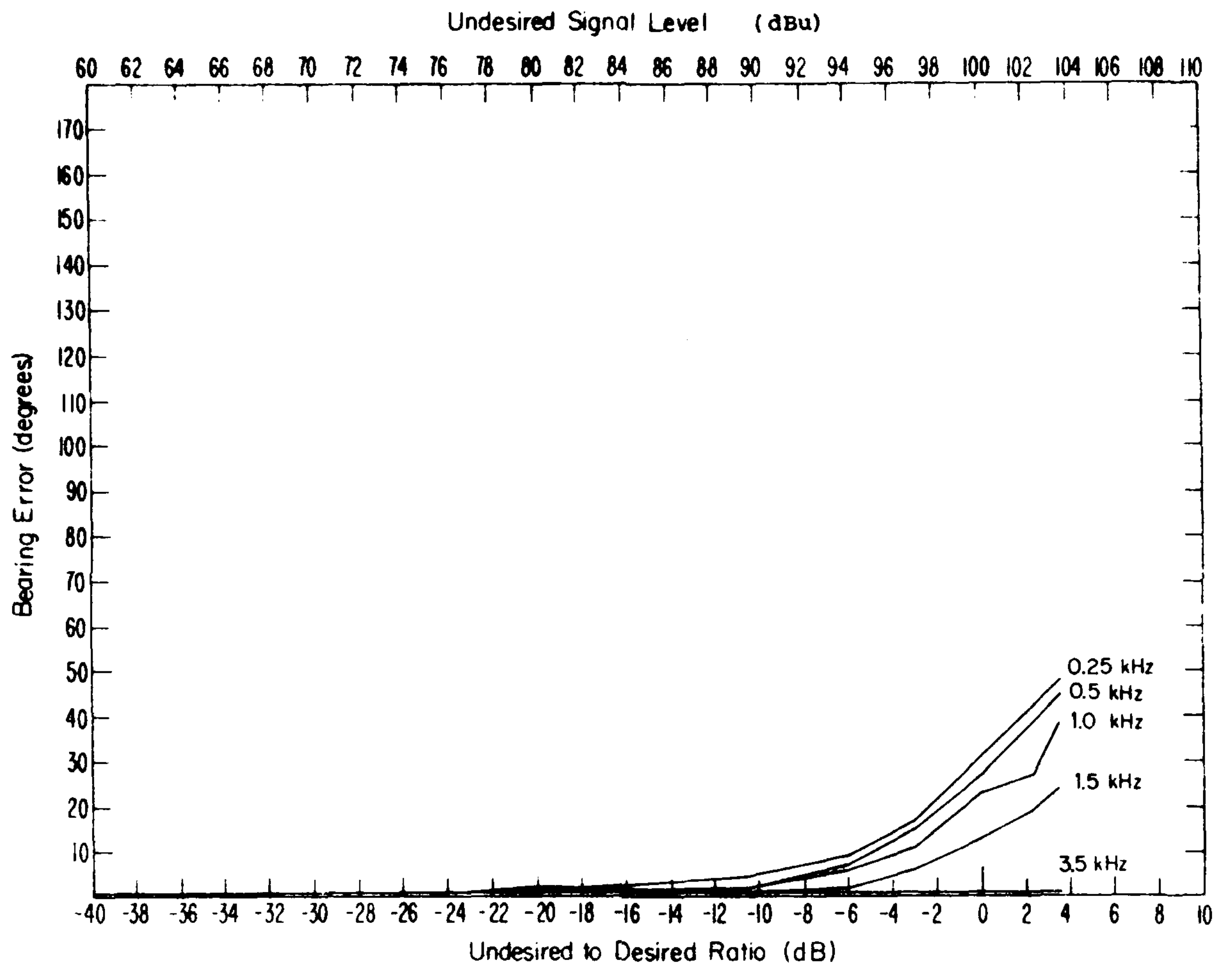

Figure A-20. Measured bearing error for ADF receiver B as a function of the undesired signal level and the frequency separation (Δf) between the desired and undesired signals. The desired signal level is 100,000 $\mu V/m$ at 400 kHz with no modulation. The undesired signal is unmodulated.

Table A-1. Measured Bearing Error for ADF Receiver A as a Function of the Undesired Signal Level and the Frequency Separation (Δf) between the Desired and Undesired Signals. The Desired Signal Level is 40 µV/m at 200 kHz with No Modulation. The Undesired Signal is Unmodulated.

UNDESIRED SIGNAL LEVEL µV/m	UNDESIRED SIGNAL LEVEL dBu	UNDESIRED TO DESIRED SIGNAL RATIO dB	BEARING ERROR, DEGREES Δf=.05 kHz	Δf=.10 kHz	Δf=.25 kHz	Δf=.50 kHz	Δf=2.0 kHz	Δf=3.75 kHz
15	23.5	-8.5	0	1	1	2	2	3
20	26.0	-6.0	0	1	1	2	2	2
25	28.0	-4.1	0	1	2	2	0	1
30	29.5	-2.5	0	1	2	2	1	2
35	30.9	-1.2	0	1	2	3	0	2
40	32.0	0.0	0	1	2	3	-1	2
50	34.0	1.9	0	1	2	0	0	5
60	35.6	3.5	0	1	2	3	0	2
70	36.9	4.9	0	1	2	3	0	2
80	38.1	6.0	0	1	2	-2	-2	-1
90	39.1	7.0	91**	1	2	-2	0	1
100	40.0	8.0	128	43**	2	-6	3	1
200	46.0	14.0	102	70	80**	90*	3	2
300	49.5	17.5	82	75	78	90*	2	2
500	54.0	21.9	80	77	78	90*	1	1
1000	60.0	28.0	78	79	83	90*	-5	2

** Receiver locked onto undesired signal from this point on

* Loss of lock entirely

Table A-2. Measured Bearing Error for ADF Receiver A as a Function of the Undesired Signal Level and the Frequency Separation (Δf) between the Desired and Undesired Signals. The Desired Signal Level is 500 μV/m at 200 kHz with No Modulation. The Undesired Signal is Unmodulated.

UNDESIRED μV/m	SIGNAL LEVEL dBu	UNDESIRED TO DESIRED SIGNAL RATIO dB	BEARING ERROR, DEGREES					
			Δf=.05 kHz	Δf=.10 kHz	Δf=.25 kHz	Δf=.50 kHz	Δf=2.0 kHz	Δf=3.75 kHz
10	20.0	-34.0	0	0	0	0	0	0
30	29.5	-24.4	0	0	0	0	0	0
70	36.9	-17.1	0	0	0	0	0	0
100	40.0	-14.0	0	0	0	0	0	0
300	49.5	-4.4	1	0	0	0	0	0
500	54.0	0.0	1	0	0	0	0	0
1000	60.0	6.0	1	0	0	0	0	0
1100	60.8	6.9	59	0	0	0	0	0
1200	61.6	7.6	61**	50	0	0	0	0
1500	63.5	9.5	64	51**	72**	90*	0	0
3000	69.5	15.6	66	64	72	90*	0	0
7000	76.9	22.9	74	69	71	90*	0	0
10000	80.0	26.0	74	71	71	90*	1	0

** Receiver locked onto undesired signal from this point on

* Loss of lock entirely

Table A-3. Measured Bearing Error for ADF Receiver A as a Function of the Undesired Signal Level and the Frequency Separation (Δf) between the Desired and Undesired Signals. The Desired Signal Level is 500 µV/m at 200 kHz with Tone Modulation. The Undesired Signal is Unmodulated.

UNDESIRED SIGNAL LEVEL µV/m	UNDESIRED SIGNAL LEVEL dBu	UNDESIRED TO DESIRED SIGNAL RATIO dB	BEARING ERROR, DEGREES					
			Δf=.05 kHz	Δf=.10 kHz	Δf=.25 kHz	Δf=.50 kHz	Δf=2.0 kHz	Δf=3.75 kHz
10	20.0	-34.0	0	0	0	0	0	0
30	29.5	-24.4	0	0	0	0	0	0
70	36.9	-17.1	0	0	0	0	0	0
100	40.0	-14.0	0	0	0	0	0	0
300	49.5	-4.4	0	0	0	0	0	0
500	54.0	0.0	0	0	0	0	0	0
1000	60.0	6.0	0	0	0	0	0	0
1100	60.8	6.9	0	0	0	0	0	0
1200	61.6	7.6	1	0	0	0	0	0
1500	63.5	9.5	58**	0	70**	0	0	0
3000	69.5	15.6	68	51**	72	90*	0	0
7000	76.9	22.9	71	62	72	90*	0	0
10000	80.0	26.0	73	68	71	90*	0	0

** Receiver locked onto undesired signal from this point on

* Loss of lock entirely

Table A-4. Measured Bearing Error for ADF Receiver A as a Function of the Undesired Signal Level and the Frequency Separation (Δf) between the Desired and Undesired Signals. The Desired Signal Level is 1,000 μV/m at 200 kHz with No Modulation. The Undesired Signal is Unmodulated.

UNDESIRED	SIGNAL LEVEL	UNDESIRED TO DESIRED SIGNAL RATIO	BEARING ERROR, DEGREES					
μV/m	dBu	dB	Δf=.05 kHz	Δf=.10 kHz	Δf=.25 kHz	Δf=.50 kHz	Δf=2.0 kHz	Δf=3.75 kHz
100	40.0	-20.0	0	0	0	0	0	0
200	46.0	-14.0	0	0	0	0	0	0
500	54.0	-6.0	0	0	0	0	0	0
700	56.9	-3.1	0	0	0	0	0	0
1000	60.0	0.0	0	0	0	0	0	0
1500	63.5	3.5	0	0	0	0	0	0
3000	69.5	9.5	61**	0	72**	90*	0	0
5000	74.0	14.0	69	61**	73	90*	0	0
7000	76.9	16.9	71	68	72	90*	0	0
10000	80.0	20.0	73	69	72	90*	0	0

** Receiver locked onto undesired signal from this point on

* Loss of lock entirely

Table A-5. Measured Bearing Error for ADF Receiver A as a Function of the Undesired Signal Level and the Frequency Separation (Δf) between the Desired and Undesired Signals. The Desired Signal Level is 1,000 μV/m at 200 kHz with No Modulation. The Undesired Signal is Frequency Shift Keyed.

UNDESIRED μV/m	SIGNAL LEVEL dBu	UNDESIRED TO DESIRED SIGNAL RATIO dB	BEARING ERROR, DEGREES					
			Δf=.05 kHz	Δf=.10 kHz	Δf=.25 kHz	Δf=.50 kHz	Δf=2.0 kHz	Δf=3.75 kHz
100	40.0	-20.0	0	0	0	0	0	0
200	46.0	-14.0	0	0	0	0	0	0
500	54.0	-6.0	0	0	0	0	0	0
700	56.9	-3.1	0	0	0	0	0	0
1000	60.0	0.0	-10	0	0	0	0	0
1500	63.5	3.5	-10	0	0	2	0	0
3000	69.5	9.5	77	90*	90*	90*	0	0
5000	74.0	14.0	-84	90*	90*	90*	0	0
7000	76.9	16.9	-84	74	90*	90*	0	0
10000	80.0	20.0	-84	82	90*	90*	1	0

* Loss of lock entirely

Table A-6. Measured Bearing Error for ADF Receiver A as a Function of the Undesired Signal Level and the Frequency Separation (Δf) between the Desired and Undesired Signals. The Desired Signal Level is 30 μV/m at 400 kHz with No Modulation. The Undesired Signal is Unmodulated.

UNDESIRED μV/m	SIGNAL LEVEL dBu	UNDESIRED TO DESIRED SIGNAL RATIO dB	BEARING ERROR, DEGREES					
			Δf=.05 kHz	Δf=.10 kHz	Δf=.25 kHz	Δf=.50 kHz	Δf=2.0 kHz	Δf=3.75 kHz
15	23.5	-6.0	0	0	0	0	1	0
20	26.0	-3.5	0	0	1	0	1	0
25	28.0	-1.6	0	0	0	-1	1	0
30	29.5	0.0	0	0	0	0	-1	0
35	30.9	1.3	0	0	0	-1	-2	0
40	32.0	2.5	0	0	0	0	0	0
50	34.0	4.4	0	0	1	-2	0	1
60	35.6	6.0	0	0	1	-2	-1	0
70	36.9	7.4	0	0	1	-3	1	1
80	38.1	8.5	63**	0	1	-3	1	1
90	39.1	9.5	62	65**	75**	-3	1	1
100	40.0	10.5	64	68	74	90*	-3	1
120	41.6	12.0	73	65	74	90*	3	-1
150	43.5	14.0	75	65	73	90*	0	-1
170	44.6	15.1	74	68	73	90*	1	0
200	46.0	16.5	76	70	73	90*	2	0
300	49.5	20.0	75	69	73	90*	2	0
500	54.0	24.4	75	71	73	90*	1	0

** Receiver locked onto undesired signal from this point on

* Loss of lock entirely

Table A-7. Measured Bearing Error for ADF Receiver A as a Function of the Undesired Signal Level and the Frequency Separation (Δf) between the Desired and Undesired Signals. The Desired Signal Level is 500 $\mu V/m$ at 400 kHz with No Modulation. The Undesired Signal is Unmodulated.

UNDESIRED	SIGNAL LEVEL	UNDESIRED TO DESIRED SIGNAL RATIO	BEARING ERROR, DEGREES					
$\mu V/m$	dBu	dB	Δf=.05 kHz	Δf=.10 kHz	Δf=.25 kHz	Δf=.50 kHz	Δf=2.0 kHz	Δf=3.75 kHz
10	20.0	-34.0	0	0	0	0	0	0
30	29.5	-24.4	0	0	0	0	0	0
70	36.9	-17.1	0	0	0	0	0	0
100	40.0	-14.0	0	0	0	0	0	0
300	49.5	-4.4	0	0	0	0	0	0
500	54.0	0.0	0	0	0	0	0	0
700	56.9	2.9	0	0	0	0	0	0
1000	60.0	6.0	57**	0	0	0	0	0
1500	63.5	9.5	59	65**	72**	90*	0	0

** Receiver locked onto undesired signal from this point on

* Loss of lock entirely

Table A-8. Measured Bearing Error for ADF Receiver A as a Function of the Undesired Signal Level and the Frequency Separation (Δf) between the Desired and Undesired Signals. The Desired Signal Level is 500 μV/m at 400 kHz with No Modulation. The Undesired Signal is Frequency Shift Keyed.

UNDESIRED μV/m	SIGNAL LEVEL dBu	UNDESIRED TO DESIRED SIGNAL RATIO dB	BEARING ERROR, DEGREES					
			Δf=.05 kHz	Δf=.10 kHz	Δf=.25 kHz	Δf=.50 kHz	Δf=2.0 kHz	Δf=3.75 kHz
10	20.0	-34.0	0	0	0	0	0	0
30	29.5	-24.4	0	0	0	0	0	0
70	36.9	-17.1	1	0	0	0	0	0
100	40.0	-14.0	2	0	0	0	0	0
300	49.5	-4.4	2	0	3	0	0	0
500	54.0	0.0	2	0	2	0	0	0
700	56.9	2.9	4	0	-2	-2	0	0
1000	60.0	6.0	3	5	-2	-2	0	0
1500	63.5	9.5	71**	90*	90*	90*	0	0

** Receiver locked onto undesired signal from this point on

* Loss of lock entirely

Table A-9. Measured Bearing Error for ADF Receiver A as a Function of the Undesired Signal Level and the Frequency Separation (Δf) between the Desired and Undesired Signals. The Desired Signal Level is 1,000 μV/m at 400 kHz with No Modulation. The Undesired Signal is Unmodulated.

UNDESIRED μV/m	SIGNAL LEVEL dBu	UNDESIRED TO DESIRED SIGNAL RATIO dB	BEARING ERROR, DEGREES					
			Δf=.05 kHz	Δf=.10 kHz	Δf=.25 kHz	Δf=.50 kHz	Δf=2.0 kHz	Δf=3.75 kHz
100	40.0	-20.0	0	0	0	0	0	0
200	46.0	-14.0	0	0	0	0	0	0
300	49.5	-10.5	0	0	0	0	0	0
400	52.0	-8.0	0	0	0	0	0	0
500	54.0	-6.0	0	0	0	0	0	0
600	55.6	-4.4	0	0	0	0	0	0
700	56.9	-3.1	0	0	0	0	0	0
1000	60.0	0.0	0	0	0	0	-1	0
3000	69.5	9.5	63**	55**	71	90*	-1	0

** Receiver locked onto undesired signal from this point on

* Loss of lock entirely

Table A-10. Measured Bearing Error for ADF Receiver A as a Function of the Undesired Signal Level and the Frequency Separation (Δf) between the Desired and Undesired Signals. The Desired Signal Level is 100,000 μV/m at 400 kHz with No Modulation. The Undesired Signal is Unmodulated.

UNDESIRED μV/m	SIGNAL LEVEL dBu	UNDESIRED TO DESIRED SIGNAL RATIO dB	BEARING ERROR, DEGREES					
			Δf=.05 kHz	Δf=.10 kHz	Δf=.25 kHz	Δf=.50 kHz	Δf=2.0 kHz	Δf=3.75 kHz
1000	60.0	-40.0	0	0	0	0	0	0
3000	69.5	-30.5	0	1	0	0	0	0
5000	74.0	-26.0	0	1	0	0	0	0
7000	76.9	-23.1	0	1	0	0	0	0
10000	80.0	-20.0	0	1	0	0	0	0
30000	89.5	-10.5	1	1	0	0	0	0
50000	94.0	-6.0	1	1	0	0	0	0
70000	96.9	-3.1	58**	39**	0	2*	0	0
100000	100.0	0.0	63	49	69**	90*	0	0
130000	102.3	2.3	66	54	70	90*	0	0
150000	103.5	3.5	66	59	69	90*	0	0

** Receiver locked onto undesired signal from this point on

* Loss of lock entirely

Table A-11. Measured Bearing Error for ADF Receiver A as a Function of the Undesired Signal Level and the Frequency Separation(Δf) between the Desired and Undesired Signals. The Desired Signal Level is 40 μV/m at 200 kHz with No Modulation. The Undesired Signal is Unmodulated.

UNDESIRED μV/m	SIGNAL LEVEL dBu	UNDESIRED TO DESIRED SIGNAL RATIO dB	BEARING ERROR, DEGREES					
			Δf=.05 kHz	Δf=.10 kHz	Δf=.25 kHz	Δf=.50 kHz	Δf=2.0 kHz	Δf=3.75 kHz
15	23.5	-8.5	1	-1	0	2	1	0
30	29.5	-2.5	1	-2	0	1	2	0
50	34.0	1.9	1	-6	0	1	2	0
70	36.9	4.9	1	-10	0	2	0	0
100	40.0	8.0	1	-10	0	2	0	2
300	49.5	17.5	1	-1	0	90*	0	3
500	54.0	21.9	1	0	0	90*	2	0
700	56.9	24.9	1	0	0	90*	1	2
1000	60.0	28.0	1	0	0	90*	1	3
1500	63.5	31.5	1	0	0	90*	2	2
3000	69.5	37.5	1	0	0	90*	90*	2
5000	74.0	41.9	1	0	0	90*	90*	2
7000	76.9	44.9	1	0	0	90*	90*	3
10000	80.0	48.0	0	0	0	90*	90*	4
15000	83.5	51.5	0	0	0	90*	90*	5

* Loss of lock entirely

Table A-12. Measured Bearing Error for ADF Receiver A as a Function of the Undesired Signal Level and the Frequency Separation (Δf) between the Desired and Undesired Signals. The Desired Signal Level is 1,000 μV/m at 200 kHz with No Modulation. The Undesired Signal is Unmodulated.

UNDESIRED μV/m	SIGNAL LEVEL dBu	UNDESIRED TO DESIRED SIGNAL RATIO dB	BEARING ERROR, DEGREES					
			Δf=.05 kHz	Δf=.10 kHz	Δf=.25 kHz	Δf=.50 kHz	Δf=2.0 kHz	Δf=3.75 kHz
200	46.0	-14.0	0	0	0	0	0	0
300	49.5	-10.5	0	0	0	0	0	0
400	52.0	-8.0	0	0	0	0	0	0
500	54.0	-6.0	0	0	0	0	0	0
600	55.6	-4.4	0	0	0	0	0	0
700	56.9	-3.1	0	0	0	0	0	0
1000	60.0	0.0	0	0	0	0	-1	0
3000	69.5	9.5	0	0	-1	90*	-1	0
5000	74.0	14.0	0	0	-2	90*	-1	0
7000	76.9	16.9	0	0	-2	90*	-1	0
10000	80.0	20.0	0	0	-1	90*	-1	0
15000	83.5	23.5	0	0	-1	90*	-1	0

* Loss of lock entirely

Table A-13 Measured Bearing Error for ADF Receiver A as a Function of the Undesired Signal Level and the Frequency Separation (Δf) between the Desired and Undesired Signals. The Desired Signal Level is 500 μV/m at 200 kHz with No Modulation. The Undesired Signal is Frequency Shift Keyed.

UNDESIRED μV/m	SIGNAL LEVEL dBu	UNDESIRED TO DESIRED SIGNAL RATIO dB	BEARING ERROR, DEGREES					
			Δf=.05 kHz	Δf=.10 kHz	Δf=.25 kHz	Δf=.50 kHz	Δf=2.0 kHz	Δf=3.75 kHz
10	20.0	-34.0	0	0	-1	0	0	0
30	29.5	-24.4	0	0	0	0	0	0
70	36.9	-17.1	0	0	0	0	0	0
100	40.0	-14.0	-2	0	0	0	0	0
300	49.5	-4.4	-2	-2	0	0	0	0
500	54.0	0.0	-6	-3	0	0	0	0
700	56.9	2.9	-6		-3	2	0	0
1000	60.0	6.0	-4		-2	2	0	0
1500	63.5	9.5			90*	90*	0	0

* Loss of lock entirely

Table A-14. Measured Bearing Error for ADF Receiver A as a Function of the Undesired Signal Level and the Frequency Separation (Δf) Between the Desired and Undesired Signals. The Desired Signal Level is 30 μV/m at 400 kHz with No Modulation. The Undesired Signal is Unmodulated.

UNDESIRED μV/m	SIGNAL LEVEL dBu	UNDESIRED TO DESIRED SIGNAL RATIO dB	BEARING ERROR, DEGREES					
			Δf=.05 kHz	Δf=.10 kHz	Δf=.25 kHz	Δf=.50 kHz	Δf=2.0 kHz	Δf=3.75 kHz
15	23.5	-6.0	0	-2	-1	0	0	0
20	26.0	-3.5	0	-2	1	-1	0	0
25	28.0	-1.6	0	-3	0	0	0	0
30	29.5	0.0	1	-4	0	-1	0	0
35	30.9	1.3	1	-7	0	0	-2	0
40	32.0	2.5	1	-9	0	0	0	0
50	34.0	4.4	1	-50	0	0	1	0
60	35.6	6.0	1	-110	0	0	0	0
70	36.9	7.4	1	-180	0	0	0	0
80	38.1	8.5	1	-190	-2**	0	0	0
90	39.1	9.5	1	4	-2**	90*	1	0
100	40.0	10.5	0	5	-2**	90*	0	0
120	41.6	12.0	0	4	-2**	90*	0	0
150	43.5	14.0	0	4	-2**	90*	-1	0
170	44.6	15.1	0	4	-2**	90*	-2	0
200	46.0	16.5	0	4	-2**	90*	2	0
300	49.5	20.0	0	5	-2**	90*	2	0
500	54.0	24.4	0	4	-2**	90*	2	0

** Receiver locked onto undesired signal from this point on

* Loss of lock entirely

Table A-15. Measured Bearing Error for ADF Receiver A as a Function of the Undesired Signal Level and the Frequency Separation (Δf) between the Desired and Undesired Signals. The Desired Signal Level is 500 $\mu V/m$ at 400 kHz with No Modulation. The Undesired Signal is Unmodulated.

UNDESIRED $\mu V/m$	SIGNAL LEVEL dBu	UNDESIRED TO DESIRED SIGNAL RATIO dB	BEARING ERROR, DEGREES					
			Δf=.05 kHz	Δf=.10 kHz	Δf=.25 kHz	Δf=.50 kHz	Δf=2.0 kHz	Δf=3.75 kHz
10	20.0	-34.0	0	0	0	0	0	0
30	29.5	-24.4	0	0	0	0	0	0
70	36.9	-17.1	0	-2	0	0	0	0
100	40.0	-14.0	0	-2	0	0	0	0
300	49.5	-4.4	0	-5	0	0	0	0
500	54.0	0.0	-2	-7	0	0	0	0
700	56.9	2.9	-3		0	0	0	0
1000	60.0	6.0	-1		-2	-1	0	0
1500	63.5	9.5	-1		-2	90*	0	0

* Loss of lock entirely

AD-A087 126 NATIONAL TELECOMMUNICATIONS/INFORMATION ADMINISTRATIO--ETC F/G 17/3
POWER LINE CARRIER RADIATION AND THE LOW-FREQUENCY AERONAUTICAL--ETC(U)
MAY 80 W A KISSICK DOT-FA79WAI-023

UNCLASSIFIED FAA-RD-80-31 NL

2 OF 2
AD A
087126

END
DATE
FILMED
9-80
DTIC

Table A-16. Measured Bearing Error for ADF Receiver B as a Function of the Undesired Signal Level and the Frequency Separation (Δf) between the Desired and Undesired Signals. The Desired Signal Level is 40 μV/m at 200 kHz with No Modulation. The Undesired Signal is Unmodulated.

UNDESIRED μV/m	SIGNAL LEVEL dBu	UNDESIRED TO DESIRED SIGNAL RATIO dB	BEARING ERROR, DEGREES				
			Δf=.25 kHz	Δf=.50 kHz	Δf=1.0 kHz	Δf=1.5 kHz	Δf=3.5 kHz
15	23.5	-8.5	1	1	1	2	2
20	26.0	-6.0	1	1	1	1	2
25	28.0	-4.0	3	1	1	2	2
30	29.5	-2.5	1	2	1	1	1
35	30.9	-1.2	2	2	2	1	2
40	32.0	0.0	4	2	3	2	1
50	34.0	1.9	2	4	2	3	2
60	35.6	3.5	1	3	3	2	3
70	36.9	4.9	3	2	2	3	3
80	38.1	6.0	1	3	1	2	2
90	39.1	7.0	4	3	2	3	2
100	40.0	8.0	3	2	2	2	2
120	41.6	9.5	2	2	2	3	2
150	43.5	11.5	4	4	3	2	3
170	44.6	12.6	2	1	3	2	2
200	46.0	14.0	6	10	8	6	2
300	49.5	17.5	35	60	75	55	5
500	54.0	21.9	65	105	130	135	3

Table A-17. Measured Bearing Error for ADF Receiver B as a Function of the Undesired Signal Level and the Frequency Separation (Δf) between the Desired and Undesired Signals. The Desired Signal Level is 500 μV/m at 200 kHz with No Modulation. The Undesired Signal is Unmodulated.

UNDESIRED μV/m	SIGNAL LEVEL dBu	UNDESIRED TO DESIRED SIGNAL RATIO dB	BEARING ERROR, DEGREES				
			Δf=.25 kHz	Δf=.50 kHz	Δf=1.0 kHz	Δf=1.5 kHz	Δf=3.5 kHz
10	20.0	-33.9	0	0	0	0	0
30	29.5	-24.4	1	0	0	1	1
70	36.9	-17.1	1	0	1	1	1
100	40.0	-14.0	1	0	1	1	1
300	49.5	-4.4	0	3	5	3	1
500	54.0	0.0	34	8	16	9	1
700	56.9	2.9	108	10	77	36	1
1000	60.0	6.0		13	94	110	0
1500	63.5	9.5		48	132	135	0

Table A-18. Measured Bearing Error for ADF Receiver B as a Function of the Undesired Signal Level and the Frequency Separation (Δf) between the Desired and Undesired Signals. The Desired Signal Level is 500 μV/m at 200 kHz with Tone Modulation. The Undesired Signal is Unmodulated.

UNDESIRED μV/m	SIGNAL LEVEL dBu	UNDESIRED TO DESIRED SIGNAL RATIO dB	BEARING ERROR, DEGREES				
			Δf=.25 kHz	Δf=.50 kHz	Δf=1.0 kHz	Δf=1.5 kHz	Δf=3.5 kHz
10	20.0	-34.0	0	0	0	1	0
30	29.5	-24.4	1	1	1	1	1
70	36.9	-17.1	1	1	1	1	1
100	40.0	-14.0	1	1	2	2	1
300	49.5	-4.4	3	2	5	3	1
500	54.0	0.0	6	5	15	8	1
700	56.9	2.9	9	11	50	25	1
1000	60.0	6.0	11	11	102	99	1
1500	63.5	9.5	15	14	105	132	1

Table A-19. Measured Bearing Error for ADF Receiver B as a Function of the Undesired Signal Level and the Frequency Separation (Δf) between the Desired and Undesired Signals. The Desired Signal Level is 1,000 μV/m at 200 kHz with No Modulation. The Undesired Signal is Unmodulated.

UNDESIRED μV/m	SIGNAL LEVEL dBu	UNDESIRED TO DESIRED SIGNAL RATIO dB	BEARING ERROR, DEGREES				
			Δf=.25 kHz	Δf=.50 kHz	Δf=1.0 kHz	Δf=1.5 kHz	Δf=3.5 kHz
100	40.0	-20.0	0	1	1	1	0
200	46.0	-14.0	2	2	2	2	0
300	49.5	-10.5	3	4	3	2	1
400	52.0	-8.0	7	6	6	3	1
500	54.0	-6.0	9	10	8	4	1
600	55.6	-4.4	12	14	12	5	1
700	56.9	-3.1	17	19	16	7	1
1000	60.0	0.0	30	32	30	12	0
3000	69.5	9.5	65	68	72	63	0

Table A-20. Measured Bearing Error for ADF Receiver B as a Function of the Undesired Signal Level and the Frequency Separation (Δf) between the Desired and Undesired Signals. The Desired Signal Level is 1,000 $\mu V/m$ at 200 kHz with No Modulation. The Undesired Signal is Frequency Shift Keyed.

UNDESIRED $\mu V/m$	SIGNAL LEVEL dBu	UNDESIRED TO DESIRED SIGNAL RATIO dB	BEARING ERROR, DEGREES				
			Δf=.25 kHz	Δf=.50 kHz	Δf=1.0 kHz	Δf=1.5 kHz	Δf=3.5 kHz
100	40.0	-20.0	0	0	0	0	0
200	46.0	-14.0	2	2	2	1	0
300	49.5	-10.5	4	4	3	1	0
400	52.0	-8.0	6	6	5	2	0
500	54.0	-6.0	8	10	8	3	0
600	55.6	-4.4	11	14	11	4	0
700	56.9	-3.1	17	17	13	5	0
1000	60.0	0.0	29	33	26	10	0
3000	69.5	9.5	73	68	70	55	0

Table A-21. **Measured Bearing Error for ADF Receiver B as a Function of the Undesired Signal Level and the Frequency Separation (Δf) between the Desired and Undesired Signals. The Desired Signal Level is 30 μV/m at 400 kHz with No Modulation. The Undesired Signal is Unmodulated.**

UNDESIRED μV/m	SIGNAL LEVEL dBu	UNDESIRED TO DESIRED SIGNAL RATIO dB	BEARING ERROR, DEGREES				
			Δf=.25 kHz	Δf=.50 kHz	Δf=1.0 kHz	Δf=1.5 kHz	Δf=3.5 kHz
15	23.5	-6.1	0	0	0	1	1
20	26.0	-3.5	1	2	0	2	1
25	28.0	-1.6	1	2	1	2	1
30	29.5	0.0	1	0	2	1	0
35	30.9	1.4	0	0	2	1	0
40	32.0	2.5	2	0	3	2	0
50	34.0	4.4	2	0	2	2	0
60	35.6	6.0	2	1	2	2	0
70	36.9	7.4	3	2	2	2	0
80	38.1	8.5	3	2	2	2	0
90	39.1	9.5	3	3	3	2	0
100	40.0	10.5	2	2	3	2	0
120	41.6	12.0	4	4	4	3	0
150	43.5	14.0	8	12	12	5	1
170	44.6	15.1	13	17	14	13	0
200	46.0	16.5	18	18	48	22	0
300	49.5	20.0	80	127	127	142	0
500	54.9	24.4	160	152	150	157	0

Table A-22. **Measured Bearing Error for ADF Receiver B as a Function of the Undesired Signal Level and the Frequency Separation (Δf) between the Desired and Undesired Signals. The Desired Signal Level is 500 μV/m at 400 kHz with No Modulation. The Undesired Signal is Unmodulated.**

UNDESIRED μV/m	SIGNAL LEVEL dBu	UNDESIRED TO DESIRED SIGNAL RATIO dB	BEARING ERROR, DEGREES				
			Δf=.25 kHz	Δf=.50 kHz	Δf=1.0 kHz	Δf=1.5 kHz	Δf=3.5 kHz
10	20.0	-34.0	0	1	0	1	0
30	29.5	-24.4	0	2	1	0	0
70	36.9	-17.1	0	1	0	0	1
100	40.0	-14.0	0	0	1	0	1
300	49.5	-4.4	0	2	3	2	0
500	54.0	0.0	2	5	4	3	0
700	56.9	2.9	2	20	22	5	0
1000	60.0	6.0	7	53	62	48	0
1500	63.5	9.5	53	86	117	110	0

Table A-23. Measured Bearing Error for ADF Receiver B as a Function of the Undesired Signal Level and the Frequency Separation (Δf) between the Desired and Undesired Signals. The Desired Signal Level is 500 μV/m at 400 kHz with No Modulation. The Undesired Signal is Frequency Shift Keyed.

UNDESIRED μV/m	SIGNAL LEVEL dBu	UNDESIRED TO DESIRED SIGNAL RATIO dB	BEARING ERROR, DEGREES				
			Δf=.25 kHz	Δf=.50 kHz	Δf=1.0 kHz	Δf=1.5 kHz	Δf=3.5 kHz
10	20.0	-34.0	1	0	0	0	0
30	29.5	-24.4	2	0	0	1	1
70	36.9	-17.1	1	1	1	1	1
100	40.0	-14.0	0	1	2	2	1
300	49.5	-4.4	2	2	2	2	1
500	54.0	0.0	3	2	3	3	1
700	56.9	2.9	6	4	6	5	1
1000	60.0	6.0	22	18	24	25	0
1500	63.5	9.5	58	78	108	83	0

Table A-24. Measured Bearing Error for ADF Receiver B as a Function of the Undesired Signal Level and the Frequency Separation (Δf) between the Desired and Undesired Signals. The Desired Signal Level is 1,000 $\mu V/m$ at 400 kHz with No Modulation. The Undesired Signal is Unmodulated.

UNDESIRED $\mu V/m$	SIGNAL LEVEL dBu	UNDESIRED TO DESIRED SIGNAL RATIO dB	BEARING ERROR, DEGREES				
			Δf=.25 kHz	Δf=.50 kHz	Δf=1.0 kHz	Δf=1.5 kHz	Δf=3.5 kHz
100	40.0	-20.0	0	0	0	0	0
200	46.0	-14.0	1	1	1	.1	0
300	49.5	-10.5	4	4	3	2	1
400	52.0	-8.0	5	5	5	3	1
500	54.0	-6.0	9	8	8	4	0
600	55.6	-4.4	22	21	21	7	0
700	56.9	-3.1	25	24	24	19	0
1000	60.0	0.0	38	36	37	28	0
3000	69.5	9.5	73	66	76	73	0

Table A-25. Measured Bearing Error for ADF Receiver B as a Function of the Undesired Signal Level and the Frequency Separation (Δf) between the Desired and Undesired Signals. The Desired Signal Level is 100,000 $\mu V/m$ at 400 kHz with No Modulation. The Undesired Signal is Unmodulated.

UNDESIRED $\mu V/m$	SIGNAL LEVEL dBu	UNDESIRED TO DESIRED SIGNAL RATIO dB	BEARING ERROR, DEGREES				
			Δf=.25 kHz	Δf=.50 kHz	Δf=1.0 kHz	Δf=1.5 kHz	Δf=3.5 kHz
1000	60.0	-40.0	0	-1	0	0	0
3000	69.5	-30.5	0	-3	-2	-2	0
5000	74.0	-26.0	1	-4	-3	-2	-2
7000	76.9	-23.1	1	-3	-3	-3	-2
10000	80.0	-20.0	1	-1	-3	-3	-3
30000	89.5	-10.5	5	2	2	0	-2
50000	94.0	-6.0	9	7	6	2	-3
70000	96.9	-3.1	17	15	11	6	-3
100000	100.0	0.0	31	27	23	13	-3
130000	102.3	2.3	42	39	27	19	-3
150000	103.5	3.5	48	45	38	24	-4

Table A-26. Measured Bearing Error for ADF Receiver B as a Function of the Undesired Signal Level and the Frequency Separation (Δf) between the Desired and Undesired Signals. The Desired Signal Level is 40 μV/m at 200 kHz with No Modulation. The Undesired Signal is Unmodulated.

UNDESIRED μV/m	SIGNAL LEVEL dBu	UNDESIRED TO DESIRED SIGNAL RATIO dB	BEARING ERROR, DEGREES				
			Δf=.25 kHz	Δf=.50 kHz	Δf=1.0 kHz	Δf=1.5 kHz	Δf=3.5 kHz
15	23.5	-8.5	-2	0	0	0	0
30	29.5	-2.5	0	0	0	0	0
50	34.0	1.9	-3	0	0	0	0
70	36.9	4.9	-2	0	0	0	0
100	40.0	8.0	0	1	0	0	0
300	49.5	17.5	0	0	0	0	0
500	54.0	22.0	-2	0	0	0	0
700	56.9	24.9	-2	0	0	0	0
1000	60.0	27.8	0	1	0	0	0
1500	63.5	31.5	0	1	0	0	0
3000	69.5	37.5	0	1	0	0	0
5000	74.0	41.9	0	1	0	0	0
7000	76.9	44.9	0	1	0	0	0
10000	80.0	48.0	0	1	0	0	0
15000	83.5	51.5	0	1	0	0	0

Table A-27. Measured Bearing Error for ADF Receiver B as a Function of the Undesired Signal Level and the Frequency Separation (Δf) between the Desired and Undesired Signals. The Desired Signal Level is 1,000 μV/m at 200 kHz with No Modulation. The Undesired Signal is Unmodulated.

UNDESIRED μV/m	SIGNAL LEVEL dBu	UNDESIRED TO DESIRED SIGNAL RATIO dB	BEARING ERROR, DEGREES				
			Δf=.25 kHz	Δf=.50 kHz	Δf=1.0 kHz	Δf=1.5 kHz	Δf=3.5 kHz
200	46.0	-14.0	0	0	0	0	0
300	49.5	-10.5	0	0	0	0	0
400	52.0	-7.9	0	0	0	0	0
500	54.0	-6.0	0	0	0	0	0
600	55.6	-4.4	0	0	0	0	0
700	56.9	-3.1	0	0	0	0	0
1000	60.0	0.0	0	0	0	0	0
3000	69.5	9.5	0	0	0	0	0
5000	74.0	14.0	0	0	0	0	0
7000	76.9	16.9	0	0	0	0	0
10000	80.0	20.0	0	0	0	0	0
15000	83.5	23.5	0	0	0	0	0

Table A-28. Measured Bearing Error for ADF Receiver B as a Function of the Undesired Signal Level and the Frequency Separation (Δf) between the Desired and Undesired Signals. The Desired Signal Level is 500 $\mu V/m$ at 200 kHz with No Modulation. The Undesired Signal is Frequency Shift Keyed.

UNDESIRED	SIGNAL LEVEL	UNDESIRED TO DESIRED SIGNAL RATIO	BEARING ERROR, DEGREES				
$\mu V/m$	dBu	dB	Δf=.25 kHz	Δf=.50 kHz	Δf=1.0 kHz	Δf=1.5 kHz	Δf=3.5 kHz
10	20.0	-34.0	0	0	0	0	0
30	29.5	-24.4	0	-1	0	0	0
70	36.9	-17.1	1	0	0	1	0
100	40.0	-14.0	-1	0	0	1	1
300	49.5	-4.4	-1	-1	-1	1	1
500	54.0	0.0	2	-1	-2	1	0
700	56.9	2.9	-2	-1	-1	1	1
1000	60.0	6.0	1	-1	-2	-1	1
1500	63.5	9.5	2	-1	-5	-1	1

Table A-29. Measured Bearing Error for ADF Receiver B as a Function of the Undesired Signal Level and the Frequency Separation (Δf) between the Desired and Undesired Signals. The Desired Signal Level is 30 μV/m at 400 kHz with No Modulation. The Undesired Signal is Unmodulated.

UNDESIRED μV/m	SIGNAL LEVEL dBu	UNDESIRED TO DESIRED SIGNAL RATIO dB	BEARING ERROR, DEGREES				
			Δf=.25 kHz	Δf=.50 kHz	Δf=1.0 kHz	Δf=1.5 kHz	Δf=3.5 kHz
15	23.5	-6.0	0	0	-1	0	-1
20	26.0	-3.5	0	0	0	0	0
25	28.0	-1.6	-1	0	1	0	0
30	29.5	0.0	0	-1	0	-1	-1
35	39.0	1.3	-1	-1	0	-1	0
40	32.0	2.5	-2	0	0	0	0
50	34.0	4.4	-1	0	0	1	0
60	35.6	6.0	-1	-1	-1	0	0
70	36.9	7.4	0	0	0	0	0
80	38.1	8.5	0	0	0	0	0
90	39.1	9.5	0	0	0	0	0
100	40.0	10.5	0	0	0	0	0
120	41.6	12.0	0	0	0	0	0
150	43.5	14.0	0	0	0	0	0
170	44.6	15.1	0	0	0	0	0
200	46.0	16.5	0	0	0	0	-1
300	49.5	20.0	0	0	0	0	-2
500	54.0	24.4	0	0	0	0	-2

Table A-30. Measured Bearing Error for ADF Receiver B as a Function of the Undesired Signal Level and the Frequency Separation (Δf) between the Desired and Undesired Signals. The Desired Signal Level is 500 μV/m at 400 kHz with No Modulation. The Undesired Signal is Unmodulated.

UNDESIRED µV/m	SIGNAL LEVEL dBu	UNDESIRED TO DESIRED SIGNAL RATIO	BEARING ERROR, DEGREES				
			Δf=.25 kHz	Δf=.50 kHz	Δf=1.0 kHz	Δf=1.5 kHz	Δf=3.5 kHz
10	20.0	-34.0	0	0	0	0	0
30	29.5	-24.4	-1	0	0	0	0
70	36.9	-17.1	-1	0	0	0	0
100	40.0	-14.0	-1	0	0	0	0
300	49.5	-4.4	0	0	0	0	0
500	54.0	0.0	0	0	0	0	0
700	56.9	2.9	1	0	0	0	0
1000	60.0	6.0	1	0	0	0	0
1500	63.5	9.5	1	0	0	0	0

APPENDIX B

MEASUREMENT AIRCRAFT CALIBRATION

B.1 Introduction and Ground-Level Measurements

One portion of the work covered in this report is the airborne measurement of the field strength of PLC signals to be made over power lines. The measurement of the actual field strength external to the aircraft required the calibration of the aircraft/receiving system as a unit. The receiving system used is a spectrum analyzer with a microprocessor controlled data storage system; see subsection 4.3 for a more detailed description of the receiving system.

The purpose of the aircraft calibration is to obtain the relationship between the measured, received signal level at the spectrum analyzer (in watts or dBm) and the actual field strength (in volts/meter or dBu) external to the aircraft. To do this, a known field was obtained by locating several suitable NDB's, then measuring the ground-level field strength, and lastly, using the ground-level data to infer the radiated power and ground constants, predicting the field strength at some altitude above the ground. An ideal NDB for this calibration procedure is one that is located on perfectly flat, homogeneous earth with no nearby obstructions and has a circularly symmetric antenna pattern. An ideal NDB does not exist, of course; hence some real ones must suffice. Three NDB's that come as close as is reasonable to the ideal conditions were found; these are:

- The NDB at the Perryton, Texas, airport. This NDB is located over very flat earth that appears to be fairly homogeneous. The antenna is not as symmetric as desired and has some nearby obstructions; but it is a very short, horizontal wire. The frequency of this NDB is 266 kHz.

- The NDB at the Alva, Oklahoma, airport. This NDB is located over relatively flat earth that appears to be reasonably homogeneous. The antenna is situated in an open and unobstructed part of the airfield and is a top-loaded vertical wire. The frequency of this beacon is 203 kHz.

- The NDB at the Elk City, Oklahoma, airport. This NDB is located on and

is surrounded by slightly rolling plains. Since there is some drainage in the area, the earth is probably somewhat inhomogeneous. The antenna is a top-loaded vertical wire with a small amount of local obstruction. The frequency of this beacon is 241 kHz.

Ground-level field strength data were taken at each of the three NDB sites. These data were taken along two carefully chosen radials for each beacon. Sufficient data points are needed to define the slope and the intercept of this field strength versus distance line. These two values can then be used to infer the ground constants and the radiated power of each NDB along each radial. The ground-level field strength data are given in Table B-1.

B.2 The Field Intensity and Structure at Non-Zero Heights

In general, the electromagnetic field radiated from a short, vertical antenna located on a smooth plane earth is vertically polarized. The field strength is (Berry, 1978*)

$$E(d) = \frac{9.487\sqrt{P}}{d} A(z) \quad , \qquad V/m \qquad (B-1)$$

where P is the effective radiated power in watts and A(z) is the flat earth attenuation function. The geometrical parameters used are defined in Figure B-1.

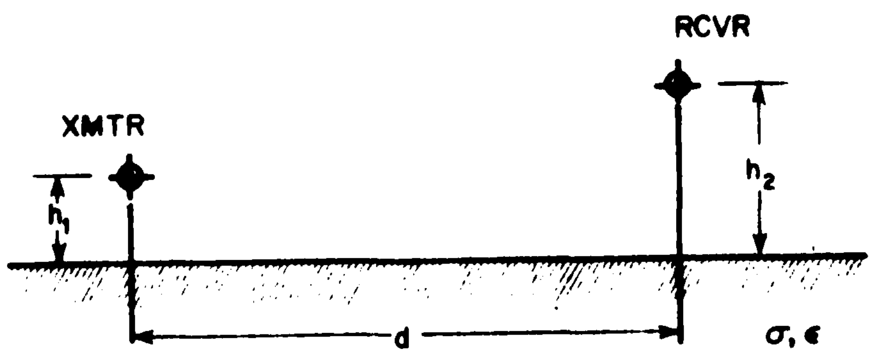

Figure B-1 Geometric parameters used to calculate the non-directional beacon field strength.

---

* An unpublished Technical Memorandum: Berry, L.A. (1978), User's guide to low-frequency radio coverage programs, OT-TM 78-274. National Telecommunications and Information Administration, Boulder, CO.

Table B-1 The Measured Ground-Level Field Strength (in decibels above 1 μV/m) for the Three Beacons Used for Aircraft Calibration

PERRYTON 266 kHz				ALVA 203 kHz				ELK CITY 241 kHz			
55° RADIAL		323° RADIAL		66° RADIAL		290° RADIAL		59° RADIAL		316° RADIAL	
DISTANCE km	STRENGTH dBu	DISTANCE km	STRENGTH dBu	DISTANCE km	STRENGTH dBu	DISTANCE km	STRENGTH dBu	DISTANCE km	STRENGTH dBu	DISTANCE km	STRENGTH dBu
4.07	60.5	1.36	69.0	0.59	74.4	0.31	81.8	1.60	68.5	1.69	67.5
4.37	59.2	3.09	61.0	2.11	62.4	1.06	68.8	2.24	65.4	2.41	65.0
7.79	53.6	5.44	56.6	2.57	61.4	2.90	60.3	2.64	64.0	3.98	61.0
8.20	52.2	7.15	54.6	4.50	56.1	4.62	56.2	3.59	60.9	4.80	58.7
9.77	51.6	8.11	52.9	4.89	56.1	5.79	53.4	5.38	57.7	6.21	56.4
11.75	49.9	10.75	50.7	6.52	53.1	6.28	53.3	7.40	54.8	7.18	55.3
13.03	48.2	11.33	50.4	7.61	51.9	7.95	52.0	9.28	52.9	8.48	54.9
		12.08	48.8	8.48	51.3	9.71	49.7	11.14	51.9	8.88	54.0
				10.32	49.4	10.47	48.6				
				10.49	49.0	11.38	48.1				
				12.55	47.6	14.84	46.2				
				13.12	47.6	15.19	47.1				
				14.49	46.5						

the flat earth attenuation function is

$$A(z) = \left[1 - R_o\, \delta\, e^{z^2}\, \mathrm{erfc}(z)\right], \tag{B-2}$$

where δ is the surface impedance of the ground, given by

$$\delta = \begin{cases} \sqrt{\eta - 1}\,/\eta & \text{for vertical polarization,} \\ \sqrt{\eta - 1} & \text{for horizontal polarization,} \end{cases} \tag{B-3}$$

and

$$\eta = \epsilon - i\,\frac{1.8(10)^7\sigma}{f} \quad , \tag{B-4}$$

where σ is the ground conductivity in mhos/m (siemens/m), ϵ is the permittivity of the ground relative to that of free space, and f is the radio frequency in kilohertz. The other parameters involved are

$$R_o = e^{i\pi/4}\sqrt{\pi k D/2} \quad , \tag{B-5}$$

$$D = \sqrt{d^2 + (h_1 - h_2)^2} \quad , \tag{B-6}$$

$k = 2\pi/\lambda = 2\pi f/c$, where $\lambda = f/c$ is the free space wavelength,

$$z = e^{i\pi/4}\sqrt{\frac{kD}{2}}\,\delta \left[1 + \frac{h_1 + h_2}{\delta D}\right] \quad , \tag{B-7}$$

and erfc (z) is the complementary error function (Abramowitz and Stegun, 1964). All units are MKS, unless noted otherwise.

Inspection of equations B-1 through B-7 shows that the following parameters must be known:

Radio system parameters: radio frequency, f, and effective radiated power, P.

Geometrical parameters: antenna heights, h_1 and h_2, and path length, d.

Ground parameters: conductivity, σ, and relative dielectric constant, ϵ.

Since σ is the usually greater than 10^{-3} and ϵ is the order of 10, equation B-4 shows that the exact value of ϵ is unimportant for frequencies less than 400 kHz - the value of η is controlled by the ground conductivity σ.

The antenna heights and path lengths are independent variables when calculating the field structure. The two remaining parameters, P and σ, can be determined from measurements made on the ground along a radial from the transmitter. The measured field strengths are plotted in decibels as a function of distance, and a straight line is fitted to the points. The slope of the line determines the ground conductivity, σ, and the value of the line at 1 km determines the radiated power P.

At distances sufficiently far from the transmitting antenna, the curvature of the earth must be taken into account. Then (Fock, 1965; Wait, 1964)

$$E = 9.487\sqrt{P}\sqrt{\frac{v}{12\ \sin\theta}}\ \frac{e^{-i3\pi/4}}{a}\int_{\Gamma} e^{-ixt}\ F_I(q,t)\ dt\ , \qquad \text{(B-8)}$$

where a is the radius of the earth, $\theta = d/a$,

$$v = (ka/2)^{1/3}\ ,\ x = v\theta,\ \text{and}\ q = -iv\ \delta\ . \qquad \text{(B-9)}$$

The contour Γ comes from ∞ to $e^{-i\pi/4}$ on a straight line with a slope of -1 to $(Re(t_o) - i/2\ Im(t_o))$ and then proceeds on a straight line with slope +1 to $\infty\ e^{-i3\pi/4}$. t_o is the first pole of $F_I(q,t)$. Re designates the "real part of" and Im designates the "imaginary part of". Here

$$F_I(q,t) = \frac{H_1(h_1)\ H_2(h_2)}{\dfrac{W_1'(t)}{W_1(t)} - q}\ . \qquad \text{(B-10)}$$

The height gain functions are

$$H_1(h) = \frac{W_1(t - y)}{W_1(t)} \qquad \text{(B-11)}$$

and

$$H_2(h) = -.5i \left\{ W_2(t - y) \left[W_1'(t) - qW_1(t) \right] - W_1(t - y) \left[W_2'(t) - qW_2(t) \right] \right\} \quad \text{(B-12)}$$

where $y = kh/v$. Note that $H_1(0) = H_2(0) = 1$. The functions $W_n(t)$ are Airy functions (Wait, 1964), which satisfy

$$W'_n(t) = tW_n(t) \quad . \quad \text{(B-13)}$$

The only parameter required to evaluate B-8 that is not required for B-1 is the radius of the earth, a, and this is known. Thus, B-8 can be used to extrapolate measurements made near the transmitter to much greater distances, assuming that the ground conductivity does not change as we move away from the transmitter.

Computer programs exist for evaluating equations B-1 and B-8 (Berry, 1978*). The computer programs have been validated by comparison with the standard CCIR curves (CCIR, 1970) with Federal Communications Commission methods developed originally by Norton (1941).

B.3 Flight Paths and the Calibration Constant

There are two basic flight path types: radials and orbits. By flying the radials both inbound and outbound and the orbits both clockwise and counter-clockwise, we were able to determine that the direction of signal arrival at the aircraft had no effect on the received signal level. The desired flight paths are shown in Figure B-2. Note that for the largest two orbits, data are taken only over two arcs of each orbit. Figure B-3, is a plot of the actual flight paths for the Perryton NDB. These paths were developed from the INS data.

The received signal level in dBm was recorded along the designated flight paths for each of three beacons. Figures B-4 through B-11 are the data for the radial flight paths. On these graphs, we have plotted the received signal level versus the distance from the beacon. A logarithmic curve was then

---

* An unpublished Technical Memorandum: Berry, L.A. (1978), User's guide to low-frequency radio coverage programs, OT-TM 78-274. National Telecommunications and Information Administration, Boulder, CO.

fitted through the data. Table B-2 gives the constants calculated for the logarithmic curve along with some associated parameters. The equation that represents the logarithmic curve is

$$S = A \operatorname{Log}_{10} d + B$$

where S = the received signal level in dBm

and d = the horizontal distance from the NDB in km.

Last, in Table B-3 are the signal statistics for the remaining flight paths--the orbits and the arcs.

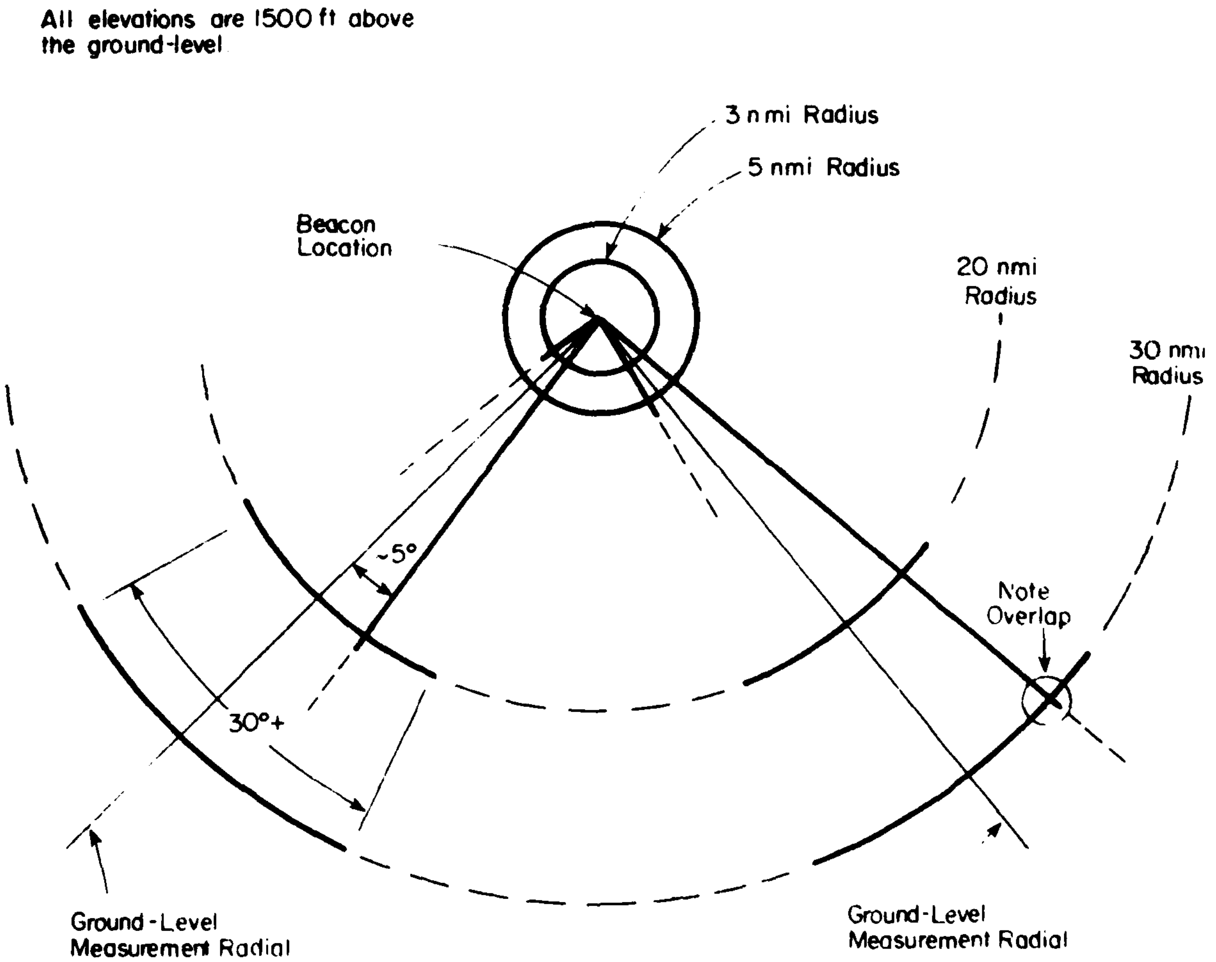

Figure B-2 Flight paths for aircraft calibration. Data are taken where solid, heavy lines are shown (1 nmi = 1.852 km, 1500 ft = 457.2 m).

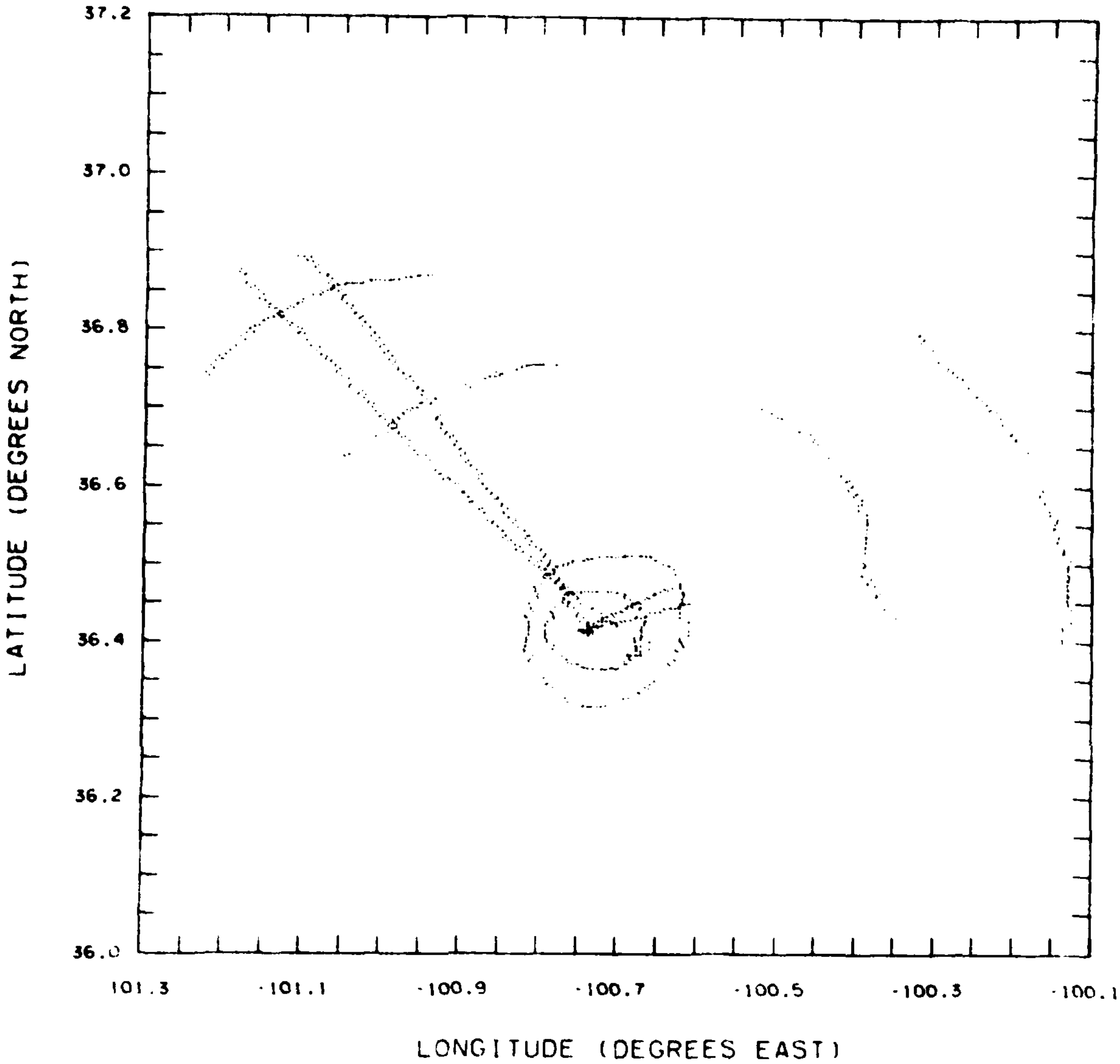

Figure B-3. The actual calibration flight paths for the Perryton NDB, taken from the INS data.

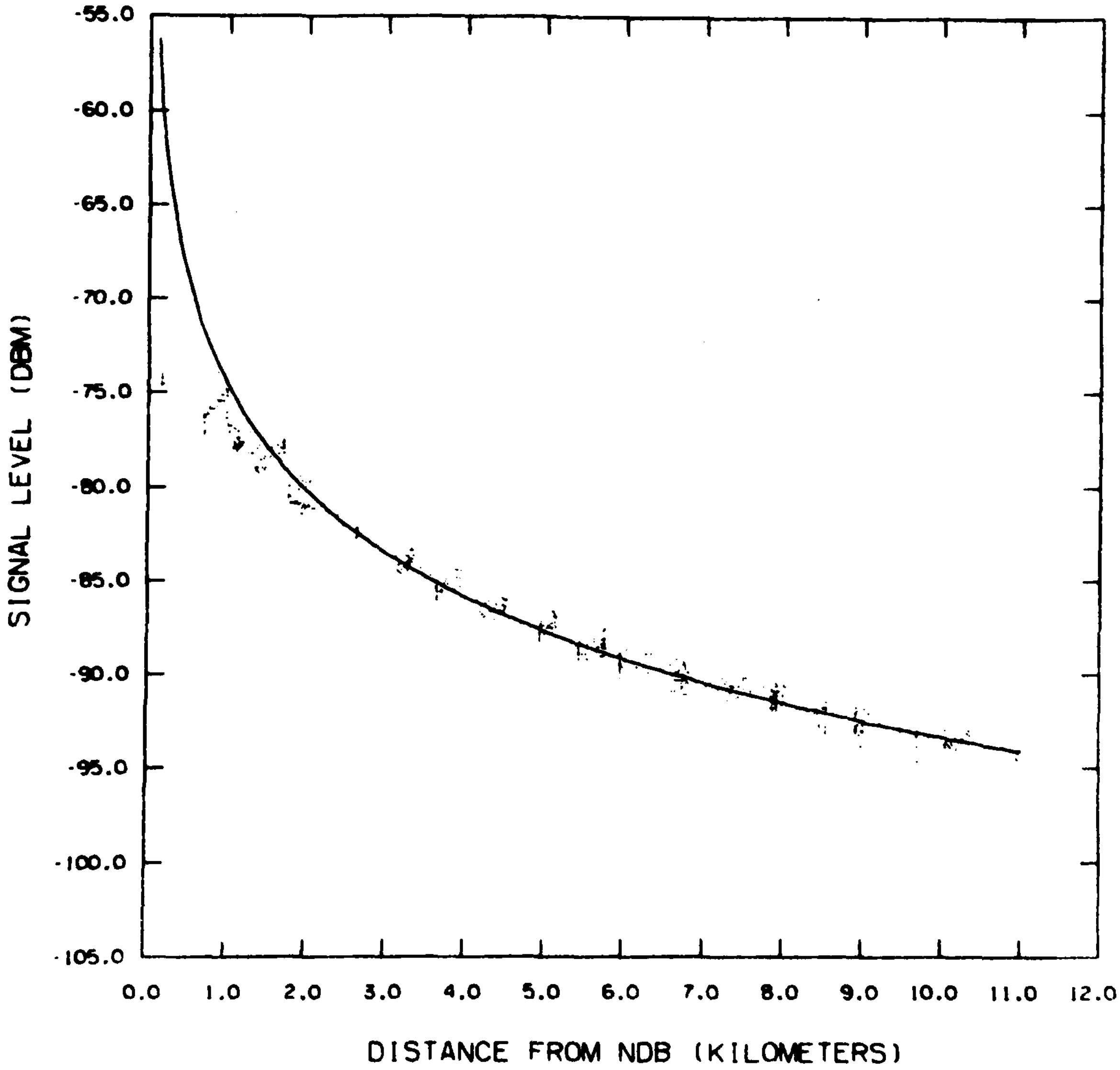

Figure B-4. The received signal level versus distance for the 50° radial at Perryton.

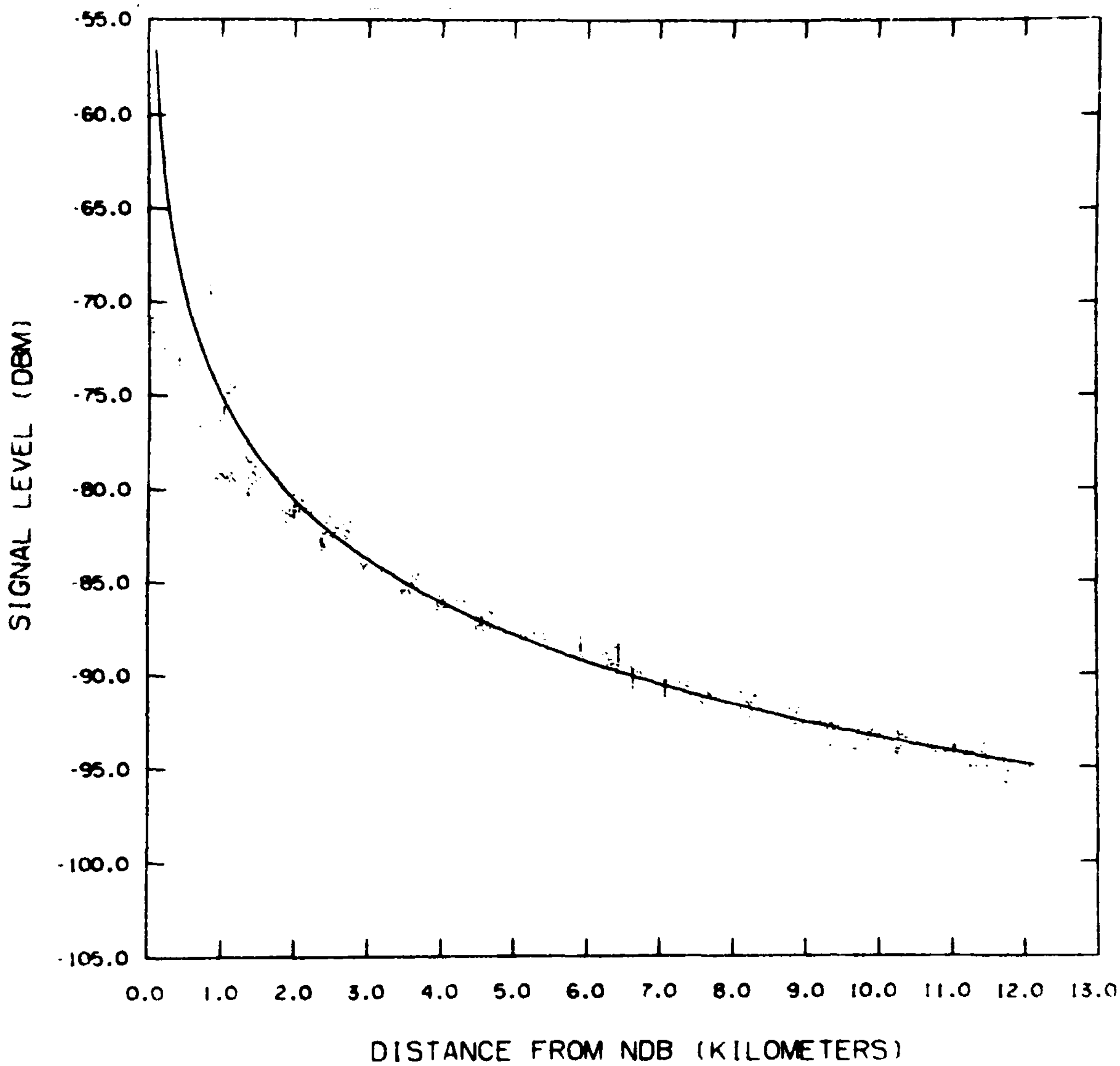

Figure B-5. The received signal level versus distance for the 60° radial at Perryton.

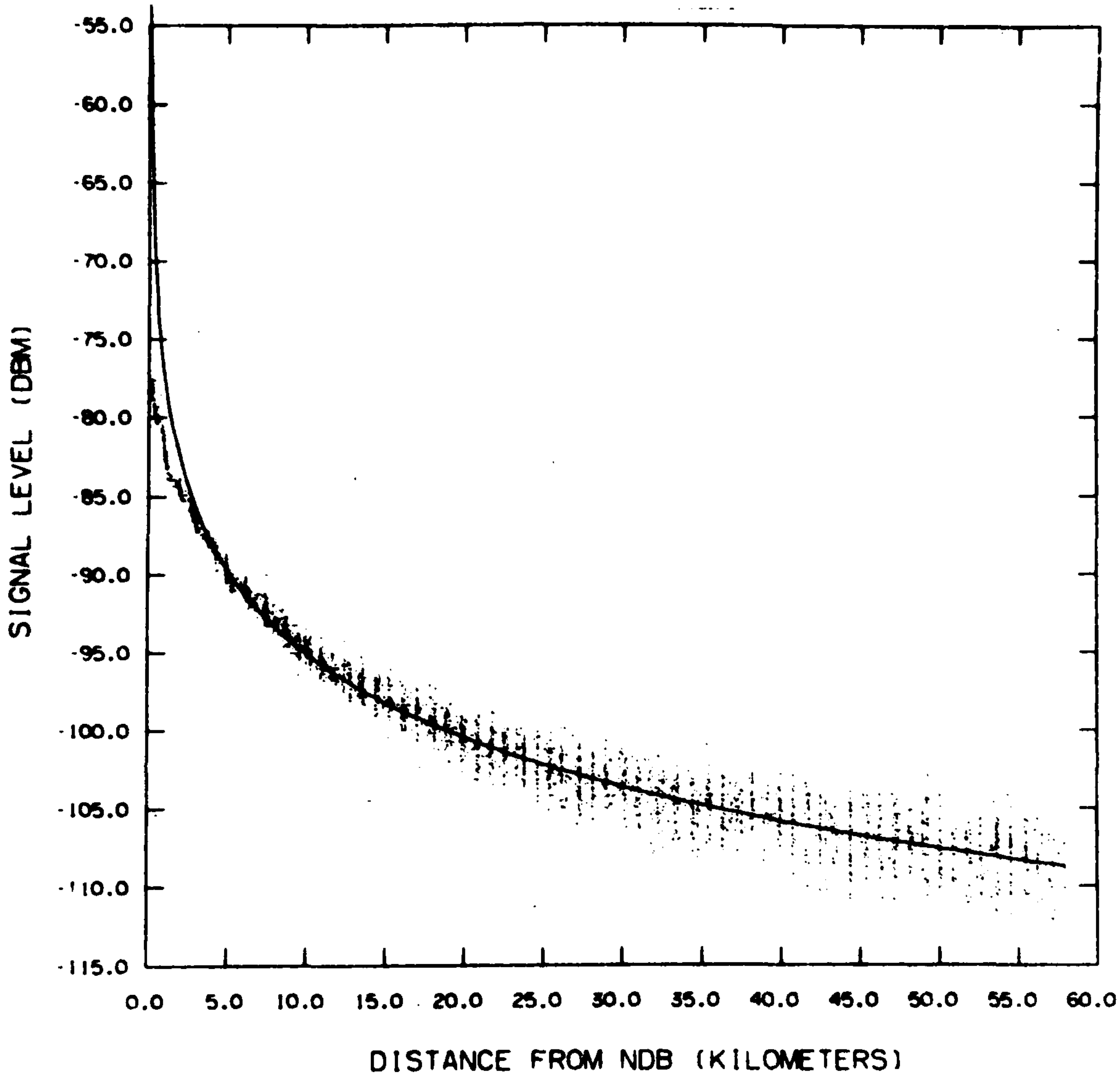

Figure B-6. The received signal level versus distance for the 318° radial at Perryton.

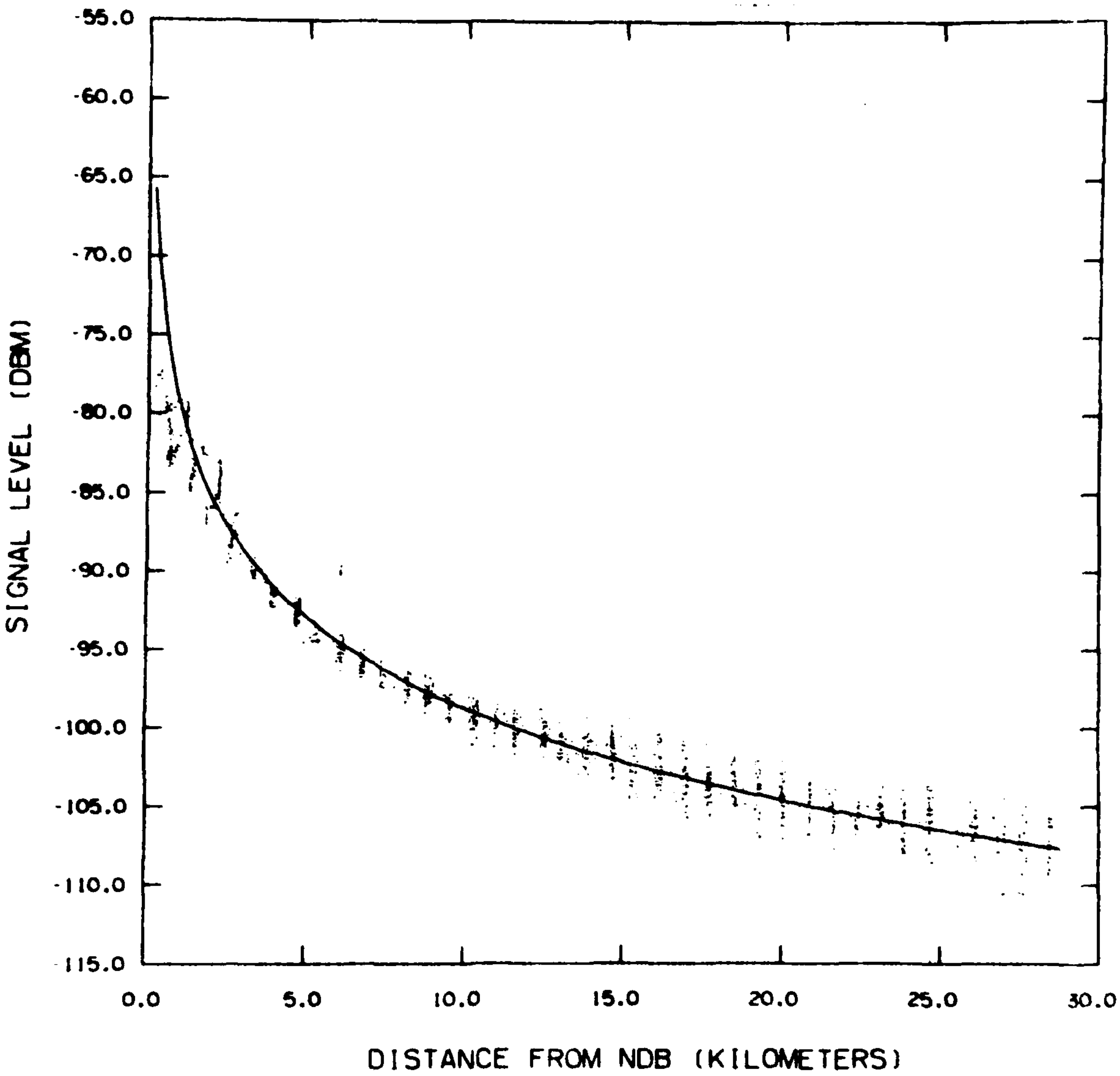

Figure B-7. The received signal level versus distance for the 328° radial at Perryton.

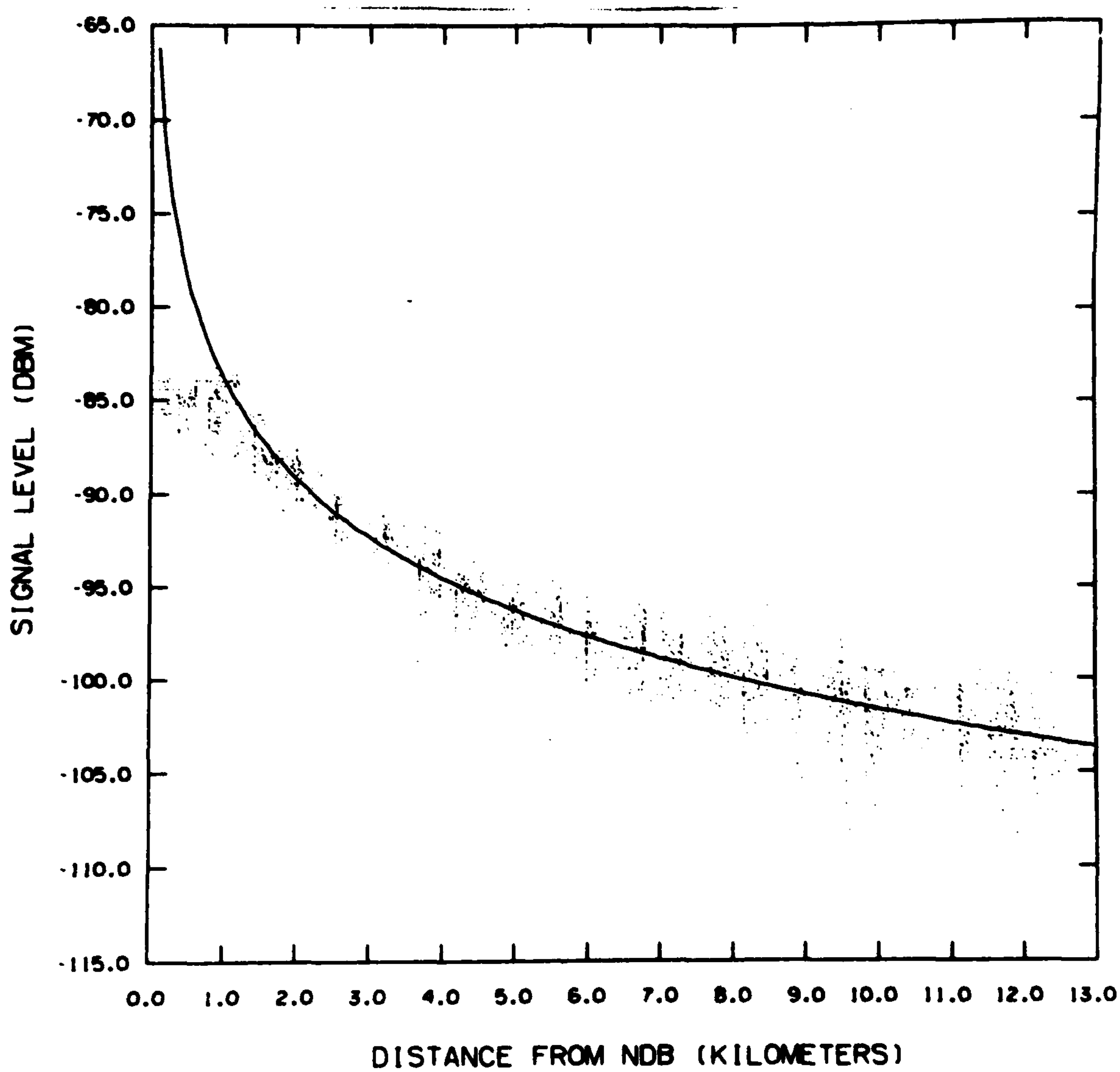

Figure B-8. The received signal level versus distance for the 61° radial at Alva.

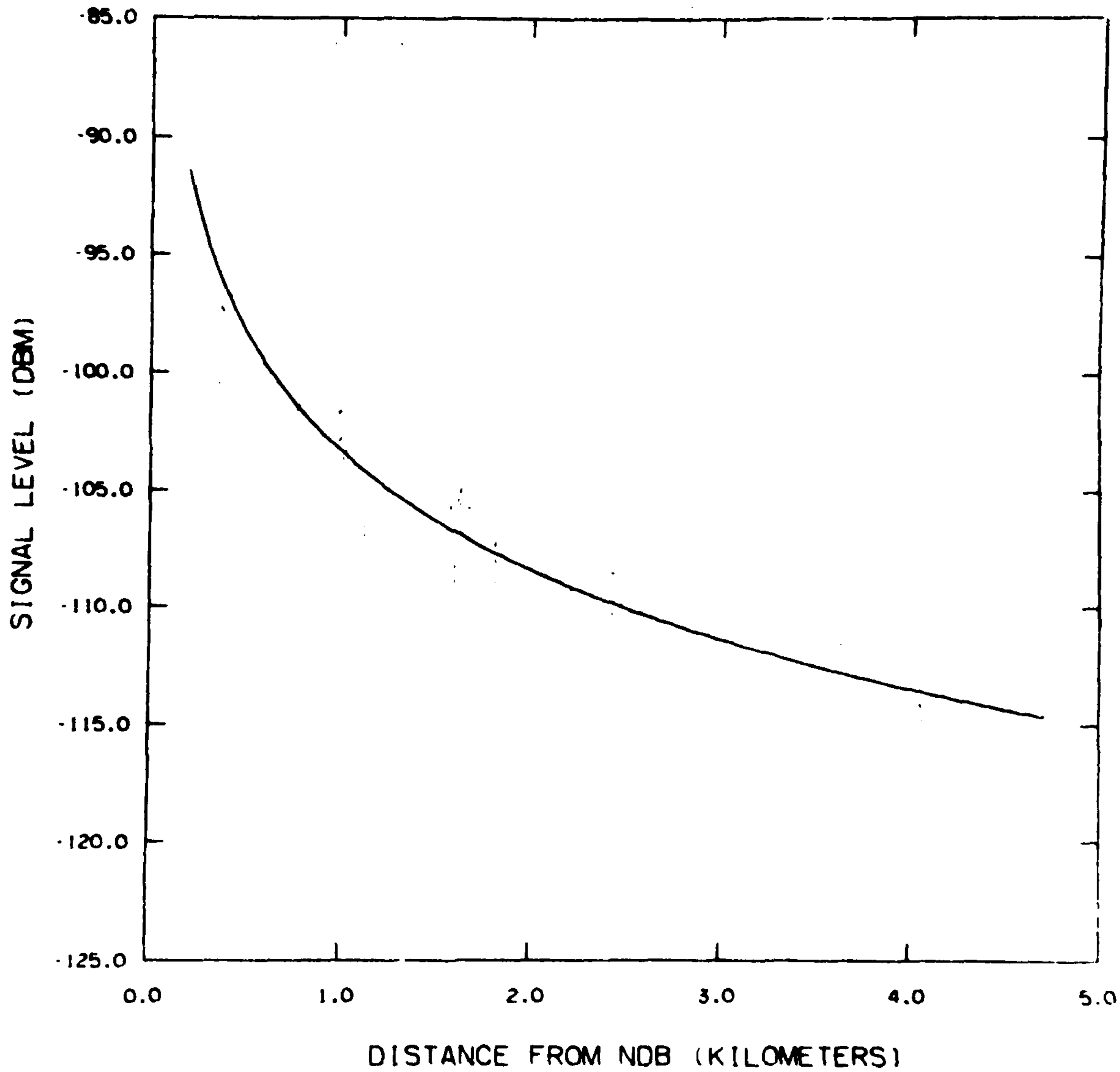

Figure B-9. The received signal level versus distance for the 54° radial at Elk City.

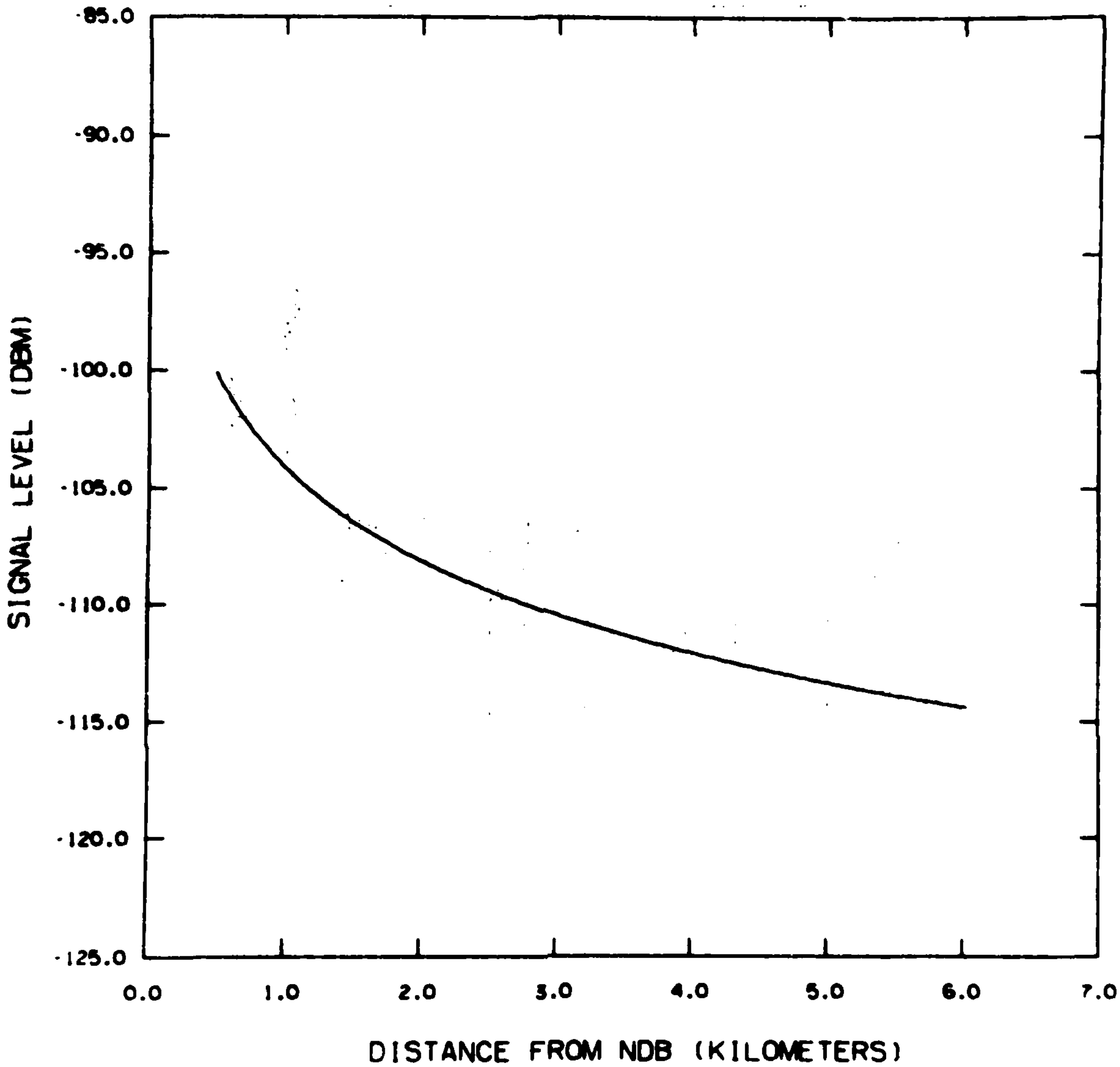

Figure B-10. The received signal level versus distance for the 64° radial at Elk City.

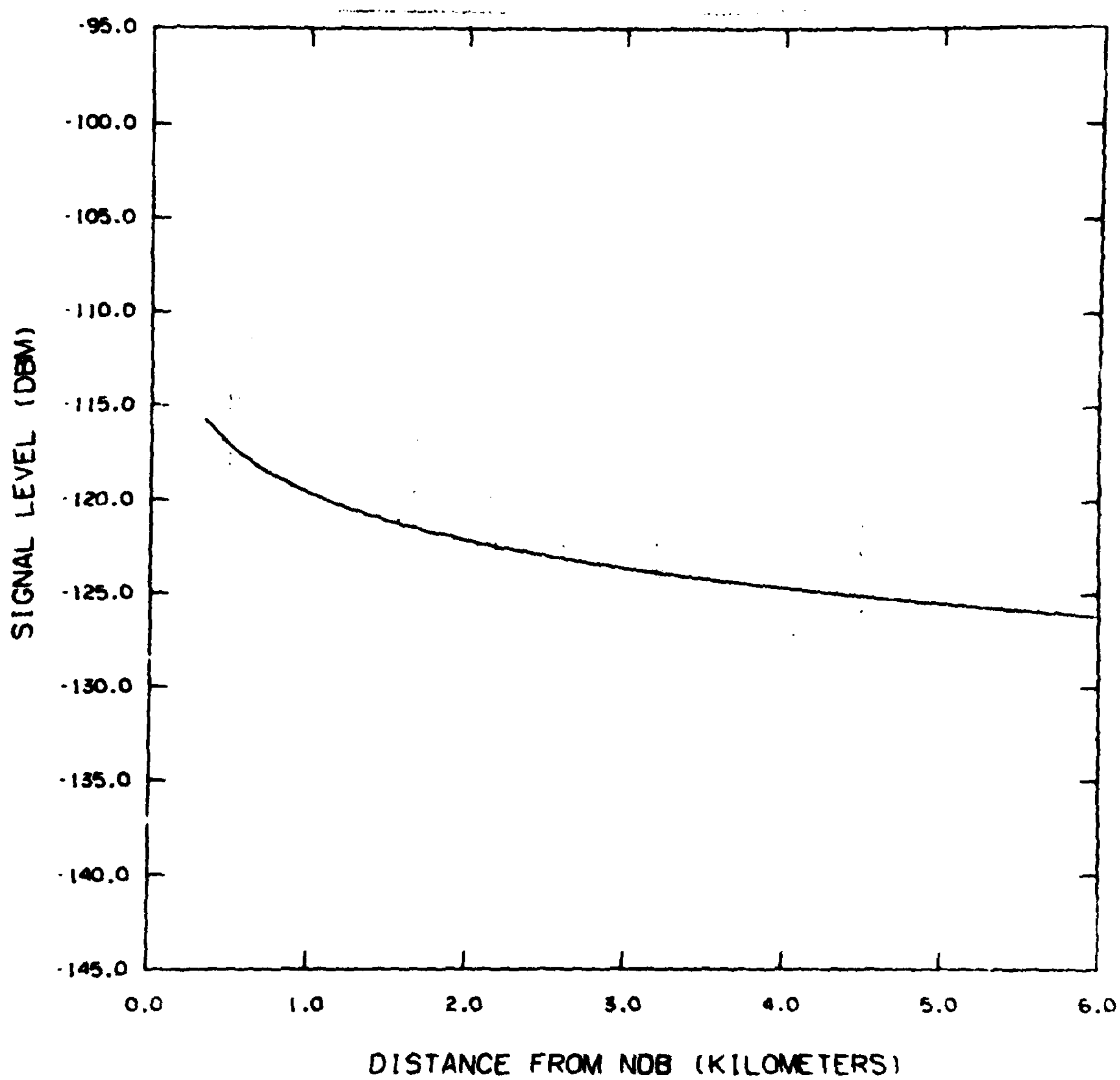

Figure B-11. The received signal level versus distance for the 311° radial at Elk City.

Table B-2. Logarithmic Curve Fit Constants and Parameters for the Radials of the Calibration Flights

LOCATION AND FREQUENCY	RADIAL BEARING	$S = A \log_{10} d + B$		VALID DISTANCE RANGE (km)	CORRELATION COEFFICIENT	MEAN SQUARED ERROR $(dB)^2$	NUMBER OF SAMPLES
		A	B				
PERRYTON 266 kHz	50°	-18.70	-74.63	1.5 - 10.9	-0.9832	0.4969	1018
	60°	-18.23	-75.11	2.0 - 12.0	-0.9873	0.5027	1097
	318°	-19.38	-79.42	4.0 - 57.0	-0.9689	2.506	2501
	328°	-17.81	-77.31	2.0 - 27.0	-0.9604	3.148	4628
ALVA 203 kHz	61°	-17.74	-83.88	1.5 - 12.0	-0.9457	2.088	1350
ELK CITY 241 kHz	54°	-16.79	-103.4	0.5 - 4.5	-0.6029	6.245	631
	64°	-13.15	-104.1	1.0 - 6.0	-0.5058	9.619	487
	311°	-8.36	-119.7	1.0 - 5.0	-0.2823	18.63	480

Table B-3. The Received Signal Level (in Decibels above 1 mW) Statistics for the Orbits and Arcs of the Calibration Flights

LOCATION AND FREQUENCY	FLIGHT PATH	STATISTICS OF RECEIVED SIGNAL LEVEL					
		MEAN (dBm)	STANDARD DEVIATION (dB)	10-PERCENTILE (dBm)	MEDIAN (dBm)	90-PERCENTILE (dBm)	NUMBER OF SAMPLES
PERRYTON 266 kHz	3 n mi ORBIT	-88.62	1.409	-90.14	-88.58	-87.51	3,590
	5 n mi ORBIT	-93.64	1.321	-95.31	-93.65	-91.90	5,209
	20 n mi ARC, 55°	-104.5	1.978	-107.1	-104.3	-102.1	3,019
	20 n mi ARC, 323°	-105.1	1.301	-106.8	-105.1	-103.6	2,117
	30 n mi ARC, 55°	-108.4	2.723	-112.0	-108.2	-105.2	3,738
	30 n mi ARC, 323°	-108.6	1.772	-110.8	-108.5	-106.5	2,495
ALVA 203 kHz	20 n mi ARC, 66°	-113.5	3.264	-117.8	-113.2	-109.8	1,888
	20 n mi ARC, 290°	-113.9	3.056	-118.0	-113.6	-110.4	2,010
	30 n mi ARC, 66°	-116.2	4.028	-121.4	-116.0	-111.4	3,041
	30 n mi ARC, 290°	-116.0	3.565	-121.0	-115.8	-111.8	3,008
ELK CITY 241 kHz	3 n mi ORBIT	-123.8	7.421	-133.6	-124.1	-114.4	3,197
	5 n mi ORBIT	-123.4	5.241	-130.4	-123.3	-116.6	4,408

B.4 REFERENCES - APPENDIX B

Abramowitz, M., and I.A. Stegun (1964), Handbook of Mathematical Functions, National Bureau of Standards AMS 55 (for sale by the Superintendent of Documents, U.S. Government Printing Office, Washington, D.C. 20402).

CCIR (1970), Recommendation 368, Ground-wave propagation curves for frequencies between 10 kHz and 10 MHz, Vol. II, Green Books (International Telecommunications Union, Geneva).

Fock, V.A. (1965), Electromagnetic Diffraction and Propagation Problems (Pergamon Press, London).

Norton, K.A. (1941), The Calculation of ground-wave field intensity over a finitely conducting spherical earth, Proc. IRE, 29, No. 12, pp. 623-639.

Wait, J.R. (1964), Electromagnetic surface waves, Advances in Radio Research (edited by J.A. Saxton), 1, pp. 157-217 (Academic Press, London).

APPENDIX C

GROUND-LEVEL MEASUREMENTS OF POWER LINE CARRIER RADIATION

During the time that we and the FAA were making the PLC radiation measurements (section 4.3) over the power lines, TVA made some observations of the field strength at the ground level. The TVA measurements were made with a calibrated field strength meter using a 15 in (38.1 cm) loop antenna mounted on the roof of an automobile.

All of these measurements (Figures C-1 through C-3) essentially indicate that the field strength decreases with lateral distance with a $1/r$ dependence.

The configurations are described by Figure 11 and 12, and the signal levels have been normalized to 1 W of injected PLC power.

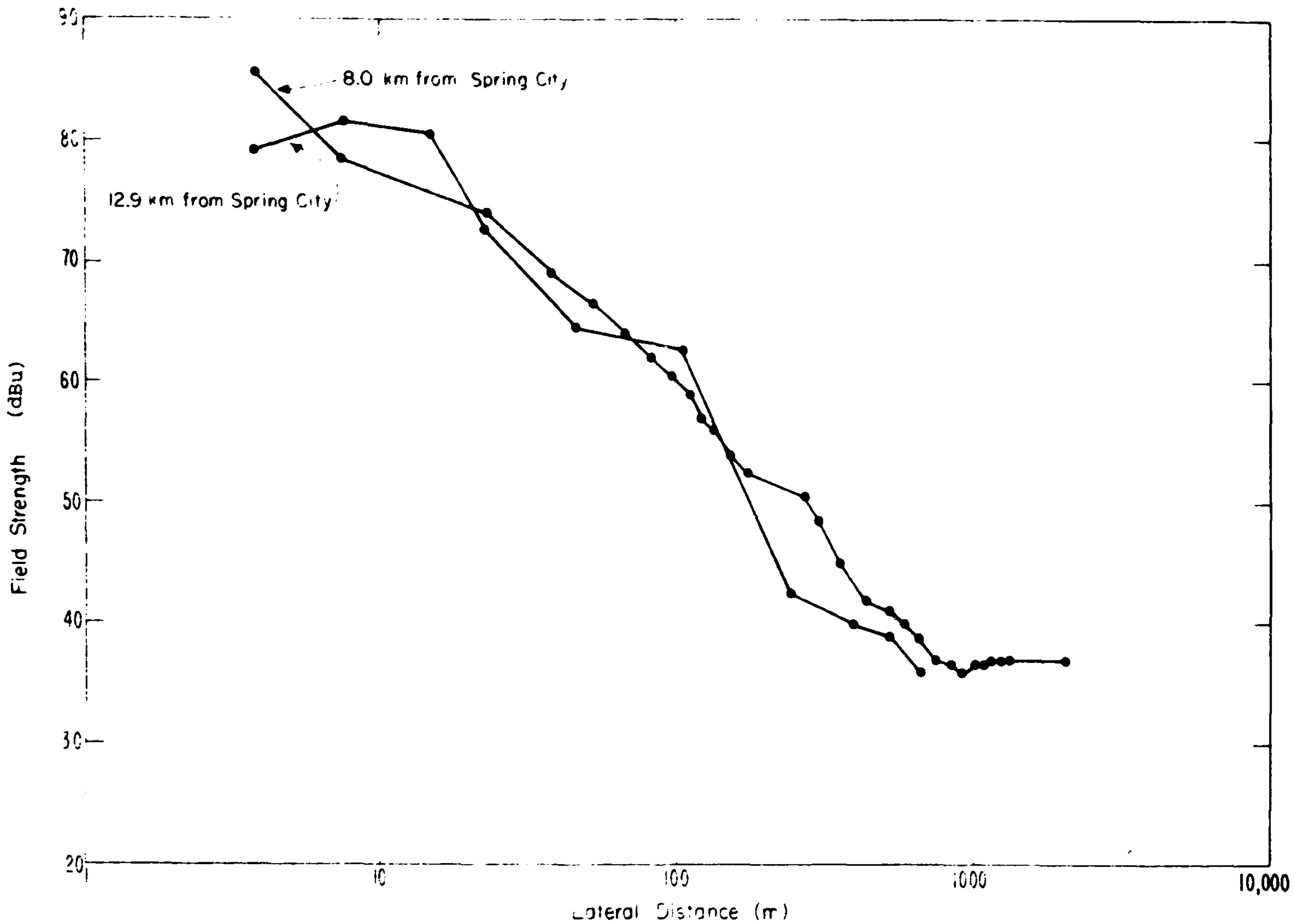

Figure C-1. Ground-level field strength measurements for the Great Falls - Spring City line, configuration I.

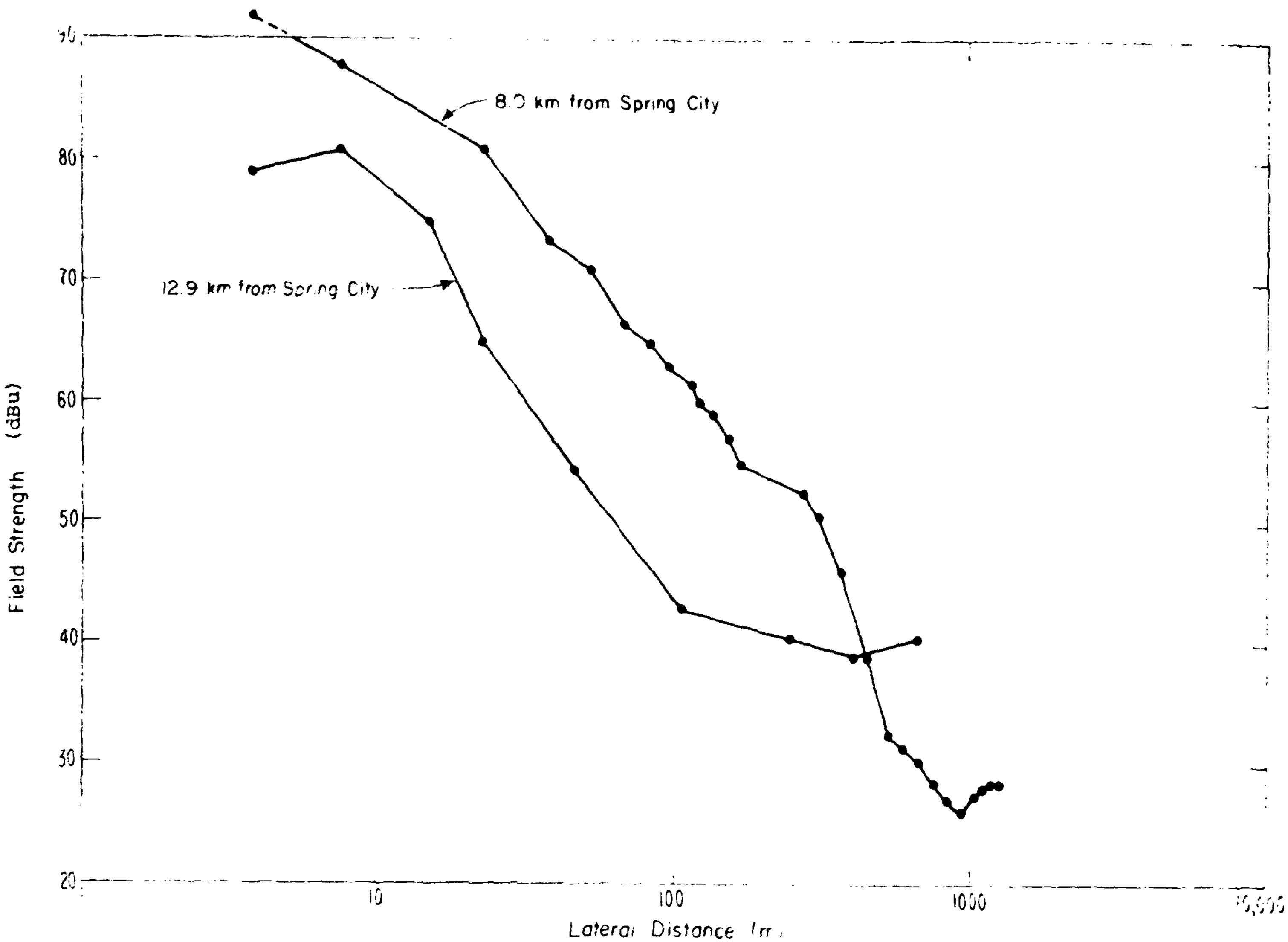

Figure C-2. Ground-level field strength measurements for the Great Falls - Spring City line, configuration II.

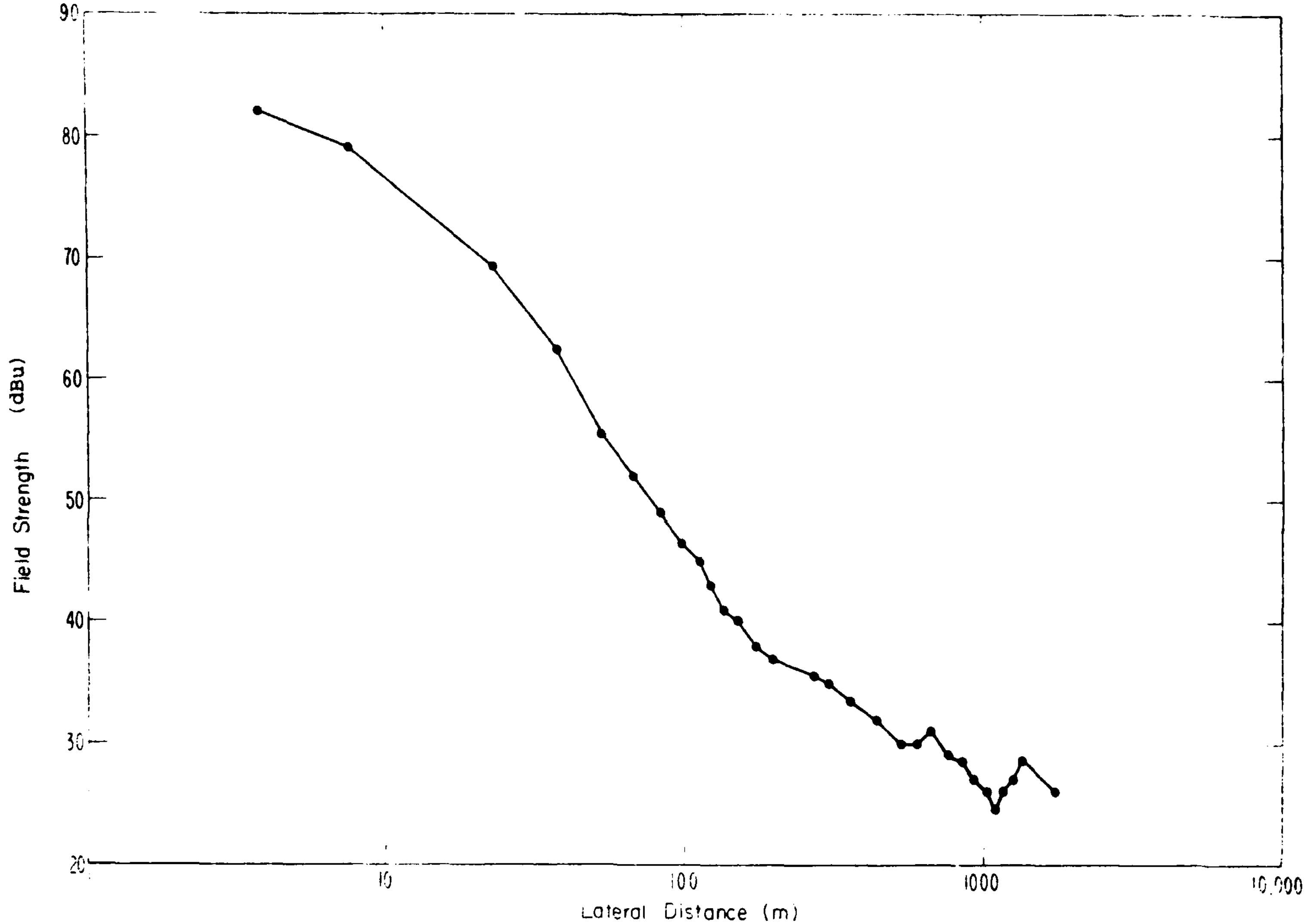

Figure C-3. Ground-level field strength measurements for the Great Falls - Spring City line, configuration III, at 8.0 km from Spring City.

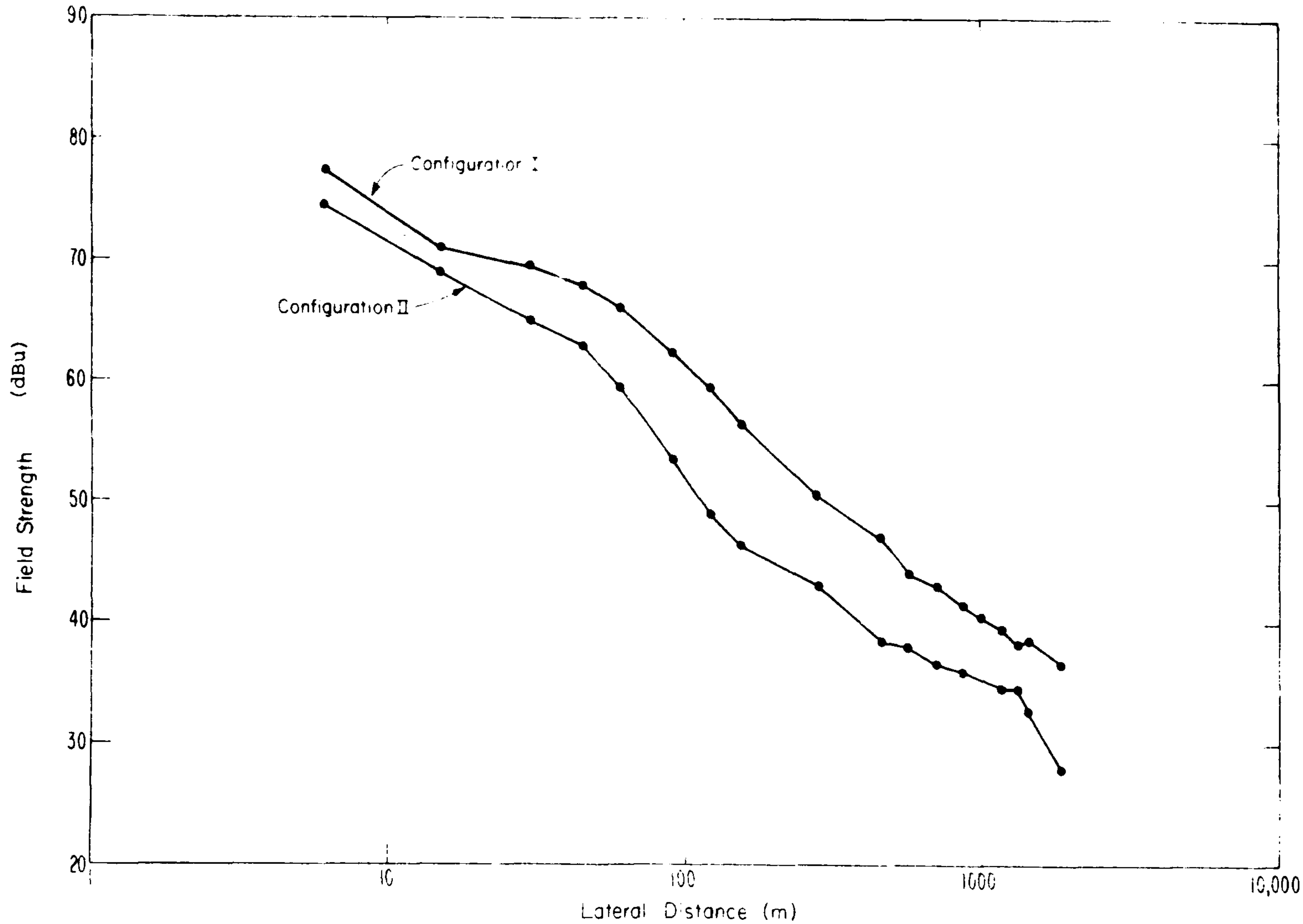

Figure C-4. Ground-level field strength measurements for the Johnsonville - Cumberland line at 13.7 km from Cumberland.

APPENDIX D

GLOSSARY AND DEFINITIONS

ADF	automatic direction-finding
AM	amplitude modulation
CW	continuous wave
D	desired
dBu	decibels above 1 $\mu V/m$
FAA	Federal Aviation Administration
FCC	Federal Communications Commission
FSK	frequency shift keying
IEEE	Institute for Electrical and Electronic Engineers
INS	inertial navigation system
LF	low frequency (30-300 kHz)
MCW	modulated continuous wave
MF	medium frequency (300-3000 kHz)
NAFEC	National Aviation Facilities Experimental Center
NDB	non-directional beacon
PLC	power line carrier
rf	radio frequency
TVA	Tennessee Valley Authority
U	undesired